

This file is part of the following work:

Yowa, Gideon Gipmai (2020) *Influence of pozzolans and plasticizer on the performance of paste backfill in underground mines*. PhD Thesis, James Cook University.

Access to this file is available from:

<https://doi.org/10.25903/bzcf%2Ddeb36>

Copyright © 2020 Gideon Gipmai Yowa.

The author has certified to JCU that they have made a reasonable effort to gain permission and acknowledge the owners of any third party copyright material included in this document. If you believe that this is not the case, please email

researchonline@jcu.edu.au



COLLEGE OF SCIENCE AND ENGINEERING

**Influence of pozzolans and plasticizer on the performance
of paste backfill in underground mines**

Gideon Gipmai Yowa

Thesis submitted to the College of Science and Engineering in partial
fulfilment of the requirements for the degree of

Master of Philosophy
(Geotechnical Engineering)

October 2020

Statement of access

I, the undersigned, the author of this thesis, understand that James Cook University will make it available for use within the university library and via Australia digital thesis network for use elsewhere.

I understand that as an unpublished work, a thesis has significant protection under copyright act, and I do not wish to place restrictions on the access of this work.

23rd October, 2020

Gideon G. Yowa

Date

Statement of sources

I declare that this thesis is my work and has not been submitted for another degree or diploma at any university or other institutions of tertiary education. Information derived from published or unpublished work of others has been acknowledged in the text and a list of references given.

23rd October, 2020

Gideon G. Yowa

Date

Acknowledgement

I would like to express my deepest gratitude to my primary supervisor Dr Nagaratnam Sivakugan for all his continuous support, guidance, and constant feedback and providing editorial support of papers and thesis throughout the research. It was a real blessing to have you as a supervisor and a mentor. I would also like to express my gratitude to Dr Rabin Thuladhar for being my co-supervisor and providing feedback and guidance throughout the research. I am also very grateful to several individuals who have contributed significantly to the completion of this research. Shaun Robinson and Troy Poole have assisted greatly in sample preparation and testing for mechanical strength properties of the cemented paste samples. Shane Askew has assisted greatly in doing the scanning electron micrograph (SEM). Ruilan Liu has assisted in using the rheometer for rheology test work. Tayla Dinnison and Lucy Bombardieri have assisted significantly in providing data of test work involving fly ash and slag.

Other important people who ensured that life in Australia and JCU was enjoyable and are worth mentioning are Melissa Norton and the GRS team, Alex and Katherine from the International Student Support Team. There were other fellow research students here at JCU namely Nafisha and Thushara who have always had time for meaningful discussions on my research progress. To my friends who became a family to me here in Townsville namely George Bopi, Warren, Jayson Wau, Stanley Amben, Dum, Teddy, Jamin, Wardman and family, Jackie Koglkia and family, and many others not mentioned here, it was a pleasure to have you all around.

This research was made possible through the Australia Award Scholarship. I would like to extend my sincere gratitude to the government and people of Australia for awarding me this prestigious scholarship to study at James Cook University.

**This thesis is dedicated to all my wonderful kids for their love and
patience while I was away from home**

Abstract

When ore is extracted underground, large voids are created which are backfilled with waste rocks or tailings to stabilise the voids. This study focuses on optimizing the mix designs of cemented paste fill, one of the most popular backfill types that uses mill tailings. Optimum paste fill design should improve strength and rheological properties while reducing cement usage and cost of backfilling.

Tailings used in paste fills have substantial clay content and a small dosage of cement binder in the order of 3 to 7 % is added to increase the strength. Even this small cement dosage adds significantly to the cost of backfilling. Partial replacement of cement with pozzolanic waste products such as slag, fly ash, or pitchstone can result in significant cost savings, and make backfilling more environmentally friendly. The possibility of partially replacing the cement with the supplementary cementitious materials was investigated in this study.

Cemented paste fill usually contains solids ranging from 70 to 85 % and water ranging from 15 to 30 %. Slurry of the cemented paste fill with high proportion of solids transported over long distances could potentially clog reticulation pipelines due to friction loss and hydration process. Thus, polycarboxylate plasticizer was used in this study to improve the flowability of the slurry.

Results from the study indicated that apart from common pozzolans like fly ash and slag, natural pozzolans like pitchstone when partially replacing cement by 10 to 20 % attained a comparable unconfined compressive strength (UCS). Cemented paste fill at binder dosage of 7 %, solid content of 74 %, and curing over 28 and 56 days produced most of the optimum mixes with UCS values reaching 1 MPa and above. Microstructure analysis of the cemented paste fill specimens of different blended binders indicated similar growth of hydration products as the control mix of 100 % Portland cement. Moreover, the application of polycarboxylate has significantly improved the workability of the slurry. The findings from this study are useful for mining industry.

Publications status

The following papers were submitted to two international conferences on Geotechnical Engineering which are in the process of acceptance and publication

Paper #1 submitted to 3rd International Conference on Geotechnical Engineering, Colombo, 2020

Investigation into strength, rheology, and microstructure of cemented paste fill using pozzolanic waste products and polycarboxylate plasticizer as partial cement replacement

G.G. Yowa, N. Sivakugan, & R. Tuladhar

Civil Engineering, James Cook University, Townsville, Australia

Paper #2 submitted to 16th International Conference, International Association for Computer Methods and Advances in Geomechanics, Turin-Italy, 2020

Influence of waste pitchstone fines and polycarboxylate plasticizer on the strength and rheology of cemented paste fill

G.G. Yowa, N. Sivakugan, R. Tuladhar

Civil Engineering, James Cook University, Townsville, Australia

Table of Contents

1	Introduction	1
1.1	Background.....	1
1.2	Research significance	4
1.3	Objectives of research	5
2	Review of literature	7
2.1	Underground mining methods	7
2.1.1	Unsupported methods	7
2.1.2	Supported methods	8
2.1.3	Caving methods	9
2.1.4	Combination methods	10
2.2	Underground backfill types.....	11
2.3	Cemented paste fill	14
2.3.1	Mill tailings	16
2.3.2	Paste plant and reticulation	18
2.3.3	Filling sequence	19
2.3.4	Curing periods.....	19
2.4	Binders	20
2.4.1	General purpose cement	21
2.4.2	Supplementary cementitious materials	22
2.4.3	Fly ash	23
2.4.4	Slag	24
2.4.5	Natural pozzolans	25
2.4.6	Pitchstone fines	25
2.5	Water.....	26

2.6	Admixtures	27
2.6.1	Plasticizer	27
2.6.2	Polycarboxylate	29
2.7	Hydration reaction	30
2.7.1	Cement hydration	30
2.7.2	Pozzolanic hydration	31
2.8	Strength development	32
2.8.1	Unconfined compressive strength	32
2.8.2	Flexural and indirect tensile strengths.....	33
2.9	Rheology of paste fill.....	34
2.9.1	Slump	34
2.9.2	Yield stress and viscosity	35
2.10	Microstructure development.....	36
2.10.1	Scanning electron micrograph	37
2.10.2	Thermogravimetry analysis.....	37
2.11	Summary	38
3	Mix design.....	39
3.1	Ingredient requirement	39
3.2	Ingredients calculation.....	44
3.3	Summary	44
4	Material characterisation	45
4.1	Physical characterisation of tailings	45
4.1.1	Particle size distribution of tailings	46
4.1.2	Grain shape of tailings	48
4.1.3	Specific gravity, bulk density, Atterberg limits of tailings.....	49
4.2	Chemical characterisation of tailings.....	51

4.2.1	X-ray diffraction of tailings.....	51
4.2.2	Thermogravimetry analysis of tailings	55
4.3	Physical characterisation of pitchstone fines	56
4.3.1	Particle size distribution of pitchstone fines	56
4.3.2	Grain size and shape of pitchstone fines.....	57
4.4	Summary	58
5	Strength development	59
5.1	Introduction	59
5.2	Materials preparation and casting.....	59
5.3	Specimen preparation for UCS	62
5.4	Unconfined compressive strength	63
5.4.1	UCS failure mode	64
5.4.2	Effect of polycarboxylate dosage on UCS.....	66
5.4.3	Effect of pozzolan and binder dosage on UCS	70
5.4.4	UCS and ground support limits	72
5.4.5	Pozzolan and strength activity index (SAI)	74
5.4.6	Effect of solid content on UCS.....	76
5.4.7	Young's modulus and UCS.....	76
5.5	Indirect tensile strength	77
5.5.1	Relevance of ITS and UCS	79
5.6	Flexural Strength	80
5.6.1	Relevance of flexural strength and UCS	81
5.7	Summary	83
6.	Microstructure development	85
6.1	Introduction	85
6.2	Scanning electron micrograph.....	85

6.2.1	Samples preparation for SEM.....	85
6.2.2	SEM of George Fisher mine tailings	87
6.2.3	Microstructure development comparison	88
6.3	TGA and DTG analysis.....	94
6.3.1	Sample preparation for TGA and DTG.....	95
6.3.2	TGA of portlandite and tailings	96
6.3.3	Effect of pozzolans on portlandite	99
6.3.4	TGA and DTG plots comparison.....	101
6.3.5	Relevance of UCS and TGA.....	105
6.4	Summary	105
7.	Rheology.....	106
7.1	Introduction	106
7.2	Preparation for yield stress and viscosity measurements	106
7.3	Yield stress measurements	109
7.3.1	Effect of solid content on yield stress	110
7.3.2	Effect of polycarboxylate dosage and binder on yield stress	111
7.3.3	Effect of rheometer and spindle on yield stress.....	113
7.3.4	Relevance of UCS and yield stress.....	114
7.3.5	Effect of solid content on viscosity.....	116
7.3.6	Effect of polycarboxylate on viscosity	116
7.3.7	Effect of time on viscosity.....	117
7.4	Slump measurement.....	118
7.4.1	Effect of polycarboxylate and solid content on slump.....	119
7.4.2	Relevance of yield stress and slump	122
7.5	Bulk density measurement for paste fill slurry	123
7.6	Summary	124

8	Summary, conclusion, and recommendation	125
8.1	Summary and key findings.....	125
8.2	Conclusion.....	130
8.3	Recommendations for future research.....	131
	Reference.....	135
	Appendix A: Example of UCS data record sheet	143
	Appendix B: Example of ITS data record sheet	144
	Appendix C: Example of slump data record sheet.....	144
	Appendix D: Example of yield stress data record sheet.....	145
	Appendix E: Example of viscosity data record sheet.....	146
	Appendix F: Example of TGA data record sheet.....	147

List of Figures

Fig. 2.1	Room and pillar method in coal mine.....	8
Fig. 2.2	Over-hand cut and fill method in hard rock mine.....	9
Fig. 2.3	Block caving method in massive hard rock mine.....	10
Fig. 2.4	Primary-secondary transverse in bulk hard rock mine.....	11
Fig. 2.5	Long section view of pure Avoca method using rockfill.....	12
Fig. 2.6	Paste fill discharge.....	13
Fig. 2.7	Ingredients for cemented paste fill slurry production.....	14
Fig. 2.8	Particle size distribution of tailings for hydraulic and paste fills.....	17
Fig. 2.9	Long section of Paste fill pour sequence of a single lift stope.....	19
Fig. 2.10	SEM of general-purpose cement.....	22
Fig. 2.11	SEM of fly ash.....	24
Fig. 2.12	UCS of Pitchstone fines replacement of CPF.....	26
Fig. 2.13	Slump comparison of various groups of plasticizers.....	28
Fig. 2.14	Impact of polycarboxylate on yield stress and plastic viscosity...29	
Fig. 2.15	Stress-strain plot.....	33
Fig. 2.16	Bingham and Newtonian fluid comparison.....	36
Fig. 3.1	Ingredients for cemented paste fill.....	39
Fig. 3.2	Combination of different mix design.....	41
Fig. 4.1	Preparation of tailing from GFM.....	45
Fig. 4.2	Equipment for particle size distribution	46
Fig. 4.3	Particle size distribution result for GFM.....	47
Fig. 4.4	Magnification of grain shape.....	49
Fig. 4.5	XRD peaks of GFM tailings.....	53
Fig. 4.6	TGA-DTG for GFM tailings.....	55
Fig. 4.7	Particle size distribution for pitchstone fines.....	56

Fig. 4.8	SEM of pitchstone fines at different magnification.....	57
Fig. 5.1	Preparation of ingredients.....	59
Fig. 5.2	Mixing the ingredients.....	60
Fig. 5.3	UCS samples removed from container for test preparation.....	62
Fig. 5.4	UCS samples preparation.....	63
Fig. 5.5	UCS testing to failure.....	63
Fig. 5.6	UCS failure modes.....	65
Fig. 5.7	Stress-strain and stiffness comparison.....	66
Fig. 5.8	UCS for different binders and dosages.....	68
Fig. 5.9	UCS for different binders types and dosages.....	71
Fig. 5.10	Strength of 5 % binder mixes.....	74
Fig. 5.11	Strength of 7 % binder mixes.....	74
Fig. 5.12	Strength activity index (SAI) comparison after 28 days.....	75
Fig. 5.13	Strength activity index (SAI) comparison over curing periods.....	75
Fig. 5.14	UCS and solid content over curing periods @ 5 % binder.....	76
Fig. 5.15	E and UCS relations	77
Fig. 5.16	ITS specimen preparation.....	78
Fig. 5.17	ITS testing to failure.....	78
Fig. 5.18	ITS with UCS relations.....	79
Fig. 5.19	Casting and storing 3-point samples.....	80
Fig. 5.20	3-Point loading to failure.....	81
Fig. 5.21	Strength comparison of UCS and flexural for 28 days cure.....	82
Fig. 5.22	Samples cracking with and without cable fasteners.....	83
Fig. 6.1	SEM machine Hitachi SU5000 for scanning specimen.....	86
Fig. 6.2	SEM of tailings at 5 μ m and 10 μ m scales.....	87
Fig. 6.3	Comparison of SEMs of mix 16.....	89

Fig. 6.4	Comparison of SEMs of mix 19.....	90
Fig. 6.5	Comparison of SEMs of mix 24.....	91
Fig. 6.6	Comparison of SEMs of mix 29.....	92
Fig. 6.7	Comparison of SEMs of mix 39.....	93
Fig. 6.8	TA SDT 650 (Discovery) model set up for TGA.....	95
Fig. 6.9	Specimen preparation for TGA and DTG.....	96
Fig. 6.10	TGA and DTG done on specimen of calcium hydroxide.....	97
Fig. 6.11	TGA and DTG of GFM tailings.....	98
Fig. 6.12	TGA of calcium hydroxide over curing days	100
Fig. 6.13	TGA and DTG of control mix16 and mix 21 @ 7 days cure.....	102
Fig. 6.14	TGA and DTG of control mix16 and mix 21 @ 14 days cure.....	103
Fig. 6.15	TGA and DTG of control mix16 and mix 21 @ 28 days cure.....	104
Fig. 7.1	Preparation of yield stress and viscosity measurements.....	108
Fig. 7.2	Yield stress @ varying binder and polycarboxylate dosages.....	112
Fig. 7.3	Yield stress and 56 days UCS @ 7% binder dosage.....	115
Fig. 7.4	Viscosity relations to different solid contents	116
Fig. 7.5	Viscosity relations to polycarboxylate dosage.....	117
Fig. 7.6	Viscosity relations to time at 76 % solids.....	118
Fig. 7.7	Slump test of cemented paste fill.....	119
Fig. 7.8	Polycarboxylate, slump and solid content.....	120
Fig. 7.9	Effect of polycarboxylate dosage on slump of 77 % solids.....	121
Fig. 7.10	Relation of yield stress and slump.....	122

List of Tables

Table 2.1	Chemical composition of binders	21
Table 2.2	Typical yield stress values of materials.....	35
Table 3.1	Mix with pure GPC (100 %).....	42
Table 3.2	Mix with pitchstone blend.....	42
Table 3.3	Mix with pitchstone blend continue.....	43
Table 3.4	Mix with fly ash and slag blend.....	43
Table 3.5	Example of calculated Ingredients.....	44
Table 4.1.	Summary of physical properties of tailings.....	51
Table 4.2	Chemical composition of GFM tailings.....	54
Table 5.1	UCS of mixes at varying polycarboxylate dosage.....	69
Table 7.1	Yield stress parameters.....	109
Table 7.2	Viscosity parameters.....	109
Table 7.3	Polycarboxylate dosage on rheological properties	111
Table 7.4	Solid content and yield stress range.....	113

1 Introduction

1.1 Background

Mineral commodities are extracted using either surface or underground mining methods. Surface mining involves the extraction of mineral commodity on the earth's surface and in the open air. Surface mining includes the open cast method for coal deposits, open pit (cut) method for non-stratified and massive deposits, quarry method for industrial minerals, placer methods for alluvial deposits, solution extraction for evaporites, and leaching methods.

Underground mining is the extraction of economic mineral commodity through the development of accesses well below the surface of the earth. Underground mining is categorized into unsupported methods, supported methods, caving methods, and combination methods.

Unsupported methods include the room and pillar, stope and pillar, sublevel stoping, and shrinkage stoping. An unsupported method does not utilize any backfill materials for support system, and instead it either utilizes the pillar left in place such as in room and pillar or the broken muck for wall support such as in shrinkage stoping.

Supported methods include cut and fill, stull and square set stoping where a backfill material or support system is introduced into the mined-out area to establish support for wall stability.

Caving methods include block caving, longwall caving, and sublevel caving. A caving method involves the caving of ore such as in block caving or caving of waste such as in longwall caving for coal mining.

Combination methods refer to mining methods that combine the supported and unsupported methods such as the primary-secondary transverse stoping, and Avoca methods. In a combination method, backfill materials are utilized for support.

Mine backfilling is mostly applied in underground mines that utilise either the supported methods such as the cut and fill or the combination methods such as the primary-secondary stoping, pure or modified Avoca methods of stoping, and the sublevel post fill methods. Backfilling is not required in caving and unsupported categories of underground mining methods.

When ore is extracted underground, large voids are created which are then backfilled with mined waste rocks or mill tailings to stabilise the voids prior to extracting the adjacent ore. The type of backfill material employed to stabilise the open stope walls depend on the mining method applied to extract the ore. Common backfill types are the hydraulic fill, waste rock fill, cemented rock or aggregate fill, and cemented paste fill.

In cases where no significant strength of the fill material is required, waste rock fill can be used to support the hanging walls and provide working horizon for extracting stopes above. In cases where fill material will serve other engineering purposes such as rib pillar or crown pillar, certain strength of the fill should be attained to serve as ground support. In such cases, cemented fill materials such as paste fill, or cemented aggregate fill are ideal engineered backfill materials to be utilized.

Cemented rock or aggregate fill consists of mined out or crushed rocks where binder and water are added to increase the strength. Cemented paste fill consists mill tailings, binder, and water to produce a competent fill. Small binder dosage of 3 to 7 % (by mass) is added to attain the desired strength over different curing periods.

Cemented paste fill (CPF) has been gaining popularity as a preferred fill material. CPF is a competent and effective fill material for engineering purposes such as pillar and wall support. CPF is also an environmentally friendly disposal method where the waste mill tailings are disposed back into the mined-out voids underground instead of surface disposal leaving minimum surface footprint.

The common type of binder used in paste filling is General Purpose Cement (GPC). Although binder is an integral component in paste filling to increase strength, it accounts for 75 to 80 % of backfilling cost (Belem et al., 2008; Panchal et al., 2018). Minimising cost and optimising backfilling are essential for the survival of mines during periods of low commodity prices. Pozzolanic binders are becoming popular and waste by products such as fly ash and slag have been widely used as supplementary cementitious materials (SCMs) to partially replace cement and reduce the cost of binder.

Paste plant is constructed on the surface to produce cemented paste fill which are pumped over longer distances. With high solid content (70 to 80 %), changing rheological properties, and hydration process, the reticulation lines can be potentially blocked (Panchal et al., 2018). To mitigate pipe blockages, admixtures have been widely used to improve the flowability of the CPF along longer distances.

Admixtures are used to alter the physical and chemical state of the mix during the slurry transportation, setting, and hardening stages of the hydration process. Admixtures are grouped according to their physical adsorption properties as accelerators, retarders, or water reducers (plasticizers). The benefits of admixtures include reducing water requirement, increasing workability, control setting, increase strength, prevent sulphide attack, and attain long term durability. The most common admixture used for improving the workability of paste filling is polycarboxylate plasticizer. Polycarboxylate also reduces water requirement at high solid content and thus improves the mechanical strength of the cemented paste fill.

Cemented paste fill is becoming a popular back fill type. Significant advances have been made in researches into using pozzolanic products as partial cement replacement in the quest to reduce cement usage and using admixtures to improve workability. The main aim of most of the studies are to optimize paste filling so to achieve a cost savings paste fill mix that still maintains the strength and flow properties.

1.2 Research significance

This research focuses on the mix designs of cemented paste fill (CPF), one of the most popular backfill types that use mill tailings. Tailings are mixed with binder and placed in voids as slurry transported through pipelines. Tailings have substantial clay content and a small dosage of cement binder (3 to 7 %) is added to increase the strength. Even this small cement dosage adds significantly to the cost of backfill operation. CPF is a major cost driver and accounts for 10 to 20 % of mine operating cost, while cement binder accounts for up to 75 % of filling cost (Belem et al., 2008; Xu et al., 2018). CPF is expensive compared to other types of backfills and requires a more cost saving approach to be continually used for wall support and establishing working level.

CPF slurry requires high water content (30 to 40 % of solid mass) to prevent blockages along pipelines. Strength development of CPF is slower at low cement dosage (< 4 %) and at high-water content. Liquefaction can occur when the UCS of CPF is less than 100 kPa during adjacent stope blasting (Belem et al., 2008). In addition, the production of clinker cement during limestone (CaCO_3) calcination is energy intensive and emits 650 to 900 kg of greenhouse gas (CO_2) per tonne of cement (Schneider et al., 2011). Approximately 5 % of CO_2 emissions are from cement industry and expected to increase into the future (Barcelo et al., 2014).

These challenges have prompted research into the application of pozzolans and admixtures to minimise the usage of clinker cement and water and still attain the desired strength and rheology of CPF for mine backfilling. Therefore, this research intends to use fly ash, slag, and pitchstone to partially replace cement binder that can result in significant cost savings, and make backfilling more environmentally friendly. Admixture polycarboxylate plasticizer is used in this study to enhance the slurry workability. Common pozzolans like slag and fly ash have been widely researched and used in the industries. While natural pozzolans like pitchstone have been studied in concrete application (Tuladhar

et al., 2018) and its viability for usage in mine backfilling remains a promising area for further investigation in this research.

1.3 Objectives of research

The research is centred on slurry rheology, hydration reaction, microstructure evolution, and strength development of cemented paste fill. The overall outcome of this research is to optimise the cemented paste fill (CPF) mixture trialling different binders, at different dosages, at different solid contents, and using plasticizer at different dosages, to achieve the desired workability and strength. The ingredients used in the study are blends of fly ash, slag, and pitchstone fines, with Portland cement as binders, polycarboxylate plasticizer as admixture, mill waste tailings (< 4.75 mm) from George Fisher Mine and tap water.

The five main objectives of this thesis are:

- To determine the physical, chemical, and mineralogical properties of the tailings, binder, and admixture used in the mix.
- To measure and compare the compressive strength (UCS), indirect tensile strength (ITS), and flexural strength of the hardened CPF cast from various mix over different curing days.
- To measure and compare the changes in the rheological properties of CPF slurry of various dosages of binder and plasticizer.
- To measure the heat and mass change of the CPF over different curing periods to determine the amount of portlandite present during the hydration and hardening process.
- To observe the microstructure and morphology of the CPF over different curing periods to determine the growth of hydration products.

The anticipated outcomes of this research are:

- To reduce cement usage with the partial replacement of clinker cement with pozzolans like slag, fly ash, and pitchstone fines, whilst maintaining strength.
- To minimise the operational cost associated with clinker cement usage with the use of pozzolans.
- To reduce the water usage and improve slurry flow with the usage of the admixture polycarboxylate plasticizer.
- To increase the solid content in the slurry with the use of polycarboxylate plasticizer, whilst maintaining optimal rheological properties.

2 Review of literature

2.1 Underground mining methods

There are four (4) different categories of underground mining methods and they are the supported methods, the unsupported methods, the caving methods, and the combination or variation methods. Supported methods utilise waste rocks, mill tailings, and timber sets to stabilise the open stope prior to extracting the adjacent ore. Unsupported methods utilise the broken ore and the pillars within the orebody to stabilise the open stope prior to extracting adjacent ore. Caving methods induce the subsidence of either ore or waste in the extraction process. No support is required in caving method due to retreat mining and subsidence. Combination methods combine either the supported, unsupported, or caving methods to form a variation to the stope extraction sequence.

2.1.1 Unsupported methods

Underground unsupported methods include room and pillar, stope and pillar, sublevel stoping, and shrinkage stoping. Room and pillar is applied on coal deposits, where part of the coal is left behind as pillar for support and part of the coal is mined out and is referred to as room (Fig. 2.1). Stope and pillar is applied on flat orebody in hard rock where portion of the orebody with the low grade are left behind as pillars for support. Sublevel stoping is applied on near vertical orebody in hard rock where predetermined pillars are left throughout the strike length of the orebody for wall support. Shrinkage stoping is applied on narrow and near vertical orebody where the blasted and broken ore are used for wall support as the mining front advances upwards. These methods are categorised as unsupported methods as they utilise the pillars and broken ore within the orebody for support and no foreign or outside materials are being introduced into the open stope for ground support.

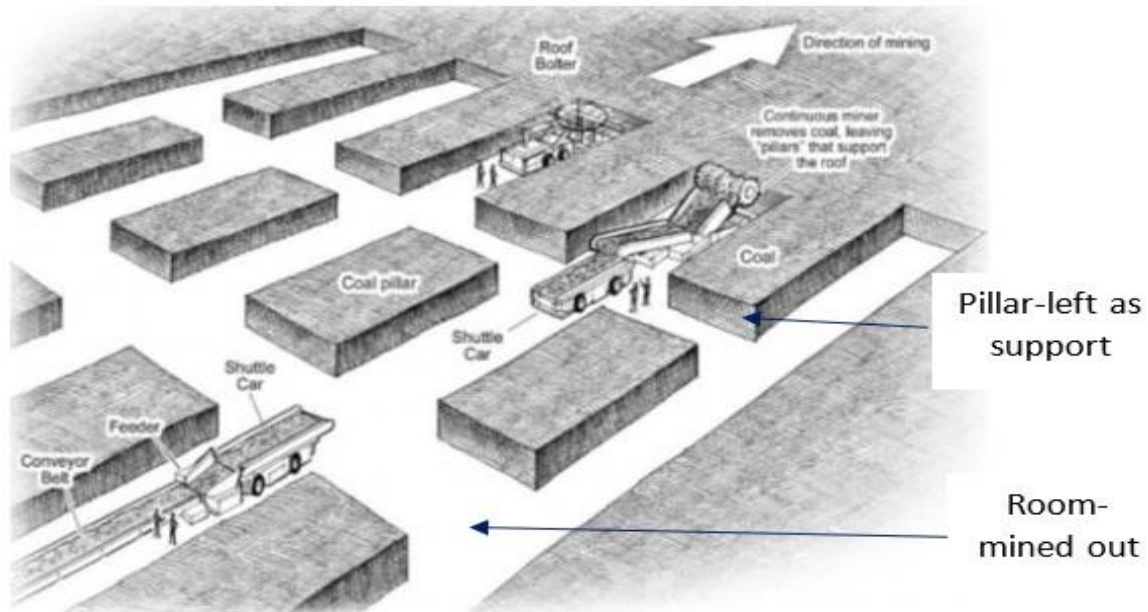


Fig. 2.1 Room and pillar method in coal (source: marketrealist.com)

2.1.2 Supported methods

Underground supported methods include cut and fill, stull and square set methods. Cut and fill is applied on narrow ore body in hard rock where the ore is mined in horizontal slices and backfill materials such as waste rock or mill tailings are introduced into the void for support (Fig. 2.2). Cut and fill can be either over-hand or under-hand depending on the direction of mining. For an under-hand cut and fill method, the ore is mined and backfilled with paste fill, and the next horizontal slice is mined under the paste fill. For an over-hand cut and fill method, the ore is mined, backfilled with either paste fill or waste rock, and the next horizontal slice is mined above the backfill placed. Stull and square set methods utilise timbers to install in the open void for support. These methods are categorised as supported as they utilise foreign materials outside the orebody for support.

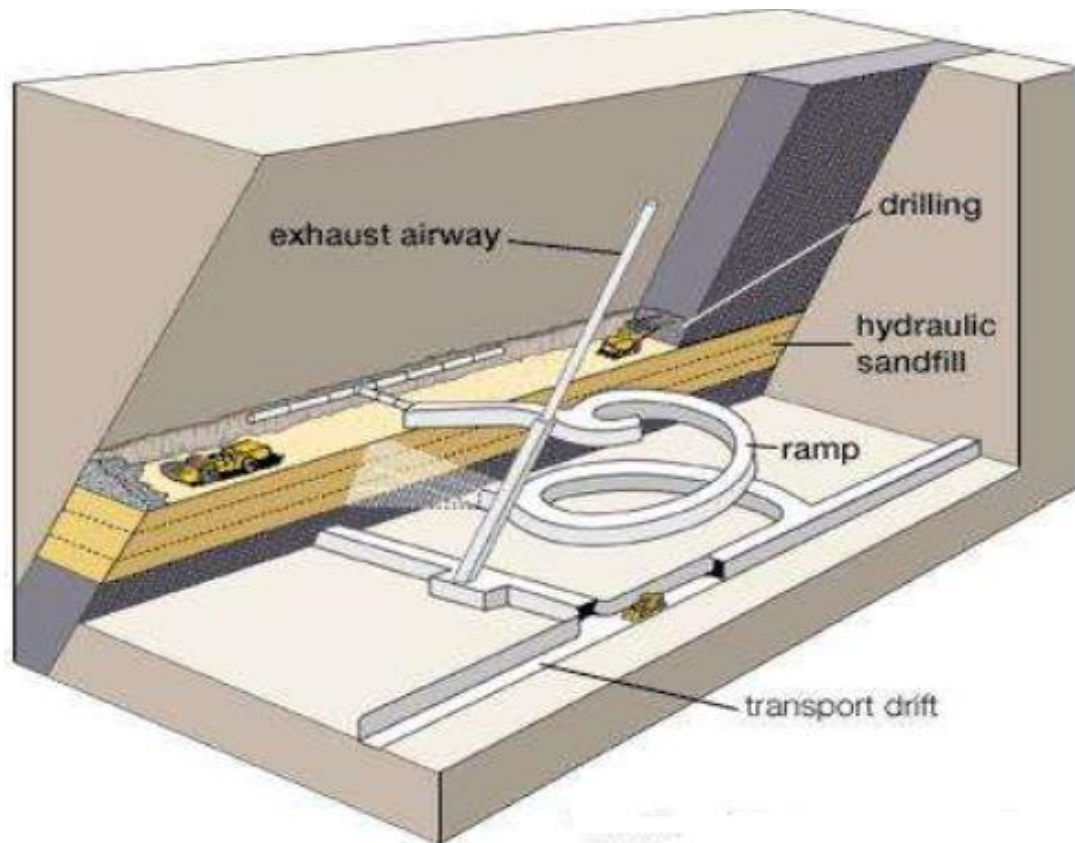


Fig. 2.2 Over-hand cut and fill method (source: cdn.britannica.com)

2.1.3 Caving methods

Underground caving methods include block caving, longwall caving, and sublevel caving. Block caving is applied on massive hard rock deposits where undercut is initiated, and vertical column of ore is drawn down through subsidence (Fig. 2.3). Longwall caving is applied on coal deposit where extraction of coal advances and the waste overburden caves into the mined-out voids as mining progresses. Sublevel caving is applied on near vertical orebody where the ore is mined through drill and blast and the waste wall caves into the mined-out void. These methods are categorised as caving as either waste or ore caves as mining progresses and besides, no materials are introduced into the stope for support.

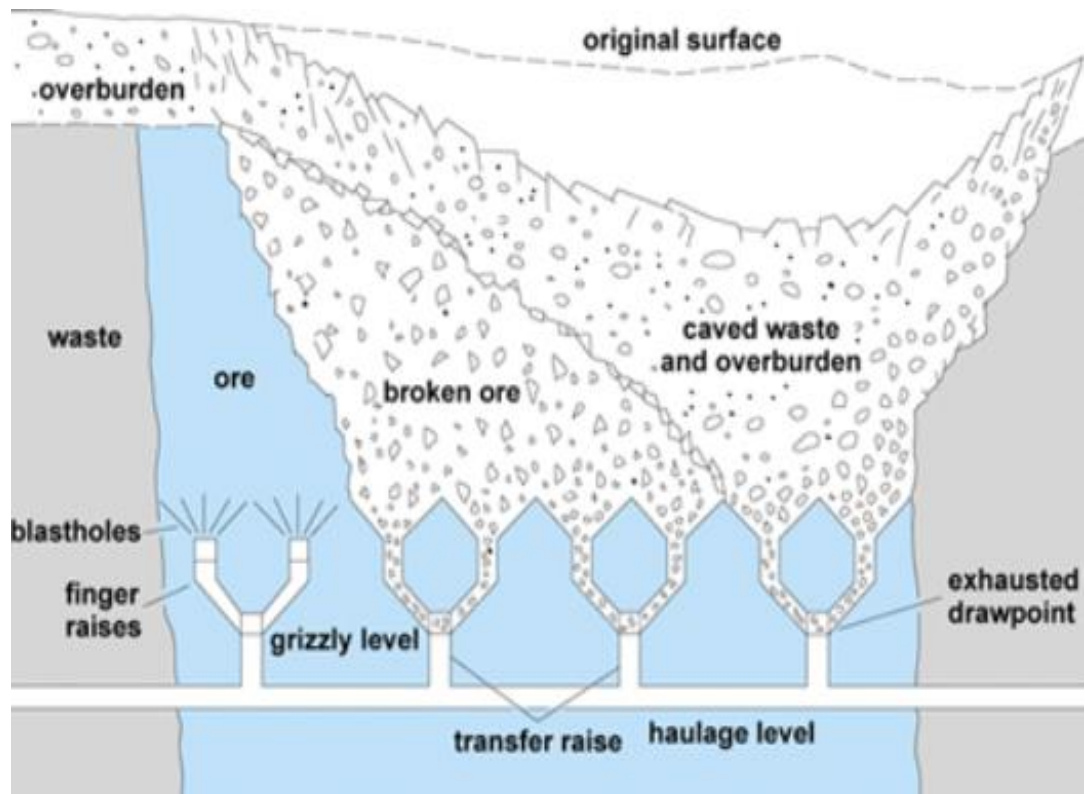


Fig. 2.3 Block caving method in massive hard rock (source: docplayer.net)

2.1.4 Combination methods

Underground combinations methods are many and the popular ones include primary-secondary, sublevel-post-fill, and Avoca methods. Primary-secondary transverse method combines the sublevel stoping method (unsupported) with backfilling (support) which replaces the need for rib pillars along the strike of orebody (Fig. 2.4). Primary-secondary stoping is applied on wide orebody in hard rock where the primary stopes are mined first and filled with competent fill and the secondary stopes are mined afterwards in a transverse mining direction (perpendicular to strike of orebody). The common competent fill materials are cemented paste fill (CPF), cemented aggregate fill (CAF), and cemented waste rockfill (CRF). The fill materials provide support and stability while the adjacent secondary stopes are mined out. The void from the secondary stopes can be left open or is usually filled with blasted rocks from waste developments. Like the primary-secondary method, the sublevel-post-

fill method combines the sublevel stoping (unsupported) with backfilling (support) which replaces the need for rib pillars and the mining direction is along the strike of the orebody (parallel to strike of orebody). Avoca method combines sublevel stoping (unsupported) with backfilling (support). Avoca method (Fig. 2.5) uses only the waste rock fill for support and uses no other fill materials like CRF, CAF, and CPF. The primary-secondary transverse method, sublevel-post-fill method, and Avoca method combine support with unsupported methods and are categorised as combination or variation methods.



Fig. 2.4 Primary-secondary transverse in bulk hard rock (source: sec.gov)

2.2 Underground backfill types

The main purpose of using backfill in underground methods is to fill the mined-out voids to provide support and stability prior to extracting the adjacent stopes. Backfill materials can be either cemented or uncemented waste from mining and milling operations. Common backfill materials utilised in underground mines are the waste rock fill (WRF), cemented rock fill (CRF),

cemented aggregate fill (CAF), cemented paste fill (CPF), hydraulic fill (HF), and cemented hydraulic fill (CHF).

Waste rock fill is the least expensive fill material compared to the other fill types. The broken waste rock from development blasting is used for filling the stope void. Loader and trucks are used to load, haul, and dump the rock fill into the open stope. With rock fill, no major service or infrastructure installation are required prior to filling, only requirements are tipping bund-wall and couple of lightings for visibility. Rock fill is used in mining methods like pure Avoca (Fig. 2.5) and cut and fill (Fig. 2.2). Waste rock fill is also used in primary-secondary transverse to backfill the secondary stope voids.

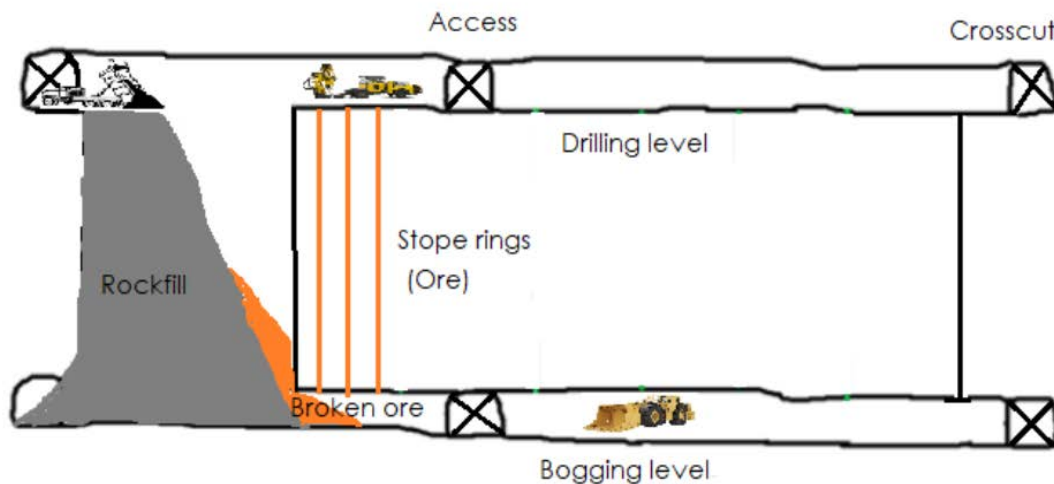


Fig. 2.5 Long section view of pure Avoca method using rockfill

With cemented rock fill (CRF), binder slurry is added to the blasted rocks from the waste developments. Water is added to cement and the paste is added to waste rocks and mixed prior to dumping into the stope voids. Agitator trucks are used to pour cement slurry onto the pile of broken rocks and a loader is used to mix the cement with the pile of rocks through heaving and tipping actions. The mix is loaded into a truck and dumped into the open stope. CRF is competent compare to rockfill due to the use of binder. CRF is used in filling the primary stope in a sublevel transverse method and cut and fill method.

Cemented aggregate fill (CAF) is produced by adding cement paste to crushed aggregates. The aggregates are crushed using crusher to pre-determined sizes such as 45 mm or 75 mm diameter. The cement paste is sprayed into the aggregates as the aggregates fall from the chutes loading the trucks. The CAF is transported using trucks and dumped in stope voids. CAF is used in cut and fill and primary-secondary where the primary stopes are filled with CAF.

Hydraulic fill uses mill waste tailings where the fine particles are deslimed prior to placement in the open stopes. Deslime is done using hydrocyclone process where clay is removed from the tailings so that water can easily drain out of the tailings through porous bulk heads. The tailings are transported via pipeline and placed in underground mined-out voids. When cement is added to the hydraulic fill, it improves the binding strength and the fill is referred to as cemented hydraulic fill.

Like hydraulic fill, cemented paste fill (Fig. 2.6) uses mill tailings and binder. However, the tailings used are not deslimed, as the fines are necessary to retain water and aid in the flowability of the paste slurry along long distance pipelines. Cemented paste fill is produced at a surface paste plant by mixing the mill tailings with water, binder, admixtures and is then transported through reticulation lines and disposed into mined out stopes.



Fig. 2.6 Paste fill discharge (source: benp.com)

2.3 Cemented paste fill

Processing of ore to recover the valuable metal leaves large quantity of waste tailings that must be safely disposed. Cemented paste filling is a popular disposal of mill tailings. Cemented paste fill (CPF) is becoming a popular backfill material in recent years due to the quick turnover from stopes as well as an effective method of disposing waste safely in underground voids. Cemented paste fill is designed to withstand liquefaction and maintain strength requirements (Grice, 1998). Cemented paste fill slurry (Fig. 2.7) is produced using mill tailings which usually contain solids ranging from 70 to 85 % (Fall et al., 2005), cement binder dosage of 3 to 7 %, water content of 15 to 30 %, and minimum dosage of admixtures to improve flow and hydration.

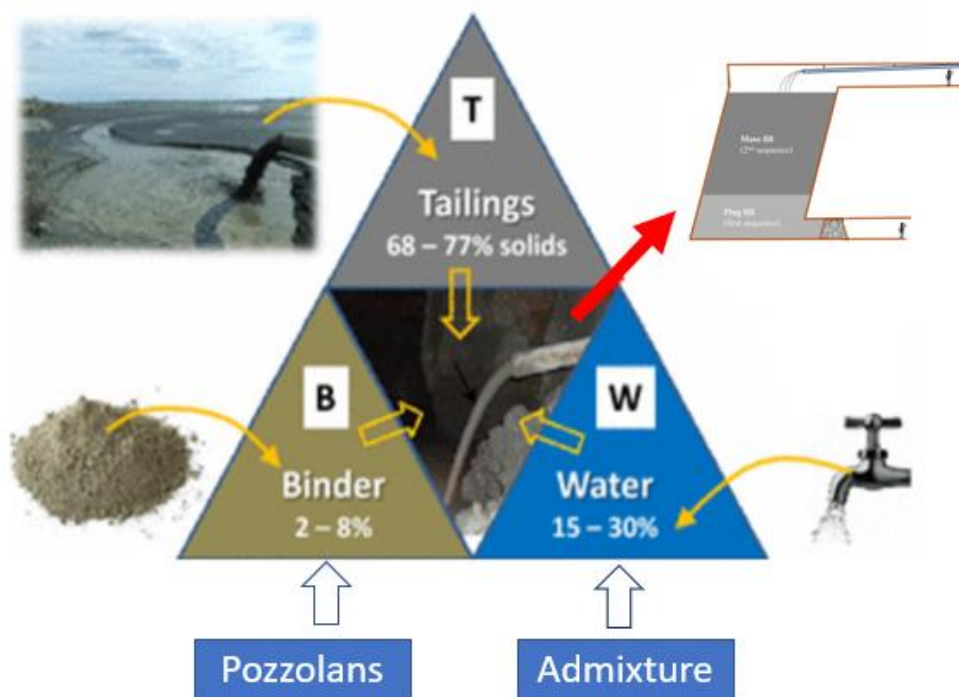


Fig. 2.7 Ingredients for cemented paste fill slurry production (modified from Belem et al., 2016)

Cemented paste fill is used in underground mines that apply cut and fill, sublevel-post-fill, and primary-secondary transverse methods where the

primary stope voids are filled with cemented paste fill. Comparing the other fill types, cemented paste fill is a competent fill material and has several advantages as a preferred mine fill material. Strength development of cemented paste fill is usually less variable and the strength integrity is maintained throughout the fill mass. Cemented paste fill transported via reticulation lines in the form of a slurry is efficient and can achieve higher rate of filling. Cemented paste fill cures and attains the desired strength within 7 to 28 days depending on the cement dosage and the adjacent stopes can be mined sooner.

Quick turnover period of stopes result in increased revenue and reduced operational cost. Cemented paste fill is disposed directly into mined voids which minimises surface footprints and environmental impacts. Cemented paste fill effectively contains within its matrix the toxic waste matter in tailings like arsenic and heavy metals. Cemented paste fill is regarded as green mining approach in the 21st century (Wu et al., 2016) and contributes to mine stability, production efficiency, mine safety, and environmental protection.

While cemented paste fill finds increasing application in underground mines, there are associated engineering and operational challenges. The construction of paste plant infrastructure is a major capital expenditure. Maintaining and operating the paste infrastructure can be costly with issues of barricade failure, pressure loss, reticulation line blockage, poor paste quality, excessive water usage, increased cement usage, and increased cement cost. Cemented paste fill is expensive and requires a more cost savings approach for its use in wall support and establishing working level (Belem et al., 2008).

Portland (clinker) cement is a widely used binder and a major operational cost driver. Cemented paste fill cost accounts for 10 to 20 % of mine operating cost with binder cost up to 75 % of filling cost (Belem et al., 2008; Xu et al., 2018). Portland cement dosage usually ranges from 3 to 7 % of dry solid mass. When the binder dosage is low (< 3 %), the cemented paste fill does not quickly attain the desired strength (> 100 kPa) for any adjacent stope blasting where

liquefaction of cemented paste fill can occur (Belem et al., 2008). When the binder dosage is high (> 4 %), the desired strength is reached within curing times (7 to 28 days) at a high cement cost.

The production of clinker cement from the decomposition of limestone (CaCO_3) emits greenhouse gas. Calcination process to produce a tonne of clinker cement emits 650 to 900 kg of CO_2 with 40 % component from fossil fuel (Schneider et al., 2011). Water consumption is high in cemented paste fill production and can range from 20 to 40 % of total mass of solids. High water content improves flow of slurry, however, the water to cement ratio increases and the strength development is slower. Furthermore, the increased water content reduces the solid content and results in low disposal rate of tailings. Low water content increases the strength of the cemented paste fill, but the workability becomes poor and line blockage can occur when CPF is transported over long distances.

These associated challenges with cemented paste fill have prompted the use of pozzolans and admixtures. Pozzolans are used to partial replace clinker cement to minimise binder cost, while admixtures are used to improve the flowability of slurry over long distance. Use of pozzolans and admixtures also improve the strength of the CPF over longer curing periods.

2.3.1 Mill tailings

Mill tailings are waste materials that are produced from ore processing plant. Tailings when uncemented, can be directly pumped through reticulation lines and disposed into underground void filling such as hydraulic filling applied in cut and fill method. Tailings when cemented become paste fill and are applied in filling underground voids in methods like cut and fill, sublevel-post-fill, and primary-secondary transverse stoping.

Tailings when used in paste fill shall contain adequate fines that can provide a larger surface area to retain water for lubrication and ease of slurry flow along

the reticulation lines (Sivakugan et al., 2006). A comprehensive study was done and the grain size distribution of tailings for hydraulic and paste filling in Australia mines were plotted as shown below (Fig. 2.8).

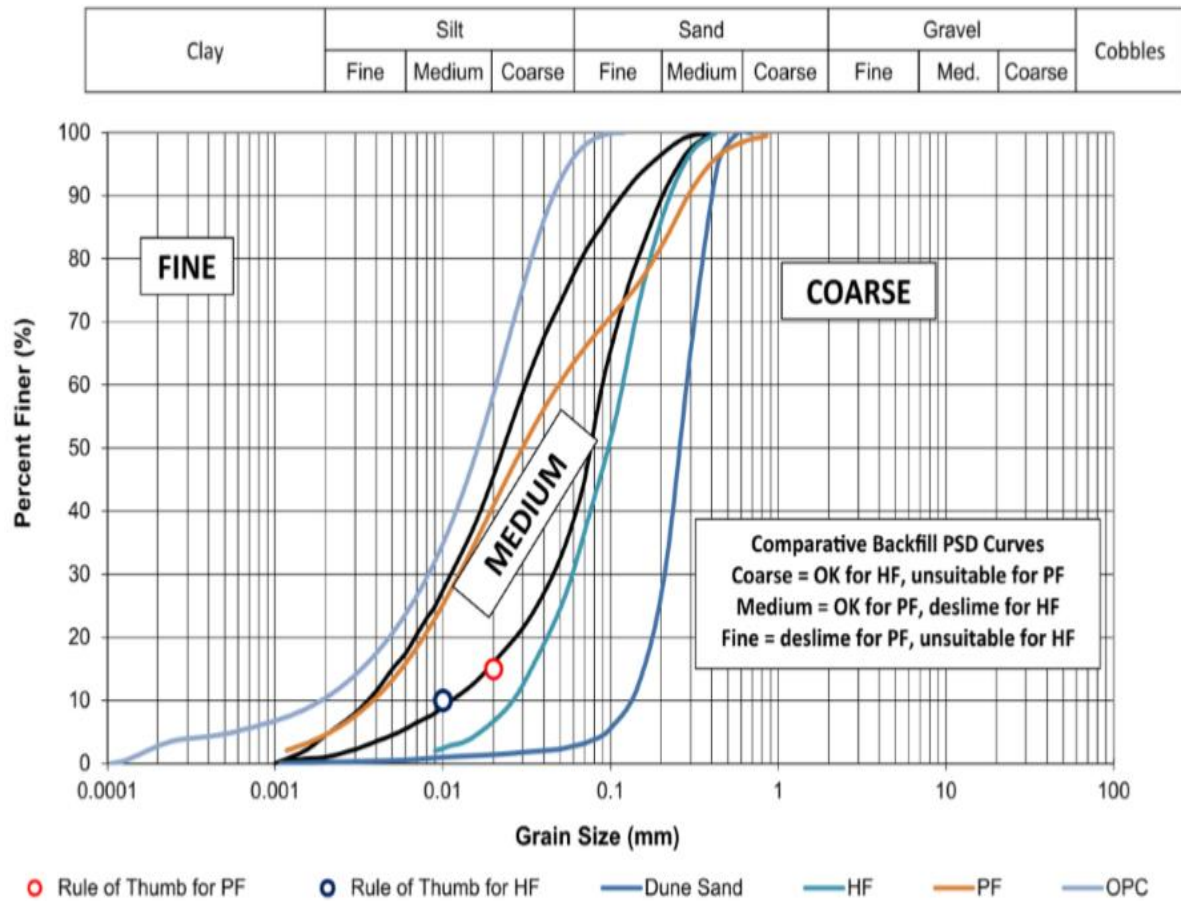


Fig. 2.8 Particle size distribution of tailings for hydraulic and paste fills (Sivakugan et al., 2015)

The mass fraction (%) of the fines less than 20 μm shall make up a minimum of 15% of the tailing mass as a rule of thumb to be used in CPF (Sivakugan et al., 2006; Kuganathan, 2005). The uniformity coefficient, curvature coefficient, and the mass fraction (%) of fines less than 20 μm are determined from grading curve. The fines (< 20 μm) have a larger surface area that allows water absorption and retention which aids flow, prevents settlement and segregation of particles along pipelines (Deng et al., 2018). Excessive fines can consume higher cement (Henderson & Revell, 2005).

The uniformity coefficient (C_u) measures the spread of the particles and is expressed as the quotient of grain size diameter at 60 % passing (D_{60}) to 10 % passing (D_{10}) and the values are obtained from the grain size distribution curve. Larger C_u (10 to 20) represents a well graded tailing and the requirement of binder is low to achieve the desired strength while a lower C_u (5 to 10) contains lesser spread in grain sizes and binder requirement is higher to attain the similar desired strength due to the presence of large voids (Kuganathan, 2005).

Tailing properties differ for each mine and thus particle size distribution is important for CPF design to attain desired strength with minimal binder. Tailings containing 35 to 55 % of fines < 20 μm gain strength slower and require tailings to contain coarse to medium sizes for improvement in the strength (Fall et al., 2005). Deslimed tailings with fines content ranging from 15 to 30 % produced higher strengths than tailings which contained fines greater than 50 % (Kesimal et al., 2003). Well graded tailings contain particles of various grain sizes that combine to reduce void and attain a CPF of high density and strength (Henderson & Revell, 2005).

2.3.2 Paste plant and reticulation

Cemented paste fill is produced at the surface paste plant by mixing the mill tailings with water, binder, admixtures and is then transported through reticulation lines and disposed into mined out stopes. Positive displacement pumps are used to force slurry through steel pipelines over longer distances. Vertical holes up to 200 mm diameter are drilled out to run paste reticulation between levels in underground to shorten the reticulation distance and save cost and resources.

Paste plant is a major capital investment in mines that use paste filling and the operational cost ranges from 20 to 30 % of the mine operational cost (Belem et al., 2008). Thus, operation of the paste plant and paste filling activities are managed by a dedicated team of technicians, operators, and engineers. Any paste plant downtime due to issues of pipeline blockage, paste wall leakage,

and electrical or mechanical faults with pumps, can have a costly impact on the stope production schedule and revenue of the mine.

2.3.3 Filling sequence

Paste filling of a stope void is usually done in stages. The Initial pour after the wall construction is referred to as plug pour and usually fills past 5 m from the backs of the drive (Fig. 2.9). The plug pour usually cures for 24 hours and the main pour commences and fills the remaining stope void. The main reason for a plug pour is to minimise the amount of slurry exerting the lateral pressure on the paste wall. Continuous paste filling can exert excessive pressure on the paste walls and in a worst-case scenario, the wall can fail and paste can overflow into the underground drives and workings.

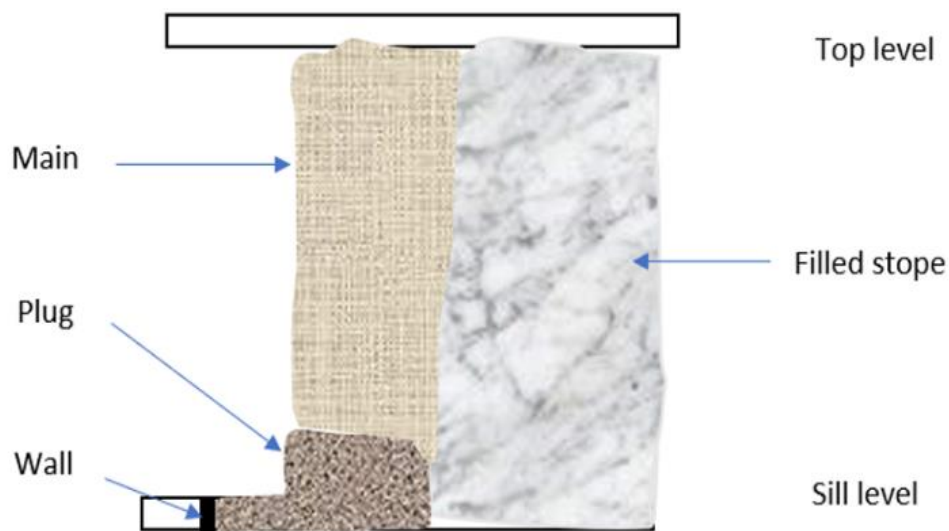


Fig. 2.9 Long section of paste fill pour sequence of a single lift stope

2.3.4 Curing periods

Cemented paste fill (CPF) must be allowed to cure in order to attain the desired unconfined compressive strength (UCS) value prior to blasting the adjacent stopes. Curing periods are usually expressed in weeks. Curing periods

of 7 to 14 days are regarded as early curing periods, 21 to 28 days as normal curing periods, while 56 days and beyond are regarded as long-term curing periods.

Most mines that use paste fill have dedicated paste fill engineers that design the ingredients of the paste mix to attain the required strength over curing periods. When a stope is scheduled to be brought forward quickly, usually the cement dosage applied is higher (6 to 7 %) to allow shorter curing period to achieve the required strength. Although the backfilling cost goes up with the increase in binder dosage, the stope turnover is quicker to get the production going according to the production schedule.

There are different strength limits that paste filling is designed and targeted to achieve over the curing periods. A minimum UCS target of 100 kPa is maintained to prevent liquefaction from blasting and UCS value of 1MPa is considered as competent for ground support. The strength requirements of paste fill is further discussed in section 2.8.1.

2.4 Binders

Binders are used in mine filling to produce a more competent back fill material that can provide support. Binder dosage has a proportional impact on the strength of the paste fill and the cost of filling (Nasir & Fall, 2010). The common binders are the general-purpose cement (GPC) and supplementary cementitious materials (SCMs).

Supplementary cementitious materials (SCMs) or pozzolans are usually blended with the GPC mainly for cost cutting measures as GPC is an expensive binder and accounts for up to 75 % of filling cost (Belem et al., 2008; Xu et al., 2018). Application of common pozzolanic materials such as fly ash and slag have been widely studied in mining and concrete industries. Pozzolans have increased the long-term strength development as well as contributed to the reduction in cement production and that has significant impact on reduction of CO₂ emissions from the calcination process of clinker production.

Binders are usually grounded to very fine powder for larger surface area for effective hydration reaction. Most binders are less than 150 microns. Common oxides in binder and pozzolanic materials are calcium oxide (CaO) or lime, silica (SiO₂), aluminium oxide (Al₂O₃) and iron oxide (Fe₂O₃), with lesser amount of other metal oxides. The Table 2.1 below shows the chemical composition for the oxides present in each binder and the abbreviation PF refers to pitchstone fines.

Table 2.1 Chemical composition of binders

Chemical composition	GPC	Fly ash	Slag	PF	Slag(60%)+GPC(40%)
CaO (%)	63.9	3.5	41.3	0.9	49.6
SiO ₂ (%)	19.2	48.1	35.2	68.53	29
Al ₂ O ₃ (%)	5	26.7	14.5	12.94	10.4
Fe ₂ O ₃ (%)	3.2	15.2	0.3	1.04	1.4
SO ₃ (%)	2.4	0.1	1.09	-	2.3
MgO (%)	1.1	1.4	5	0.02	4.2
Na ₂ O (%)	0.4	0.6	0.21	4.51	0.4
K ₂ O (%)	-	-	-	2.58	-

(Values sourced from Niroshan et al., 2017 & Vessala et al., 2009)

2.4.1 General purpose cement

General purpose cement (GPC) is the most common binder that is used in mine fills. Cemented fills such as cemented rock fill, cemented aggregate fill, cemented hydraulic fill, and cemented paste fill use GPC. General purpose cement is made from the calcination process of limestone with addition of ingredients such as iron oxide, aluminium oxide, silica, and gypsum to improve the performance. The clinker granules from the calcination grounded with the additives to produce very fine solids. The fines are angular as observed from the different magnifications of the scanning electron micrograph (Fig. 2.10) below.

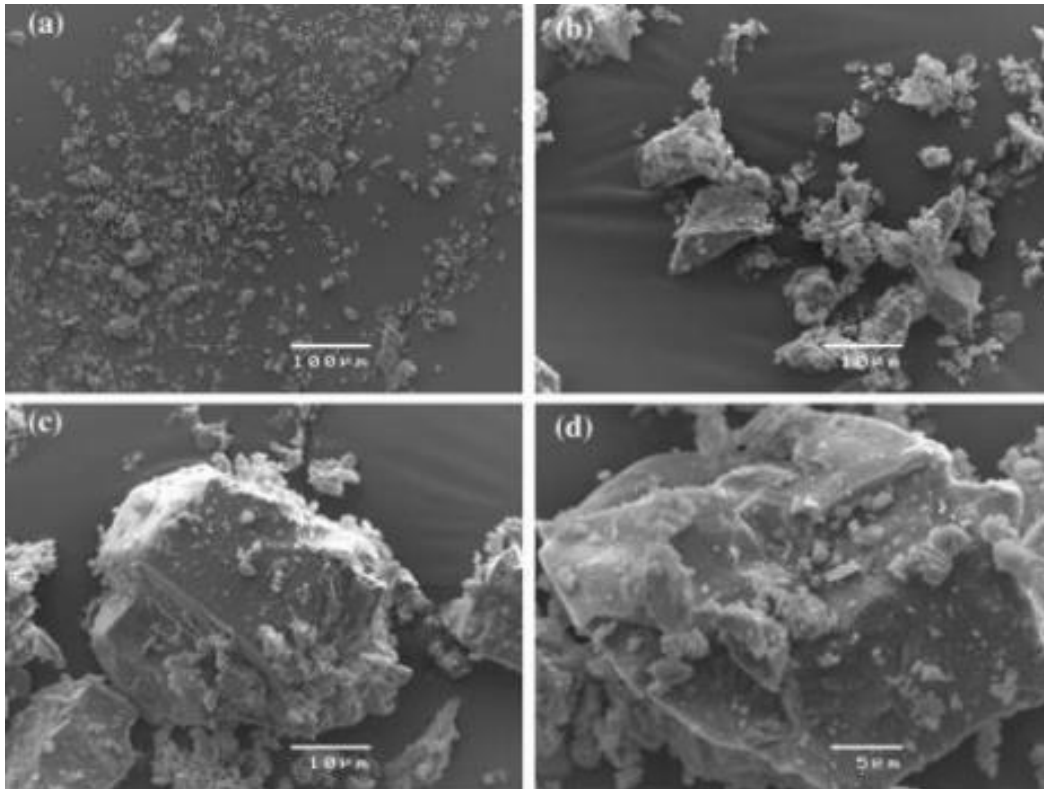


Fig. 2.10 SEM of general-purpose cement (Niroshan et al., 2018)

2.4.2 Supplementary cementitious materials

Pozzolans are low cost supplementary cementitious materials (SCMs) that are blended with clinker cement to reduce cement usage. Pozzolans consist amorphous silica mineral that react with calcium hydroxide during the hydration process to form calcium silicates (Walker & Pavia, 2011). Pozzolans are milled to fines to produce higher surface and can increase the reactivity of pozzolans. The pozzolan in concrete reduces permeability, reduces heat of hydration, reduces sulphate attack, and attains higher strength at later ages (ACI, 2001; Berodier et al., 2018).

Pozzolan to cement ratio can vary and is dependent on the reactivity of the pozzolan to attain a comparable strength compared to the control mix. Strength activity index (SAI) is a measure of reactivity of pozzolan with cement and varies with the amount of cement and pozzolan used. SAI is defined as the UCS of pozzolanic mix relative to the control mix over the same curing period and is expressed as percentage. ASTM C618 requires that pozzolanic

materials must attain SAI above 75 % of control mix within 7 to 28 days curing periods in order to be used as pozzolans.

2.4.3 Fly ash

Fly ash is a waste product from coal burning and is commonly used as a pozzolan in concrete production. The chemical composition of fly ash can be low or high in calcium. The low calcium fly ash is from burning anthracite or bituminous coal and the high calcium fly ash is from burning lignite or sub-bituminous coal (Nochaiya et al., 2010).

An increase in the fly ash content reduces the reactivity of the pozzolans. Usually, fly ash can replace cement up to 15 to 25 % to attain a higher long-term strength, however, at a higher content of fly ash (45 to 55 %), the reactivity decreases and the strength is not comparable to the control mix of 100 % GPC (Wang & Park, 2015).

Fly ash is blended with Portland cement in various ratios for use. The fines are rounded as seen from the SEM (Fig. 2.11) below.

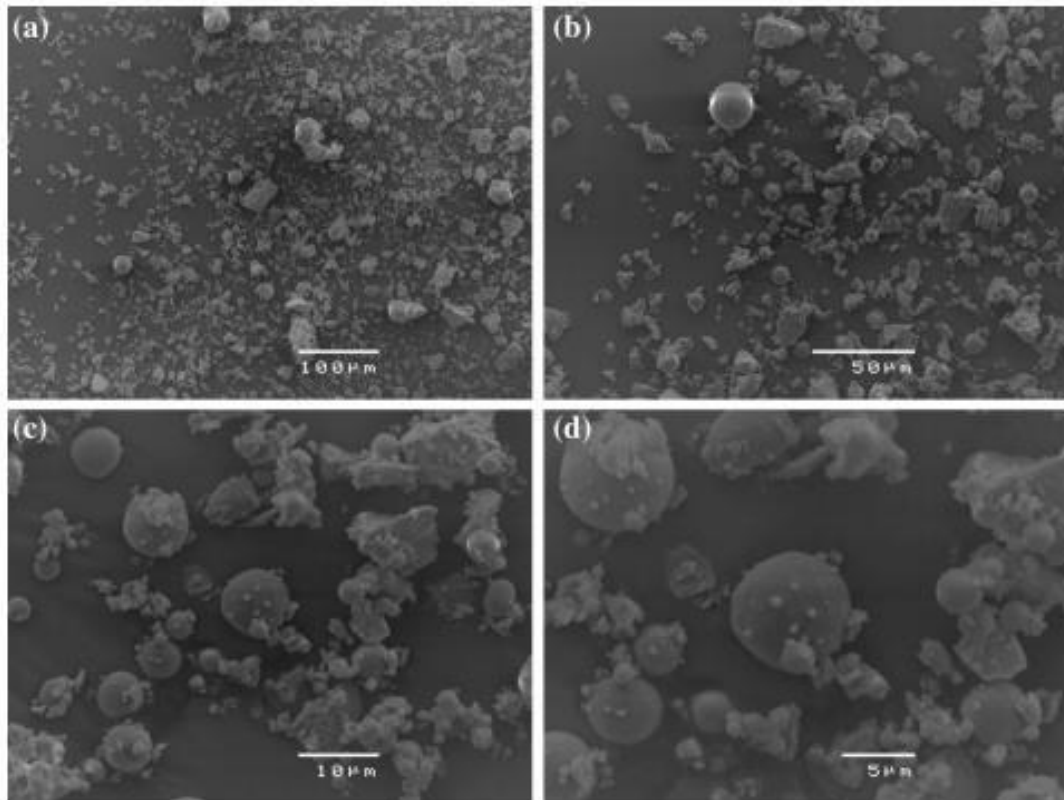


Fig. 2.11 SEM of fly ash (Niroshan et al., 2018)

2.4.4 Slag

Slag has several grades as per the ASTM C989 and ACI 233R-03 such as the grade 120, 100 and 80. The reactivity of slag with cement varies with the grade of slag and in most cases with the increase dosage of slag, the early strength (1 to 7 days curing) reduces. The long-term strength increases due to the pozzolanic reactions of the portlandite with the slag (Bougara et al., 2018). According to Niroshan et al. (2017), the slag in cement gives lower strength during early curing periods (7 to 14 days), however, the reactivity of slag can be further increased in the presence of alkaline activators. According to Pirapakaran et al. (2007), slag blend (70 % slag and 30 % GPC) produced higher strength compared to 100 % GPC and fly ash blend (25 % cement replacement).

2.4.5 Natural pozzolans

Natural pozzolans are volcanic rocks like pitchstone, obsidian, pumice, tuff, basalt, and zeolite that contain reactive silica. When the volcanic rocks are grounded to fines, they react when in contact with water. Literatures have documented the use of many of these natural pozzolans in construction which improved the long-term strength.

Natural basaltic ash from Saudi Arabia was used to replace cement up to 30 % of Portland cement that produced UCS value of 39 MPa after 28 days curing and increased further to 57 MPa after one-year curing period (Celik et al., 2014). Pitchstone fines were studied in concrete application, and a replacement of Portland cement of 10 to 20 % indicated comparable strength to control mix (Tuladhar et al., 2011). Volcanic tuff from Jordan were used to replace Portland cement from 10 to 20 % which attained higher compressive strength to the control mix after 56 to 90 days (Ababneh et al., 2018). Volcanic scoria from Cameroon was used to replace Portland cement from 25 to 45 % to determine its influence on the rheological properties and the results indicated a decrease in the yield stress as the pozzolan dosage increases (Juimo Tchamdjou, 2017).

Natural pozzolanic materials behave like the industrialised waste products such as fly ash and slag. The common attribute for pozzolans is their influence on the long-term strength development when replacing cement up to 30 %.

2.4.6 Pitchstone fines

Pitchstone and obsidian when crushed and hydrated form perlite, which has several industrial applications. Pitchstone fines as by-product from the perlite production has pozzolanic properties indicated by the reduction in calcium hydroxide content over time when blended with Portland cement (Vessalas et al., 2007). The reactivity of pitchstone fines and strength development is comparable to other SCMs like fly ash over 28 days cure (Ray et al., 2007).

Tuladhar et al. (2011) studied pitchstone fines for application in concrete that attained a comparable strength (> 30 MPa) at 10 to 20 % replacement of cement after 28 days at a binder content of 12.66 % as shown (Fig. 2.12) below.

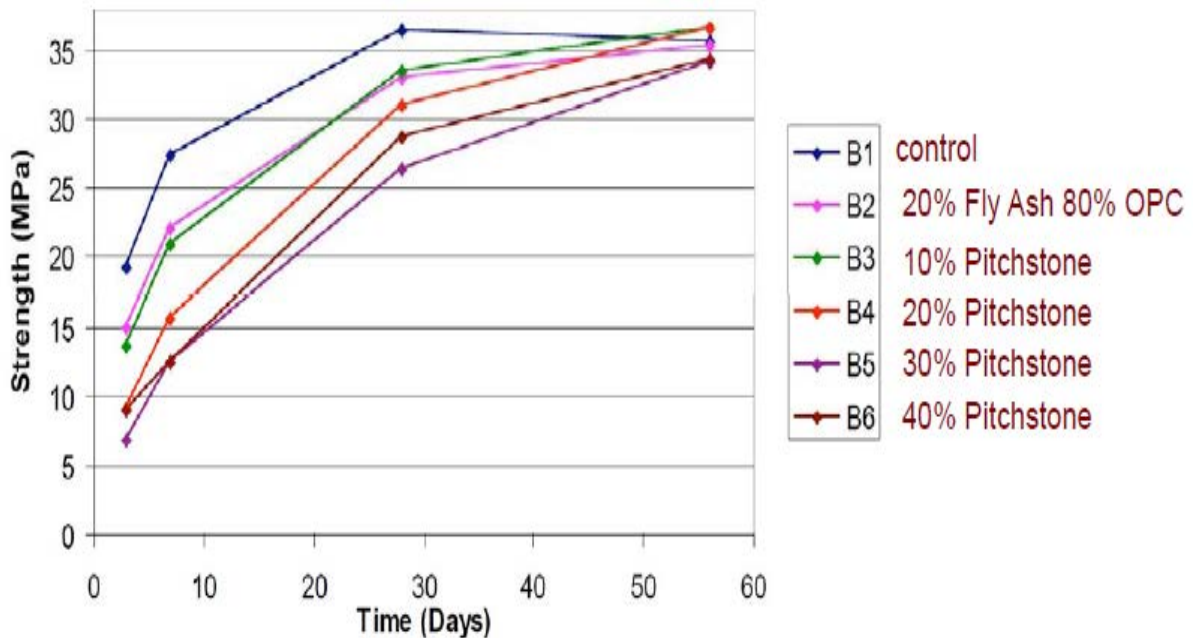


Fig. 2.12 UCS of Pitchstone fines replacement (Tuladhar et al., 2011)

Slow reaction of pitchstone fines form calcium silicate crystals that occupy space, reduce permeability, and increase strength (Tuladhar et al., 2013). Several studies on the application of pitchstone fines as a partial cement replacement in the concrete production showed promising results.

2.5 Water

Water is the universal solute where chemical reactions occur. The addition of water to produce the cemented paste fill mix aids the dissolution and diffusion of cement molecules and ions in the hydration reaction (Bullard et al., 2011). The ratio of water to cement is essential for hydration process that yields optimal strength. Too much water can slow hydration and strength requirement cannot be attained (Belem and Benzaazoua, 2008). Water aids

the paste fill slurry to flow through reticulation lines over long distances. The water content of around 28 to 35 % is applied to maintain an optimum rheology of the slurry. Chemistry of water affects the strength and durability of the cemented paste fill. Presence of sulphate salts in the tailings can attack the cementitious bonds and after some time reduce the strength of the cemented paste fill (Belem and Benzaazoua 2008). The pH and temperature of the water also influence the hydration process and strength development.

2.6 Admixtures

Admixtures are used to alter the physio-chemical properties of the binder and improve flow and strength properties of the CPF. Admixtures are grouped according to ASTM C494 standard and are used for different purposes such as to accelerate hydration reaction, to reduce water requirement, to disperse the flocculation of binder particles, and to retard the flash setting.

2.6.1 Plasticizer

Dispersant based water reducers are known as either plasticizer or superplasticizers. Plasticizers reduce the amount of water required and reduce cement required for a given strength (Schneider et al., 2011). Superplasticizer from polycarboxylate technologies can reduce water requirement up to 30 %. However, the associated costs and undesirable effects limit the dosage of superplasticizer to reduce water requirement in the range of 10 to 15 % (Cheung et al., 2017).

The ability of plasticizer to reduce water improves both the strength and durability of concrete. The dispersion action of admixture is achieved by the steric hindrance, which improves workability of CPF over longer reticulation lines (Berodier et al., 2018). The retardation action prevents flash setting, exposes binder surface areas for maximum reaction, and attains higher strength over time. According to Nagrockiene et al. (2013), the electrostatic

repulsion produced from the plasticizer prevents the cement particles from flocculating and thus improves the workability of the CPF. Reduction of water requirement from the repulsion effects of plasticizer improves workability and increases the strength. Use of plasticizer also allows for the increase in solid content which increases the disposal rate of mill tailings into the underground voids (Fan et al., 2014).

Mangane et al. (2018) trialled admixtures of various plasticizer or superplasticizer groups (lignosulfonate, naphthalene, melamine, and polycarboxylate) with ordinary Portland cement (20 %) and pozzolan (slag 80 %) with various types and dosages of superplasticizers (SP). The results from the trial (Fig. 2.13) affirmed that the type and dosage of the admixture influences the rheological properties of the paste slurry.

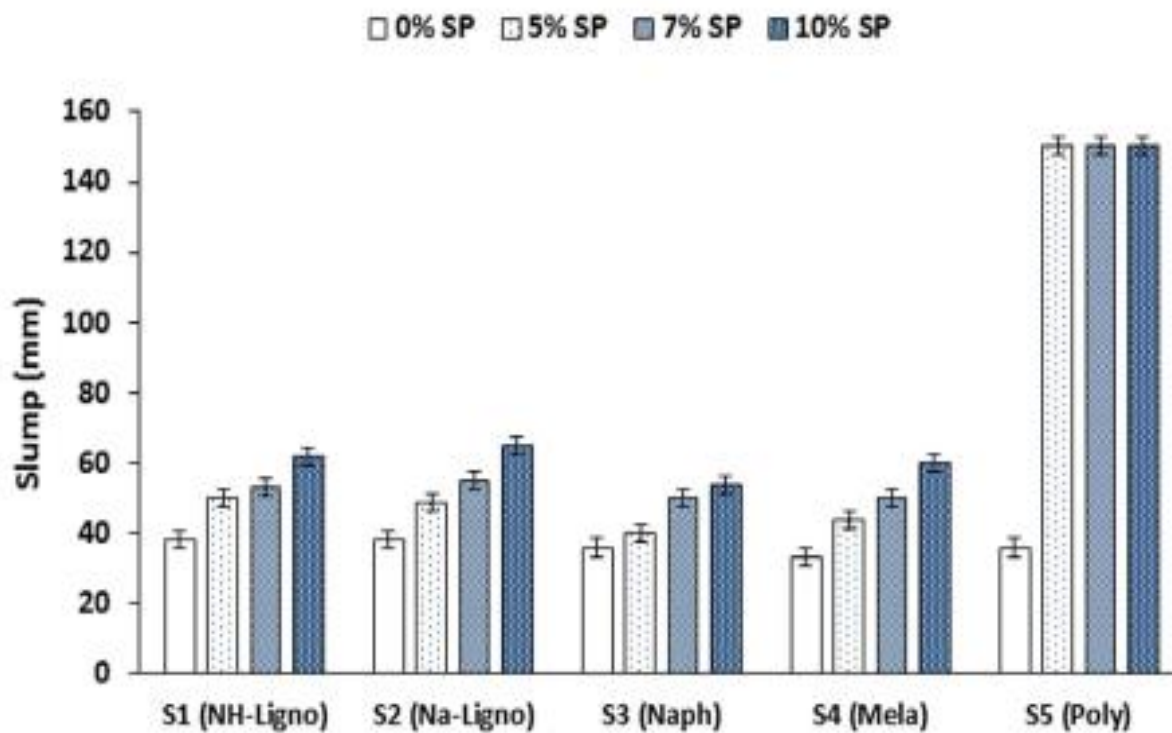


Fig. 2.13 Slump comparison of various groups of superplasticizers (SP)
(Mangane et al., 2018)

Polycarboxylate based plasticizers performed better in improving the slump of the paste slurry compared to the other types of plasticizers trialled. The slump also increases with the increase in the dosage (%) of plasticizer.

2.6.2 Polycarboxylate

Polycarboxylate is a group of plasticizers that improve the workability and influence the strength of the paste fill. Polycarboxylate plasticizers are comb-like polymers composed of polyethylene chains that get adsorbed onto the surface of the cement particles causing the cement particles to disperse thus slowing down hydration process (Yu et al., 2016). Mangane et al. (2018) trialled different types and dosages of plasticizers and affirmed that the polycarboxylate based plasticizer attained a higher workability and strength. Ouattara et al. (2017) trialled two polycarboxylate (PC) based plasticizer at 80 % solid content and at plasticizer dosages of 0.045 to 0.153 % (ratio of mass of PC to dry mass tailings) and affirmed that polycarboxylate reduce yield stress and viscosity (Fig. 2.14) in higher solid content (80 %) and maintain workability.

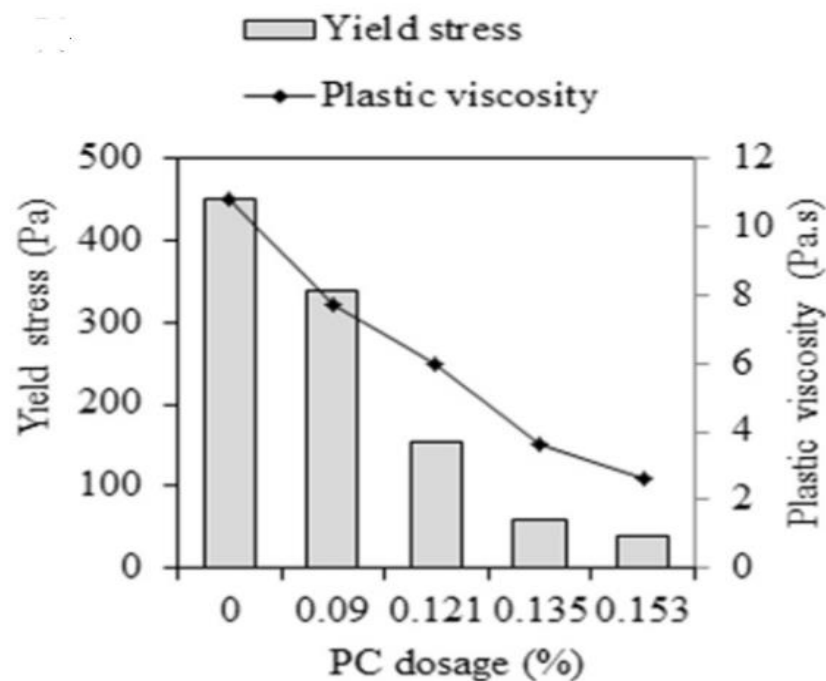


Fig. 2.14 Impact of polycarboxylate dosage on yield stress and viscosity (Ouattara et al., 2017)

Liu et al. (2013) investigated the effect of plasticizer on gypsum (α -calcium sulphate hemihydrate) and affirmed that absorption of plasticizer to binder surface was due to Van der Waals force, the dispersion was due to steric hindrance, and the optimum dosage of plasticizer was from 0.4 to 0.6 % of the binder content. Admixtures improve workability and strength of a slurry with high (80 %) solid content by dispersing and retarding the binder (Ouattara et al., 2017). The dispersion action of plasticizer improves the flow of slurry without additional water requirement while the retardation action exposes more surface areas for optimum hydration reaction.

2.7 Hydration reaction

The chemical reaction of cement when in contact with water is primarily responsible for the strength development. There are several chemical processes that take place during hydration and the main ones include dissolution when cement in contact with water, diffusion of ions within the slurry, nucleation (forming of solids), and growth of crystalline structures (Bullard et al., 2011).

2.7.1 Cement hydration

Hydration reaction occurs when cement is in contact with water and undergoes stages of dissolution, precipitation, and development of microstructures. Hydroxide ions (OH^-) are released during dissolution and the pH of the paste varies between 12 and 13 (Belem et al., 2008). Hydration process undergoes formation of different phases of reaction. Phases are grouped into the oxides of calcium, silicon, aluminium, iron, sulphate, and water ($\text{CaO} = \text{C}$, $\text{SiO}_2 = \text{S}$, $\text{Al}_2\text{O}_3 = \text{A}$, $\text{Fe}_2\text{O}_3 = \text{F}$, $\text{SO}_3 = \text{\$}$ or $\text{\$}$, and $\text{H}_2\text{O} = \text{H}$). Tricalcium silicate ($3\text{CaO}.\text{SiO}_2$) or alite is denoted as C_3S , dicalcium silicate ($2\text{CaO}.\text{SiO}_2$) or belite as C_2S , and tricalcium aluminate ($3\text{CaO}.\text{Al}_2\text{O}_3$) or celite

as C_3A , ferrite ($4CaO \cdot Al_2O_3 \cdot Fe_2O_3$) or brownmillerite as C_4AF (Scrivener et al., 2017).

Portland cement consists 60 % C_3S , 15 % C_2S , 8 % C_3A , and 10 % C_4AF (Henderson and Revell, 2005). Hydration and microstructure evolution take place in stages where the reaction of C_3S forms the initial strength while C_2S takes longer for strength development. The dissolution, diffusion of ions, and formation of calcium silicate (C-S-H), ettringite, and portlandite phases alter the strength properties. The strength of the material is mostly influenced by the growth of the C-S-H phases.

2.7.2 Pozzolanic hydration

Hydration of C_3S and C_2S forms C-S-H (usually $C_3S_2H_3$) and releases calcium hydroxide (CH) based on the following reaction (Vessalas et al., 2007).



The by-product calcium hydroxide (portlandite) reacts with silica from pozzolan to form additional calcium silicates (C-S-H). With the increase precipitation and flocculation of C-S-H within 3 to 28 days, the strength increases (Xu et al., 2018). Microstructure development reduces at later stages due to stable formation of hydration products.

Gypsum present in cement prevents the premature stiffening of hydration when the C_3A reacts with water to form calcium aluminate hydrate ($4CaO \cdot Al_2O_3 \cdot 19H_2O$) or ettringite ($3CaO \cdot Al_2O_3 \cdot 3CaSO_4 \cdot 32H_2O$) which reduces the mobility and hinders further reaction to form calcium silicates (Henderson and Revell, 2005). Plasticizers behave similarly like gypsum in retarding flash setting which is beneficial in preventing premature stiffening of CPF and optimising the hydration reaction.

2.8 Strength development

Cemented paste fill is designed to attain certain strength for application as rib or pillar support. The strength is mostly influenced by the binder dosage, solid content, tailings properties, and admixtures used. Mechanical strength gain increases with the binder dosage and solid content (Xu et al., 2018). The strength is proportional to the curing period and increases with the increase in curing period. Unconfined compressive strength is the commonly used strength in mine back filling. Besides UCS, there are other strength properties that are determined including indirect tensile strength (Brazilian Test), and flexural strength.

2.8.1 Unconfined compressive strength

Unconfined compressive strength (UCS) is the most common indicator of strength property of CPF used in mines. UCS values vary significantly with binder dosage and solid content. When binder dosage increases, higher strength is attained over short curing periods (within 7 to 14 days). Increase in solid content significantly increases the strength of paste fill. The longer the curing period, the strength increases due to the growth of calcium silicates that further binds the tailings and reduces the voids.

Different UCS limits have been adapted for paste filling for different strength requirements. UCS of 100 kPa is the minimum strength that can withstand blasting without having to liquefy under a seismic magnitude of 7.5 on Richter scale and is adapted from the work of Clough et al. (1989). Undercutting paste fill requires the UCS value of CPF to be above 1000 kPa while mining adjacent would require UCS values above 500 kPa. Although the strength requirement slightly differ from site to site, generally a UCS value ranging from 700 kPa is regarded as adequate to provide long term stability (Cihangir et al., 2012).

UCS and Young's modulus (stiffness) values are determined from the stress and strain plot as indicated below from a uniaxial compression test (Fig. 2.15).

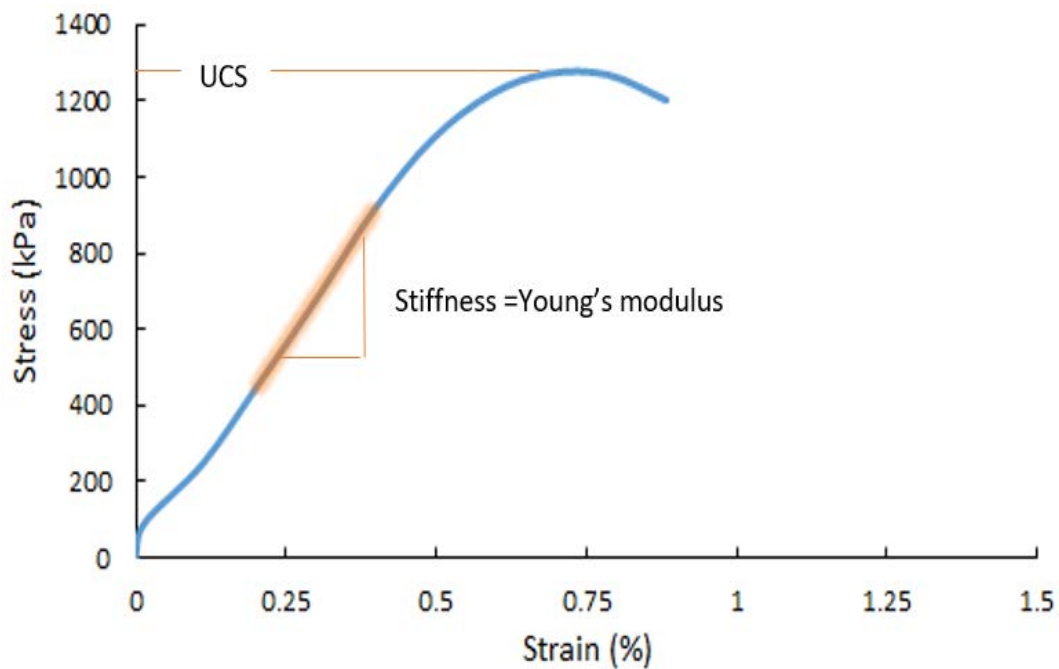


Fig. 2.15 Stress-strain plot

Most materials have range of values for the ratio of Young's modulus (E) to UCS. According to Niroshan et al. (2017), the ratio of E/UCS for cemented paste fill ranges from 150 to 350. This ratio is helpful when the UCS is estimated through simple site tests such as point load or hammer blows, where the range of Young's modulus can be estimated.

2.8.2 Flexural and indirect tensile strengths

The tensile strength of the cemented paste fill is determined using the Brazilian test method or often called indirect tensile strength (ITS) test. The flexural strength is determined using the 3-point bending test. Flexural strength of the cemented paste fill (CPF) is essential in mine filling when excavations are to be made through or below the CPF. For instance, when the stope below CPF is to be mined, the stable thickness (height) of CPF is required over the span (strike or width) so that failure of the undercut of the CPF crown is prevented and the

stope below is mined safely. Like the UCS test values, the ITS and flexural strength values are influenced by the binder dosage, solid content, and the curing period.

2.9 Rheology of paste fill

Cemented paste fill flows through reticulation lines over longer distances and thus, the rheological properties of the slurry should be optimum to avoid pipeline blockages. The optimum mix should produce desired yield stress and viscosity at a minimal pumping energy (Boger et al., 2006). Common rheology property tests are the slump, yield stress, and bulk density.

There is interrelationship among the solid content, bulk density, yield stress, and slump. Solid content affects the rheology of paste fill slurry significantly. When solid content is increased (either the tailings or binder), the bulk density and yield stress increases while the slump reduces (Niroshan et al., 2018). The flow properties of paste fill are also affected by the particle size distribution, water chemistry and temperature (Panchal et al., 2018).

2.9.1 Slump

Slump measures the degree of wetness, consistency of batch, and workability. Rheological properties of CPF are difficult to determine in practice with experimental devices, thus slump cone is the quickest and conventional mode of relating to the shear yield stress of the paste. A slump of 150 to 250 mm is optimum for pumping through reticulation lines (Belem et al., 2008). Slump varies depending on the material properties, however, the general slump for mine fills is from 235 to 275 mm (Li, 2013; Sivakugan et al., 2015). Slump can be related to yield stress, where a slump of 260 mm gives a yield stress of 150 to 200 Pa (Niroshan et al., 2017). Slump recording can be similar for different materials, however, different bulk density and yield stress of material behave differently and affect pressure along pipeline (Boger et al., 2006).

Slump cone test is done using ASTM C143 procedure. A truncated cone of 100 mm top diameter, 200 mm bottom diameter, and 300 mm height is used.

2.9.2 Yield stress and viscosity

The flowability of the cemented paste fill along reticulation lines is affected by the yield stress and the viscosity of the slurry. Cemented paste fill is a non-Newtonian fluid and exhibits Bingham flow characteristics whereby the yield stress must be overcome to initiate plastic deformation which results in slurry exhibiting plug flow (Sivakugan et al., 2006; Boger et al., 2006). Paste fill slurry flows when the driving head exceeds the pipeline wall resistance (or shear stress). Yield stress of paste fill in mines can range from 50 to 500 Pa and some mines can operate higher than up to 800 Pa as in the case of Cannington-Mt Isa (Sivakugan et al., 2015, Niroshan et al., 2018). The Table 2.2 below indicates the typical yield stress values of common materials.

Table 2.2 Typical yield stress values of materials (Boger, 2006)

Material	Yields Stress (Pa)
Tomato sauce	15
Yoghurt	80
Toothpaste	110
Peanut butter	1900
Thickened tails	30 - 100
Cemented paste fill	250 - 800

Bingham model indicates that at very low shear rate (close to zero rpm), the paste slurry indicates a non-linear behaviour. The linear Bingham model indicates a higher yield stress compared to the actual yield stress (Sivakugan et al., 2015). The behaviour of a Bingham and Newtonian flow is shown below (Fig. 2.16).

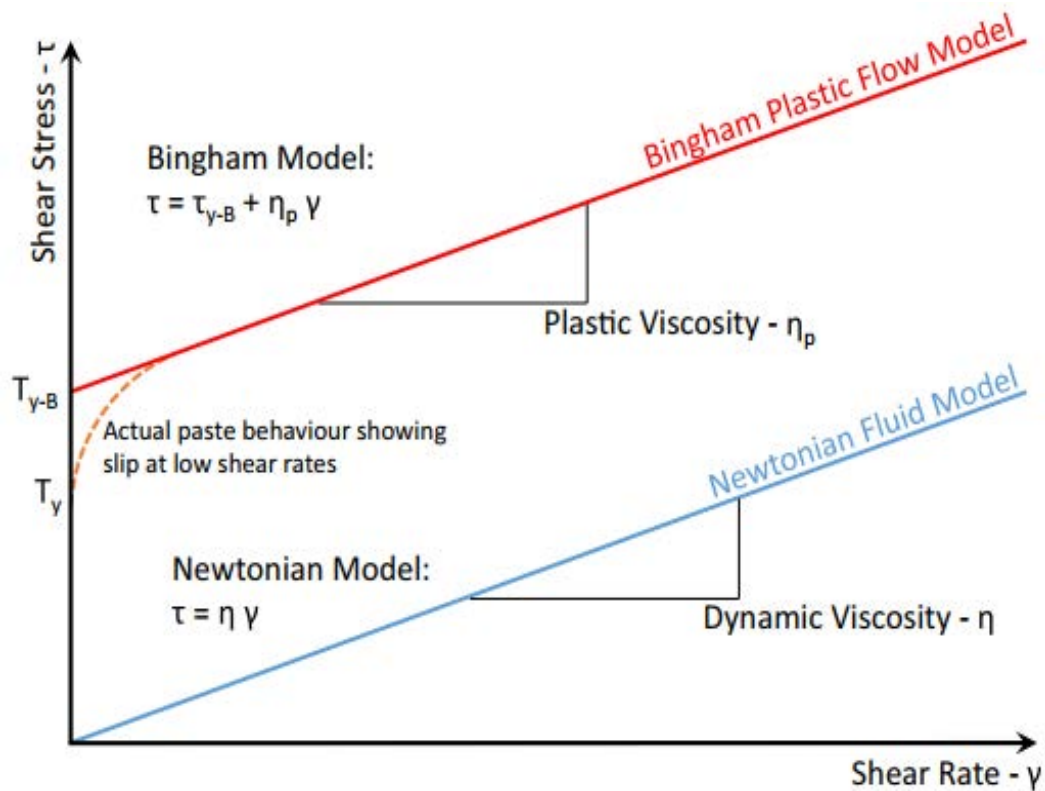


Fig. 2.16 Bingham and Newtonian fluid comparison (Niroshan et al., 2018)

Niroshan et al. (2018) showed that with an increase in the solid content, the bulk density increases, the slump height reduces, yield stress and viscosity increase resulting in lower workability. Rheological studies of tailings from George Fisher Mine (GFM) indicated a slump of cemented paste fill slurry ranging from 237 to 275 mm, with solid content ranging from 70 to 80 %, corresponded to yield stress ranging from 50 to 500 Pa with 250 Pa as a typical value in many operating mines (Sivakugan et al., 2015). Moreover, the yield stress should be within the optimal range to ensure flow along reticulation lines at velocities 0.1 m/s to 1.0 m/s without settling of the solids (Panchal et al., 2018).

2.10 Microstructure development

During the hydration process, crystal structures grow and develop. The growth of these crystals contribute to the increase in the strength of the paste fill. Microstructure studies are done to observe the growth of the hydration

products and relate it to the development of strength over curing periods. Two of the commonly known methods are the scanning electron micrograph (SEM) and thermogravimetry analysis (TGA).

2.10.1 Scanning electron micrograph

Scanning electron micrograph (SEM) is done on hard and dried specimen to observe the microstructure (crystal and precipitate) developments over curing periods. SEM films are examined to understand the formation of hydration products like portlandite (CH), calcium silicate (C-S-H), ettringite and how it affects the strength development (Scrivener, 2017).

SEM images show the porosity and distribution of voids. Pore space distribution in CPF is influenced by curing time, binder type, and solid content (Xu et al., 2018). SEM images for each curing period is related to the UCS values and can be useful to establish the relationships of the microstructure with strength development.

SEM involves directing beams of electrons to produce high image with high magnification and resolution. Specimen slice is extracted from sample, polished, and coated with gold or platinum or carbon on one side for scanning.

2.10.2 Thermogravimetry analysis

Thermogravimetry analysis (TGA) is done to determine the amount of portlandite present in the cemented paste fill specimen after different curing periods. As the curing period increases, the amount of portlandite reduces indicating that the calcium hydroxide has reacted with the silicates to form calcium silicates.

Specimen for the TGA test are oven dried, grounded, and a tiny mass of 3 to 10 mg is placed in a pan and heated. The changes in the phase over different temperature range is recorded to determine the mass loss of different minerals present in the specimen.

2.11 Summary

The four different categories of underground mining methods are the supported methods, unsupported method, caving methods, and the combination methods. The supported mining methods utilise fill materials to stabilise the voids created underground from mining the stopes. The fill materials are either cemented or uncemented.

Common back fill materials are the rock fill, cemented rock fill, cemented aggregate fill, hydraulic fill, and the cemented paste fill. Cemented paste fill is a popular fill material in recent years due to its benefits in providing stability, limiting exposure to unsafe ground conditions and most importantly being environmentally friendly in disposing waste in underground voids. The main ingredients that are used to produce the paste fill are the mill tailings, binder, water, and the addition of pozzolans and admixtures to improve strength and rheology.

Cemented paste fill is an expensive fill type compared to the other fills. Paste fill uses cement dosage ranging from 3 to 7 % which contributes to 70 to 80 % of the filling cost. Therefore, pozzolanic materials have been used to partially replace the cement and save cost.

The common strength property of paste fill is UCS, however other strengths such as tensile and flexural strengths are also necessary. A minimum strength of 100 kPa is set as liquefaction limit.

Paste fill is transported through pipelines and discharged as slurry into the stope voids, thus its rheological properties are paramount for an efficient flow without pipe blockage. Plasticizers have been used successfully to improve the workability to maintain flow over longer distances.

Microstructure development of CPF is studied with methods like scanning electron micrograph (SEM) and thermogravimetry analysis (TGA) to determine the presence of hydration products and how the strength is impacted with the growth of these products such as calcium silicates.

3 Mix design

Mix design of cemented paste fill (CPF) affects its rheological and strength properties. The characteristics of mill tailings, binder type and dosage, solid content, water content, and admixture dosages directly influence the slump, yield stress, viscosity, bulk density, microstructure and strength development of the cemented paste fill.

In this study, the mill tailings used were from George Fisher Mine (GFM) in Mt Isa in Queensland, Australia. Four different binders used in this study were general Portland cement (GPC), fly ash blend, slag blend, and pitchstone blend.

3.1 Ingredient requirement

Common ingredients used in producing cemented paste fill (CPF) are mill tailings, water, admixtures, and pozzolans which are used to partially replace cement. The content and dosage of ingredients are shown below (Fig. 3.1).



Fig. 3.1 Ingredients for cemented paste fill

Calculations of the mass of ingredients required were done in accordance with the equations used in a similar study done previously and as practised in

the mines (Niroshan et al., 2018). These mix equations outlined below have been used consistently throughout the study.

$$\text{Solid content:} \quad SC (\%) = \frac{(M_{ds}+M_b)}{(M_{ds}+M_b+M_w)} \times 100 \quad (\text{Eqn. 3.1})$$

$$\text{Binder content:} \quad BC (\%) = \frac{M_b}{(M_{ds}+M_b)} \times 100 \quad (\text{Eqn. 3.2})$$

$$\text{Water content:} \quad w (\%) = \frac{M_w}{(M_{ds}+M_b)} \times 100 \quad (\text{Eqn. 3.3})$$

$$\text{Admixture dosage:} \quad AD (\%) = \frac{M_a}{M_b} \times 100 \quad (\text{Eqn. 3.4})$$

where M_{ds} is the mass of dry solid, M_b is the mass of binder, M_w is the mass of water, and M_a is the mass of admixture.

Increasing the solid content enabled more tailings to be placed but made it difficult for slurry to flow without pipe blockages. Through a series of trials, it was found that the solid content of 74 %, giving 260 mm slump, was the optimum mix. With these threshold values, mix designs were carried out. Solid contents of majority of the mixes were set at 74 %, however, few mixes were set at 75 %, 76 %, 77 % and 78 %. The binder dosages applied were 3 %, 5 % and 7 % for the different binder types. In this study, the admixture polycarboxylate plasticizer was added to the slurry to enhance the rheological properties. Polycarboxylate plasticizer was added to the slurry at various dosages of 2 %, 4 %, 6 %, and 8 % of the mass of the binder calculated for each of the mixes. It was observed from series of trials that mixes with high dosage of polycarboxylate (> 8 %) took longer time to set, thus dosages between 2 % to 8 % were used in this study. The complete tests program is summarized below (Fig. 3.2).

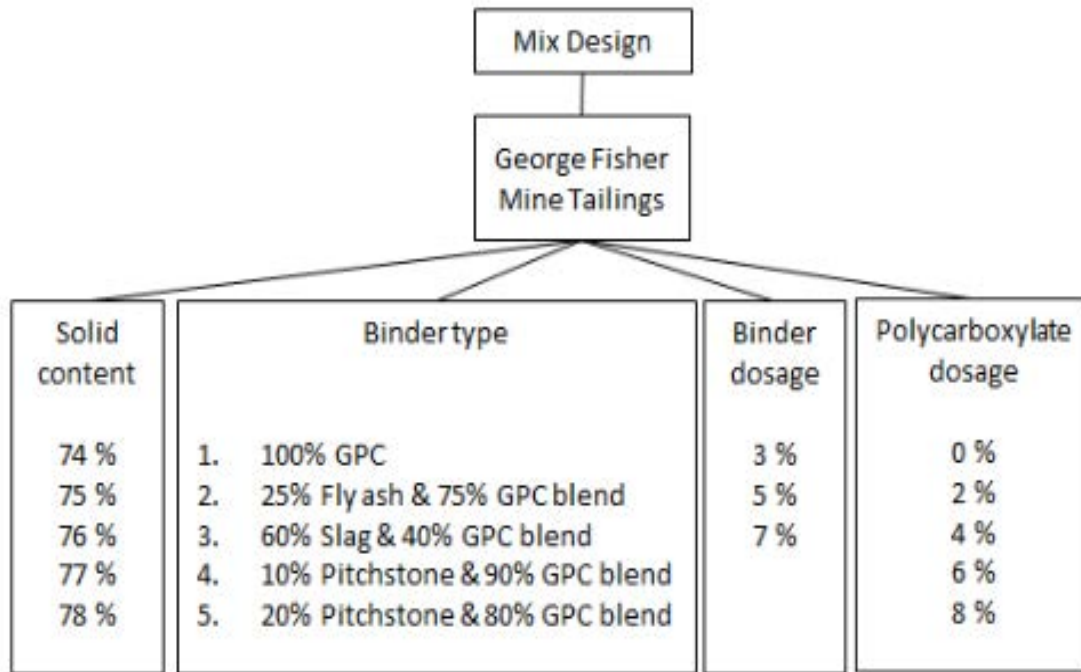


Fig. 3.2 Combination of different mix design

A total of 68 different mixtures were cast and tested for their strength and rheological properties. Mill tailings used were from George Fisher Mine in Mt Isa in Queensland, Australia. Four different binders used were general Portland cement (GPC) for control mix, fly ash blend (containing 25 % fly ash and 75 % GPC), slag blend (containing 60 % slag and 40 % GPC), pitchstone blend (containing 10 % pitchstone and 90 % GPC, and 20 % pitchstone and 80 % GPC). In this study, pitchstone fines were trialled as potential supplementary cementitious material for paste fill application apart from the common pozzolans like fly ash and slag. The yield stress and slump tests were done on the paste slurry right after preparation while the strength tests were done on cast and cured samples for 7, 14, 28, 56, and 112 days curing periods.

The 68 different mixes were sorted and tabulated according to the binder type used in the mix. Table 3.1 captures all the mixes that used 100 % GPC, Tables 3.2 and 3.3 captures all mixes that used pitchstone blend, and Table 3.4 captures all the mixes that used fly ash and slag blends.

Table 3.1 Mix with pure GPC (100 %)

Mix	1	2	3	4	5	16	17	18	19	20	51	52	53	60	61	62
Mix ID	Mix1	Mix2	Mix3	Mix4	Mix5	Mix16	Mix17	Mix18	Mix19	Mix20	MixT9	MixT11	MixT12	MixT21	MixT23	MixT24
PC-Admixture	0%	2%	4%	6%	8%	0%	2%	4%	6%	8%	0%	4%	6%	0%	4%	6%
Binder	3%	3%	3%	3%	3%	7%	7%	7%	7%	7%	3%	3%	3%	5%	5%	5%
Portland	100%	100%	100%	100%	100%	100%	100%	100%	100%	100%	100%	100%	100%	100%	100%	100%
Pitchstone																
Slag																
Flyash																
Solid content	74%	74%	74%	74%	74%	74%	74%	74%	74%	74%	74%	74%	74%	74%	74%	74%

Table 3.2 Mix with pitchstone blend

Mix	6	7	8	9	10	11	12	13	14	15	21	22	23	24	25	26	27
Mix ID	Mix6	Mix7	Mix8	Mix9	Mix10	Mix11	Mix12	Mix13	Mix14	Mix15	Mix21	Mix22	Mix23	Mix24	Mix25	Mix26	Mix27
PC-Admixture	0%	2%	4%	6%	8%	0%	2%	4%	6%	8%	0%	2%	4%	6%	8%	0%	2%
Binder	3%	3%	3%	3%	3%	3%	3%	3%	3%	3%	7%	7%	7%	7%	7%	7%	7%
Portland	80%	80%	80%	80%	80%	90%	90%	90%	90%	90%	80%	80%	80%	80%	80%	90%	90%
Pitchstone	20%	20%	20%	20%	20%	10%	10%	10%	10%	10%	20%	20%	20%	20%	20%	10%	10%
Slag																	
Flyash																	
Solid content	74%	74%	74%	74%	74%	74%	74%	74%	74%	74%	74%	74%	74%	74%	74%	74%	74%

Table 3.3 Mix with pitchstone blend continue

Mix	28	29	30	31	32	33	34	35	36	37	38	39	40	41	42	43	44
Mix ID	Mix28	Mix29	Mix30	Mix31	Mix32	Mix34	Mix35	Mix36	Mix38	Mix39	Mix40	Mix49	Mix50	Mix59	Mix61	Mix62	Mix63
PC-Admixture	4%	6%	8%	0%	4%	6%	8%	0%	4%	6%	8%	6%	8%	6%	0%	6%	6%
Binder	7%	7%	7%	5%	5%	5%	5%	5%	5%	5%	5%	5%	5%	5%	5%	5%	5%
Portland	90%	90%	90%	90%	90%	90%	90%	90%	90%	90%	90%	90%	90%	90%	80%	80%	80%
Pitchstone	10%	10%	10%	10%	10%	10%	10%	10%	10%	10%	10%	10%	10%	10%	20%	20%	20%
Slag																	
Flyash																	
Solid content	74%	74%	74%	75%	75%	75%	75%	76%	76%	76%	76%	77%	77%	78%	74%	74%	76%

Table 3.4 Mix with fly ash and slag blend

Mix	45	46	47	48	49	50	54	55	56	57	58	59	63	64	65	66	67	68
Mix ID	MixT1	MixT3	MixT4	MixT5	MixT7	MixT8	MixT13	MixT15	MixT16	MixT17	MixT19	MixT20	MixT25 (FA)	MixT26(FA)	MixT27(FA)	MixT25(Slg)	MixT26(Slg)	MixT27(Slg)
PC-Admixture	0%	4%	6%	0%	4%	6%	0%	4%	6%	0%	4%	6%	0%	4%	6%	0%	4%	6%
Binder	3%	3%	3%	3%	3%	3%	5%	5%	5%	5%	5%	5%	7%	7%	7%	7%	7%	7%
Portland	40%	40%	40%	75%	75%	75%	40%	40%	40%	75%	75%	75%	75%	75%	75%	40%	40%	40%
Pitchstone																		
Slag	60%	60%	60%				60%	60%	60%							60%	60%	60%
Flyash				25%	25%	25%				25%	25%	25%	25%	25%	25%			
Solid content	74%	74%	74%	74%	74%	74%	74%	74%	74%	74%	74%	74%	74%	74%	74%	74%	74%	74%

3.2 Ingredients calculation

A worked example showing the calculation of mass and content of ingredients using the equations 3.1 to 3.4 is shown in Table 3.5 below. The mix used as an example is a blend of pitchstone fines with Portland cement at ratio 10:90 respectively, at 77 % solid content, 5 % binder dosage, and 6 % polycarboxylate dosage.

Table 3.5 Example of calculated Ingredients

Ingredient	Mass
Tailings (kg)	1
Binder (g)	52.64
Binder (%)	5
<i>Portland</i> (g)	47.37
<i>Pitchstone</i> (g)	5.26
Water (kg)	0.31
Water (%)	29.87
Solid content (%)	77
Admixture (g)	3.16
Admixture (%)	6
Total Mass (kg)	1.37

3.3 Summary

A total of 68 different mixes were produced to cast a total of 900 samples for the unconfined compressive tests, 300 samples for indirect tensile test, and 40 samples for flexural strength tests. Slump tests were done on 54 different mixes, and 127 samples were tested for yield stress and viscosity. For each mix, samples were prepared for 7, 14, 28, 56, and 112 days curing periods. For UCS tests, 2 to 3 samples were casted for each curing periods. For ITS and flexural strength, 1 to 2 samples were casted for curing periods 28 and 56 days.

4 Material characterisation

Physical characteristics of mine tailings were determined using standard test and procedures such as particle size distribution (PSD), specific gravity, bulk density, and Atterberg limits. Mineralogical properties of tailings were studied using scanning electron micrograph (SEM), x-ray diffraction (XRD), and thermogravimetry analysis (TGA) to determine chemical structure and composition.

Characterisation of the binders have been discussed in the literature review. Particle size distribution and SEM were done on pitchstone fines only. Other binders like slag, flay ash, and GPC are common binders and their characteristics were discussed in the literature review.

4.1 Physical characterisation of tailings

Mill tailings used for the research were from George Fisher lead-zinc mine (GFM) in Mt Isa-Australia. Wet tailings received from GFM were oven dried at 105 °C and over 24-hour period to remove the free water. The dried tailings were stored in closed lid buckets and stored in dry compartments in the soil's laboratory as shown below (Fig. 4.1).



Fig. 4.1 Preparation of tailing from GFM

Prior to using the tailings, manual sieving was done with a 4.75 mm diameter sieve to separate the boulders and cobbles. Particle size distribution (PSD) was done only on the tailings that pass through the 4.75 mm sieve. The cylinder mould diameter was 50 mm, so the size of tailings used were smaller than cobbles and boulders to have a proper representation of the tailings when cast as well as to maintain consistency with similar studies done previously.

4.1.1 Particle size distribution of tailings

Particle size distribution of the tailings was done using mechanical sieving with openings from 75 μm to 4.75 mm as per AS 1289.3.6.1 standard. The fines less than 75 μm collected from the pan were further analysed using Malvern Mastersizer 3000 (laser analyser) shown below (Fig. 4.2).

Mechanical sieve



Laser analyser

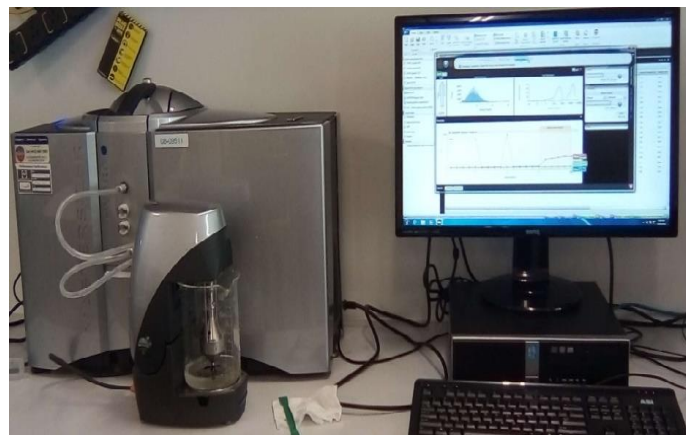


Fig. 4.2 Equipment for particle size distribution

As a generic rule of thumb, tailings should have a minimum of 15 % finer than 20 μm for water retention and lubricating effect (Sivakugan et al., 2006; Kuganathan, 2005). The fines (< 20 μm) have a larger surface area that allows

water absorption and retention which aids flow, prevents settlement, and segregation of particles along pipelines (Deng et al., 2018).

The grain size distribution for GFM tailings (Fig. 4.3) indicated that approximately 5 % by mass of particles were less than 20 μm which indicated less fines. GFM tailings with less fines will require either higher water to solid ratio or increased dosage of polycarboxylate plasticizer. The preferred option to maintain workability is to increase the dosage of polycarboxylate due to the reason that high water content will reduce the strength of the cemented paste fill (CPF).

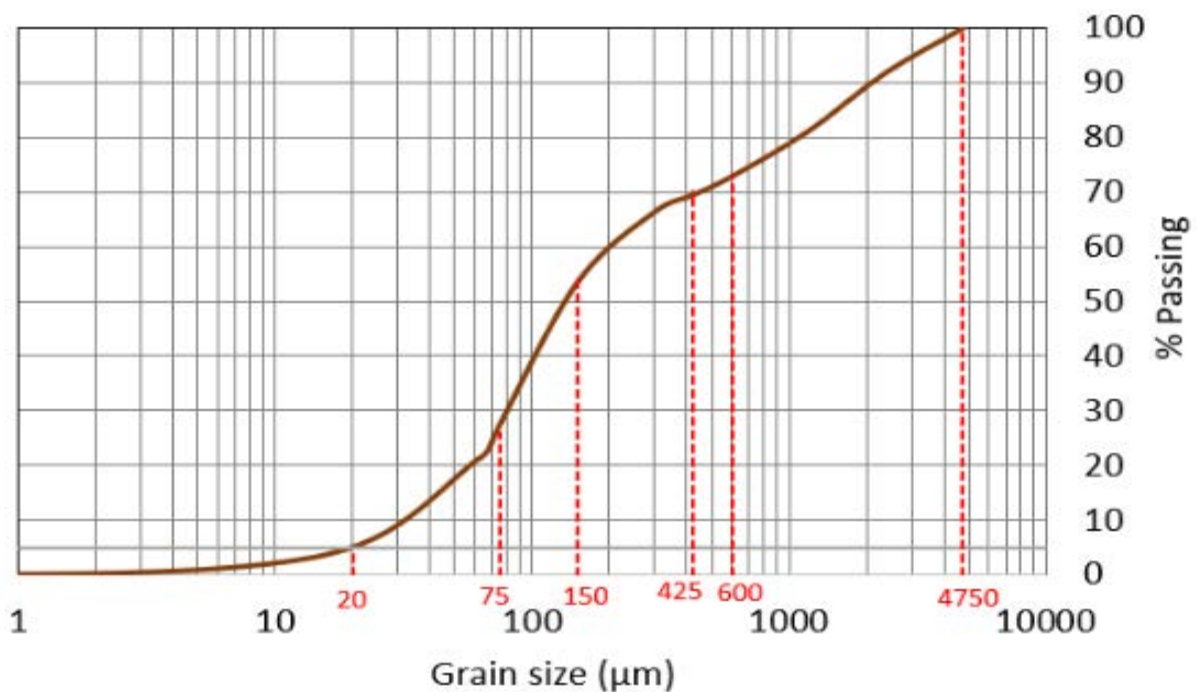


Fig. 4.3 Particle size distribution result for GFM tailings

The parameters of soil like uniformity coefficient (C_u) and coefficient of curvature (C_c) were determine from the PSD curve (Fig. 4.3) as;

$$C_u = \frac{D_{60}}{D_{10}} \quad (\text{Eqn. 4.1})$$

$$C_c = \frac{D_{30}^2}{(D_{10} * D_{60})} \quad (\text{Eqn. 4.2})$$

where D_{10} , D_{30} , and D_{60} are grain size diameters at 10 %, 30 %, and 60 % passing respectively and are obtained from particle size distribution curve. The parameters of GFM tailings are summarised in Table 4.1.

The C_u and C_c are used to measure the spread of the particle sizes and grade and the values determined were 6.5 and 1 respectively. Results (Fig. 4.3) indicated that the tailings contained 72 % sand. Using the soil parameters (C_u and C_c), the GFM mill tailings were classified as poorly graded sand with fines according to Unified Soil Classification System (USCS).

According to Kuganathan (2005), larger C_u (10 to 20) represents a well graded tailing and the requirement of binder is low to attain the desired strength while a lower C_u (5 to 10) contains lesser spread in grain sizes and binder requirement is higher to attain the similar desired strength due to the presence of large voids. Well graded tailings contain particles of various grain sizes that combine to reduce void and attain a cemented paste fill of high density and strength (Henderson & Revell, 2005).

GFM tailings with C_u of 6.5 is within the range from 5 to 10 that contain lesser spread of grain sizes and indicate a poorly graded tailing. GFM tailings with lower C_u will require either additional binder dosage to attain the similar strength to a well graded tailing due to the presence of voids or addition of fillers to reduce the voids. Fines of silica and limestone have been used as fillers and can be trialled with tailings with lower C_u . Further studies will be required to understand feasibility of using other options without increasing the cost of the operation. Tailing properties differ for each mine and thus PSD is important for CPF design to attain desired strength with minimal binder.

4.1.2 Grain shape of tailings

Scanning electron micrograph (SEM) was done on the fines and the grain shape of the tailings was lumpy due to the crushing and grinding process. The

tailing ultra-fines (< 75 μm) contained clay and indicated a flaky shape as shown below (Fig. 4.4).

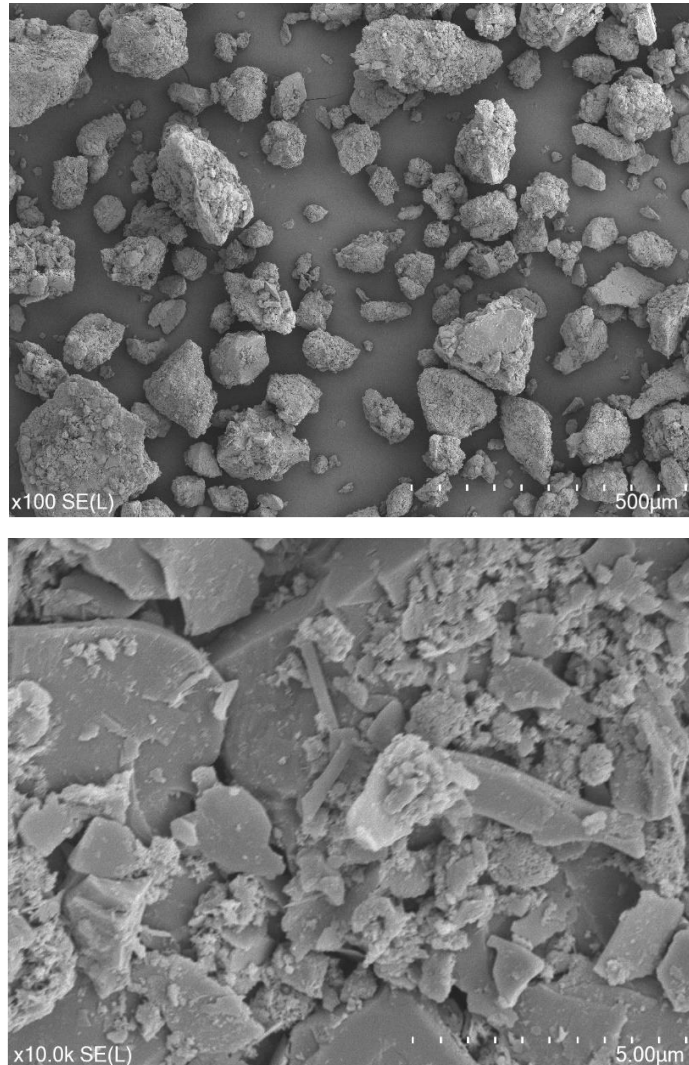


Fig. 4.4 Magnification of grain shape

4.1.3 Specific gravity, bulk density, Atterberg limits of tailings

Specific gravity tests were done on the tailings to determine the particle (grain) density which indicates how heavier the tailings is compared to water. Solids with high specific gravity require increased volume of water to aid smooth slurry flow.

Pycnometer (density bottle) and dried tailings of sizes smaller than 150 mm were used for specific gravity (G_s) test on dry samples using AS 1289.3.5.1 procedure. Results indicated an average specific gravity of 2.77 which is also the particle density of tailings (2.77 g/cc). Specific gravity values are spread out due to the mineralogy of the ore mined and can range from 2.8 to 4.4 for heavier minerals (Sivakugan et al., 2005). GFM ore body has high content of silica (40.74 %) and calcareous (18.4 %) minerals and therefore the specific gravity is at the lower range (Table 4.2).

The bulk unit weight of the tailings was determined as per the standard ASTM D2216 procedure for determining material bulk density as;

$$\text{Bulk density (kg.m}^{-3}\text{)} \qquad Y_b = \frac{W_b}{V_b} \qquad \text{(Eqn. 4.3)}$$

where γ_b is the bulk unit weight, W_b is total weight of in situ sample (water + void + solids), and V_b is the total volume of sample.

Results indicated that the bulk density of the tailings without any form of vibration or compaction was measured to be within the range of 1300 to 1480 kg/m³. The bulk densities measured are similar to the range of bulk densities of soil (1.0 to 1.6 kg/m³) due to the high content of silica (40.74 %) and calcareous (18.4 %) minerals present in the GFM tailings (Table 4.2). Silica and carbonates are common minerals that make up the Earth's crust and are present in soils.

Atterberg limits indicate the state in which the soil exists either as solid, plastic or liquid with respect to the moisture content. These limits are the liquid limit, plastic limit, and shrinkage limit. Similar tests were done on the same tailings previously by Niroshan (2018) using the falling cone method as per AS1289.3.9.1 standard, plastic limit using AS 1289.3.2.1 standard, and linear shrinkage using AS 1289.3.4.1 standard.

Results indicated a liquid limit of 22 %, plastic limit of 15 %, shrinkage limit of 2.5 %, and plastic index of 7 %. Those results together with C_c and C_u were used to classify the tailings as low plasticity, poorly graded sand with fines. The Table 4.1 summarises the physical properties of the GFM mill tailings.

Table 4.1. Summary of physical properties of tailings

Physical property	Value
Bulk density of dry tails (kg/m^3)	1300-1480
Specific gravity	2.77
D_{10} (μm)	33.5
D_{30} (μm)	78
D_{60} (μm)	200
Coefficient of uniformity, C_u	5.97
Coefficient of curvature, C_c	0.91
Liquid limit, LL (%)	22
Plastic limit, PL (%)	15
Plastic index, PI (%)	7
Linear shrinkage limit, LS (%)	2.5

4.2 Chemical characterisation of tailings

Chemical analysis were done on the tailings from George Fisher Mine (GFM). The two methods used to study the chemical composition of the GFM tailings are x-ray diffraction (XRD) and thermogravimetry analysis (TGA).

4.2.1 X-ray diffraction of tailings

X-ray diffraction (XRD) is done on particles to determine their mineralogy and elemental composition. The mineralogy of tailings is not necessarily inert and

can influence the chemical reaction in the hydration process. The presence of clay minerals (sericite) makes the CPF retain water and lowers the strength, while quartz is abrasive and wears out the pipeline, and oxidation of sulphide minerals can deteriorate the hydrated cement over longer period (Henderson & Revell, 2005).

The chemical composition of the GFM mill tailings was determined from the x-ray diffraction (XRD) method. The XRD analysis plots the peaks which indicate which minerals are present when referencing to known minerals. The concentration of minerals detected in abundance from the XRD done on the tailings were quartz (silica), dolomite, bassanite, pyrite, and muscovite. The XRD peaks and the minerals present in the tailings are shown below (Fig. 4.5).

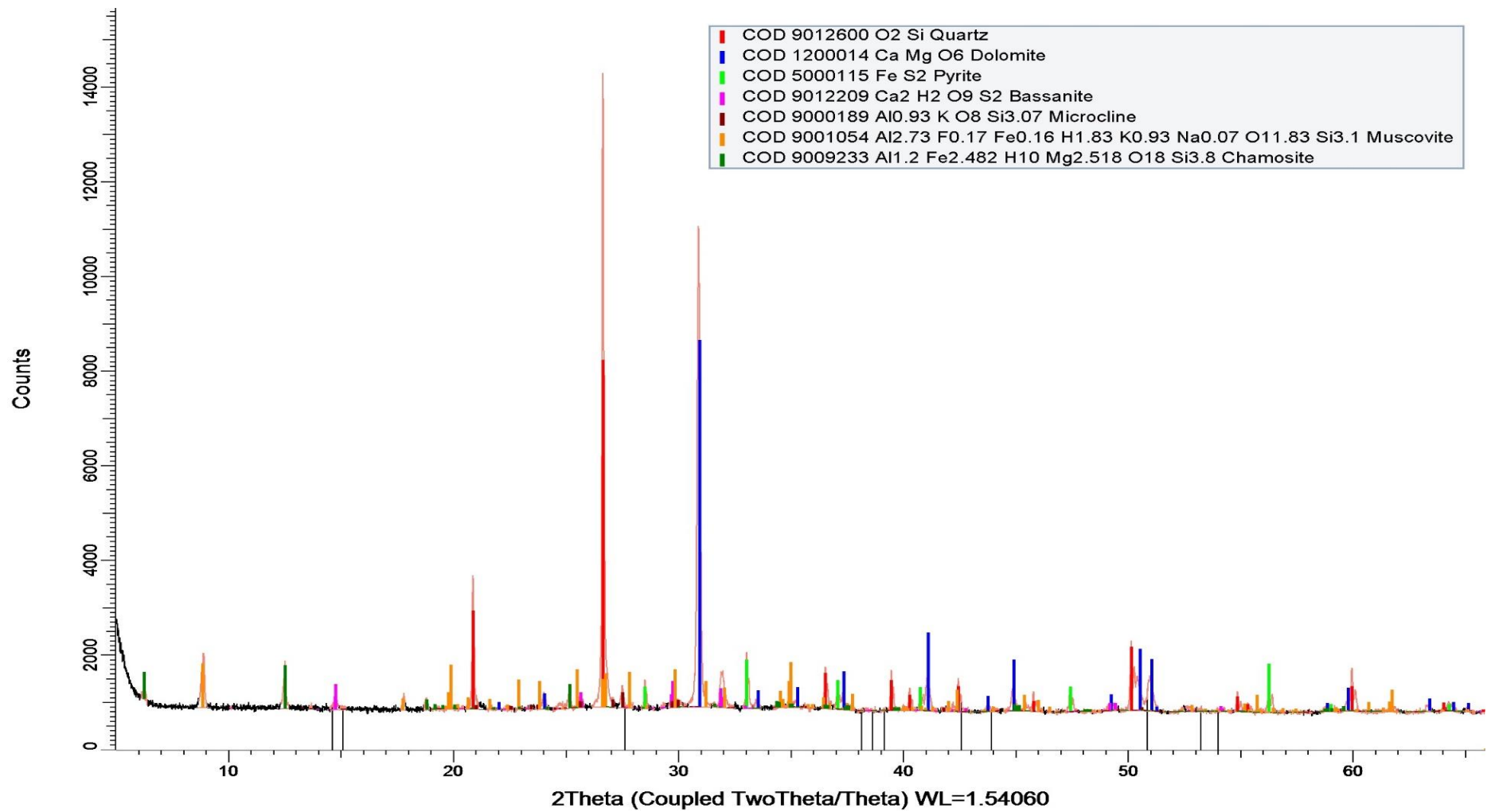


Fig. 4.5 XRD peaks of GFM tailings

Quantitative analysis of the XRD peaks were made and the chemical composition is shown in Table 4.2 below.

Table 4.2 Chemical and mineralogical composition of GFM tailings

Oxide	Percent (%)	Source rock/mineral
SiO ₂ (%)	40.74	Shale (pyritic)
Fe ₂ O ₃ (%)	19.11	Pyrite
SO ₃ (%)	12.65	Pyrite
CaO (%)	12.23	Calcareous-dolomitic siltstones
MgO (%)	6.17	Calcareous-dolomitic siltstones
Al ₂ O ₃ (%)	5.23	Shale (pyritic)
K ₂ O (%)	1.48	Shale (pyritic)
ZnO (%)	0.69	Sphalerite (zinc mineral)
MnO (%)	0.66	Shale (pyritic)
PbO (%)	0.49	Galena (lead mineral)

The chemical compositions of the tailings reflect the type of mineralisation and the host rocks of the orebody. The dominant minerals from the x-ray diffraction (XRD) analysis of GFM tailings were silica (40.74 %), iron oxide (19.11 %), sulphite (12.65 %), dolomite (18.4 %), and other lesser content of metal oxides. The high silica (SiO₂) content is from shale, a sedimentary rock. The sulphite (SO₃) and iron oxide (FeO₃) are from the mineral pyrite (FeS₂). The dolomite is from the calcareous siltstones. The tailings also contained sphalerite (ZnO) which is the mineral that contained zinc, and galena (PbO) which is the mineral that contained lead.

The minerals galena and sphalerite are the source of lead-zinc and silver and are hosted in pyritic shales and calcareous siltstone. The tailings are expected to have higher content of sulphur and iron from the pyritic shale (FeS₂) and higher calcium oxide (CaO) from the calcareous (dolomitic and carbonaceous) siltstones. The commodities mined in George Fisher Mine (GFM) are lead and zinc, with silver as a by-product.

4.2.2 Thermogravimetry analysis of tailings

Thermogravimetry analysis (TGA) and derivative thermogravimetry analysis (DTG) were done on the tailings to compliment the results from the XRD. TGA and DTG results (Fig. 4.6) indicated a phase change occurring within the temperature range of 450 to 550 °C. The phase change indicates the decomposition of dolomite which occurs around these temperature ranges.

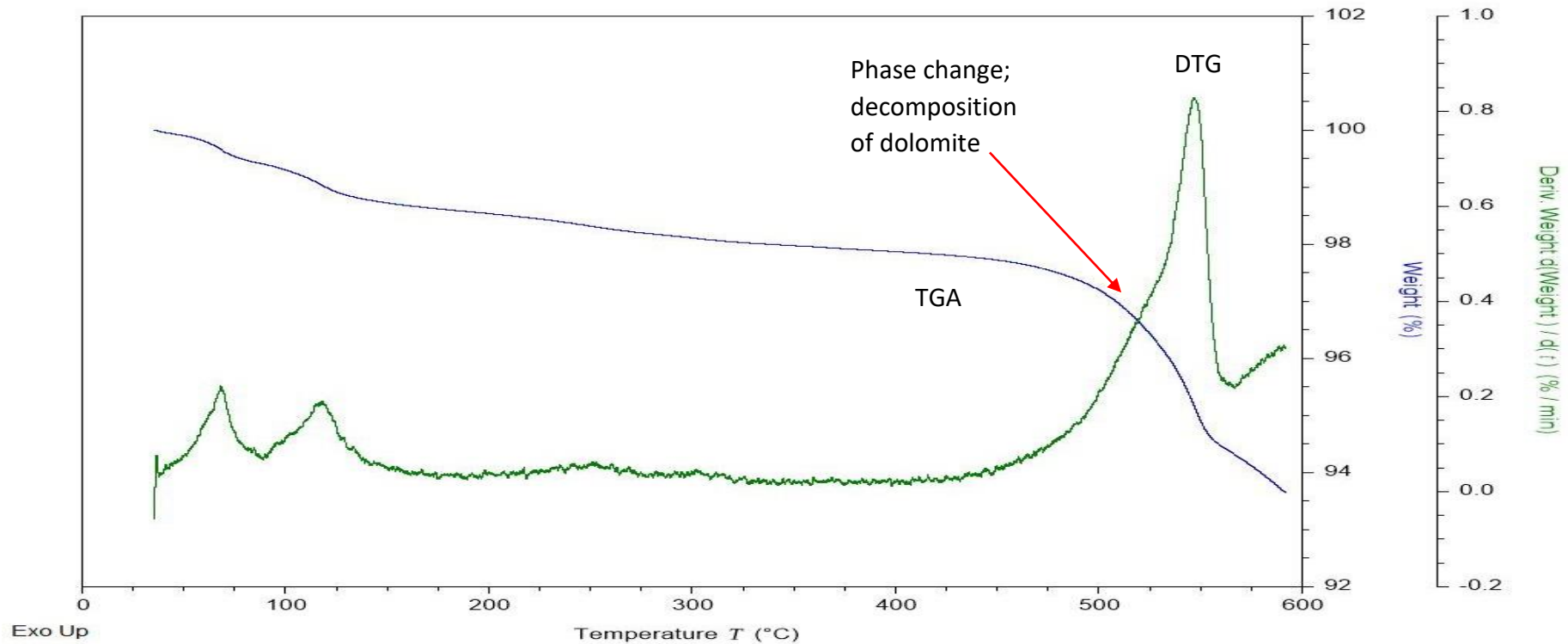


Fig. 4.6 TGA-DTG for GFM tailings

4.3 Physical characterisation of pitchstone fines

Characterisation of the binders was limited to the pitchstone fines as the other binders like slag, flay ash, and GPC are common binders and their characteristics were discussed in the literature review. Characterisation of pitchstone fines involved PSD and SEM to determine the grain distribution and the grain shape.

4.3.1 Particle size distribution of pitchstone fines

The pitchstone fines were analysed for particle size distribution using AS 1289.3.6.1 standard and Malvern (3000) laser. Particle size distribution plots for the pitchstone fines (Fig. 4.7) indicated that about 85 % of the pitchstone fines were within the range of sand from 0.075 to 1.18 mm, while the fines (< 75 μm) made up 13 %.

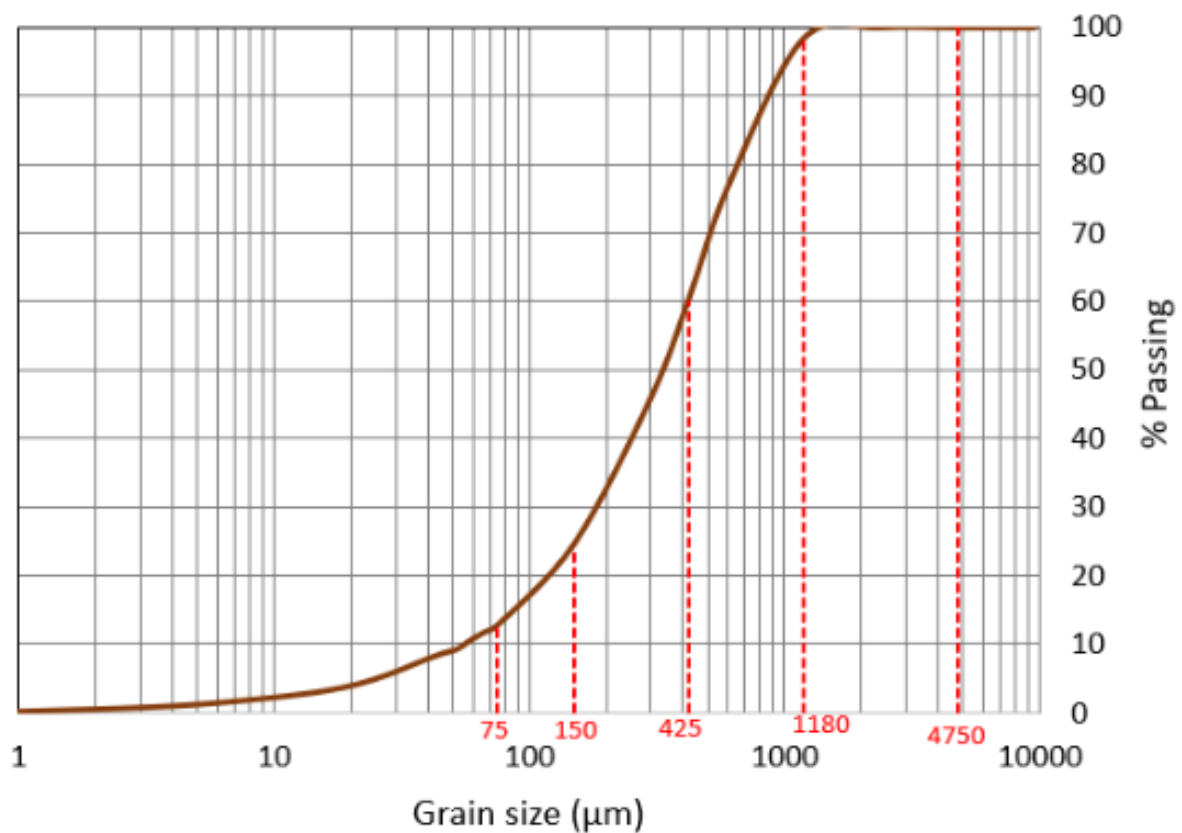


Fig. 4.7 Particle size distribution for pitchstone fines

4.3.2 Grain size and shape of pitchstone fines

SEM was done at different magnification to capture the grain shape of the pitchstone fines (Fig. 4.8). The grain shape of the pitchstone fines were lumpy and indicated a variety of sizes.

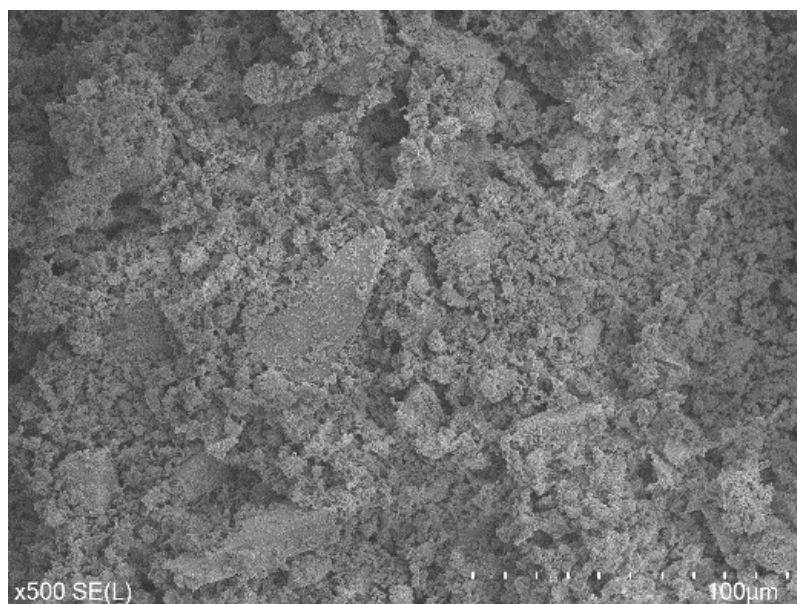
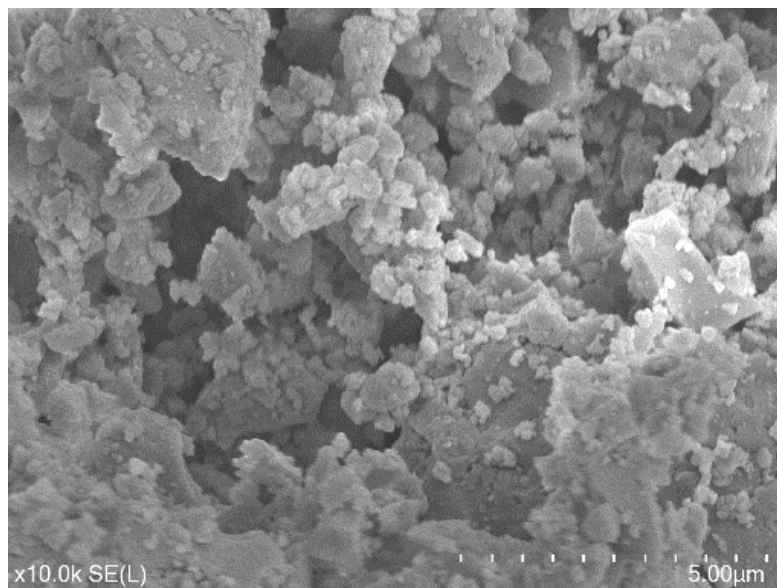


Fig. 4.8 SEM of pitchstone fines at different magnification.

4.4 Summary

Material characterisation was mostly done on the tailings from the George Fisher Mine and the pitchstone fines. Grain size distribution for GFM tailings showed approximately 5 % by mass of particles were less than 20 μm which indicated less fines. As a rule of thumb, the tailings should consist a minimum of 15 % with less than 20 μm . GFM tailings that were used for this research had less fines than normally used for paste filling. From the particle size distribution and the Atterberg limits, the GFM tailings were classified as low plasticity, poorly graded sand with fines.

The particle size distribution done for the pitchstone fines indicated that about 85 % of the pitchstone fines were within the range of sand from 0.075 to 1.18 mm, and the fines made up 13 %.

The high silica presence from the XRD analysis done on the tailings came from the presence of shale, a sedimentary rock type. The pyritic shale and calcareous siltstone formed the host rocks for the deposition of the minerals galena and sphalerite which are the source minerals for lead and zinc respectively. The thermogravimetry analysis (TGA) done on the tailings indicated presence of calcareous minerals with phase change around temperature range of 500 to 550 $^{\circ}\text{C}$. The maximum temperature set for the TGA was 600 $^{\circ}\text{C}$ so any minerals with phase change above 600 $^{\circ}\text{C}$ were out of the range and were not analysed.

5 Strength development

5.1 Introduction

Strength of cemented paste fill (CPF) that are used in mine planning and designs can be the tensile strength, unconfined compressive strength (UCS), flexural strength, and shear strength. Although design engineers tend to utilise all the different strengths, UCS is the commonly used strength for engineering purposes in mining. When CPF serves as crown or sill pillar, all the strength parameters are taken into consideration. When blasting adjacent to a CPF, UCS value is used to design the blast pattern. In this study, samples were cast for the UCS test, indirect tensile strength (ITS) or Brazilian test, and flexural 3-point bending test.

5.2 Materials preparation and casting

The main ingredients used to produce cemented paste fill were oven dried GFM tailings (< 4.75 mm), tap water, general purpose Portland cement, and polycarboxylate plasticizer. The moulds were prepared and labelled prior to mixing the ingredients. The general steps followed in mixing and casting samples are listed below.

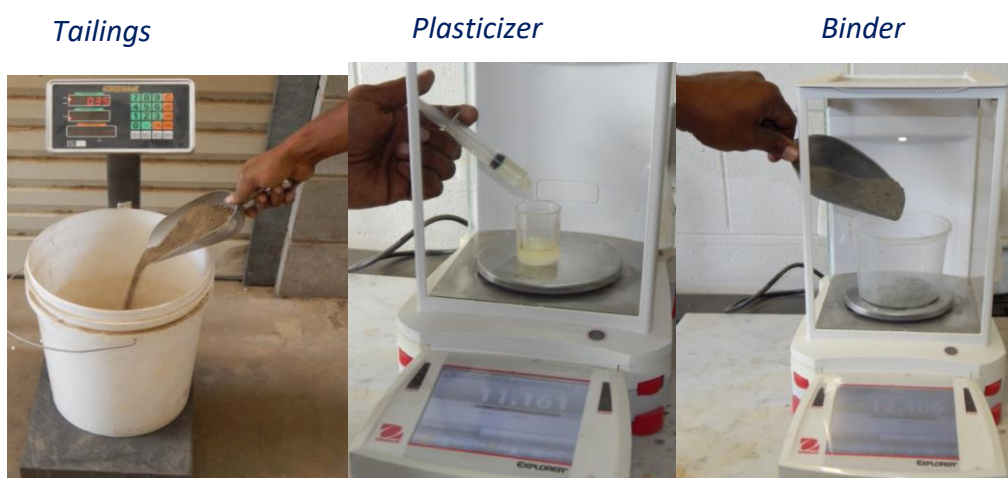


Fig. 5.1 Preparation of ingredients.

- i) The mass of ingredients were determined and weighted out using equations 3.1 to 3.4 in chapter 3. (For this study, 9 to 10 kg of tailings per mix was adequate for casting samples for UCS, ITS and 3-point bending).
- ii) Binder was added to the tailings and manually mixed with a small scoop.
- iii) Water was added to the mix and electrical mixer was used to stir the mixture until it was homogenous.
- iv) Polycarboxylate plasticizer was added afterwards and further stirred. Sika® ViscoCrete® polycarboxylate plasticizer in liquid form was used at dosage 2 %, 4 %, 6 %, and 8 %.



Fig. 5.2 Mixing the ingredients.

- v) Slump test was done immediately on the mix using standard slump cone as per ASTM C143 standard.
- vi) After slump, the mix was scooped back into the buckets and stirred by a paint stirrer to attain homogeneity, as shown above (Fig. 5.2).
- vii) For UCS tests, split-cylindrical PVC moulds of 120 mm height and 50 mm diameter were used to cast the samples. For ITS tests, split-cylindrical PVC moulds of 40 mm height and 50 mm diameter were used to cast samples. For flexural strength tests, wooden triangular

prism moulds of 300 mm length and 75 mm width were used to cast the samples.

- viii) No lubricants were used to polish the interior of the moulds to prevent any reactions with the polycarboxylate plasticizers which retards hydration process.
- ix) For UCS samples, total of 10 moulds were prepared for casting 2 samples per curing period for each mix. For ITS samples, total of 4 moulds were prepared for casting 1 sample per curing period for each. Extra samples each were cast in case samples get damaged. The curing periods were 7 days, 14 days, 28 days, 56 days, and 112 days.
- x) The moulds for the UCS and ITS tests were then filled with the paste slurry. The moulds were positioned on the vibration table. Vibration table was used to expel air in the slurry.
- xi) Cast moulds were stored in containers. The base of containers were filled with water to height of 1 cm to maintain a constant humidity. The containers were tightly sealed off with sticky tape preventing entry of air.
- xii) The remainder of the paste mix was used to cast the samples for the 3-point bending test. Wooden triangular prism moulds of 300 mm length and 75 mm width were used.
- xiii) For 3-point bending tests, total of 2 moulds were prepared for casting 1 sample per curing period of 28 and 56 days only. An additional sample was cast in case the samples get damaged.
- xiv) The moulds were positioned on the vibration table and the filling was done. Vibration table was used to expel air in the slurry as well as avoiding gaps within the slurry.

- xv) After casting into the wooden mould, the samples were left in a dry room for 24 hours. The moulds were removed, and the samples were stored in a closed humidity chamber at 23 degrees at set humidity of 90 %.

5.3 Specimen preparation for UCS

UCS samples due for tests were removed from container on the date of testing (Fig. 5.3). The container was re-sealed with sticky tape and stored while the samples removed were prepared for testing.



Fig. 5.3 UCS samples removed from container for test preparation

Sample height was trimmed to 100 mm with 50 mm diameter to maintain a ratio of 1:2 (Fig. 5.4). The mass of sample was recorded, and the samples were tested according to ASTM D2166 standard.



Fig. 5.4 UCS samples preparation

5.4 Unconfined compressive strength

The sample was placed directly under the loading plate of triaxial machine (Wykeham Farrance Tritech 50 kN) and centralised prior to loading. The procedure from AS1289.6.4.1 standard was used to do the UCS test. The loading rate for the UCS test was set at 2 mm per minute over a duration of 5 minutes.



Fig. 5.5 UCS testing to failure

Load and deformation data from the triaxial data logger were analysed to plot the stress-strain curve (Fig. 5.7) using the following equations;

Initial sample area (m²): $A_0 = \pi r^2$ (Eqn. 5.1)

Instantaneous area (m²): $A = \frac{A_0}{(1 - \varepsilon)}$ (Eqn. 5.2)

Stress (Pa): $\sigma = \frac{F}{A}$ (Eqn. 5.3)

Strain (%): $\varepsilon = \frac{\Delta L}{L_0} * 100$ (Eqn. 5.4)

UCS (Pa): $\sigma_{max} = \frac{F_{max}}{A}$ (Eqn. 5.5)

Young's modulus (Pa): $E = \frac{\Delta \sigma}{\Delta \varepsilon}$ (Eqn. 5.6)

where, F is the applied load, F_{max} is the maximum applied load prior to failure, ΔL is the vertical change in length, L₀ is the initial length of sample, Δσ is the change in stress and Δε is the change in strain over the elastic region.

Cross-sectional area of CPF samples undergoing loading increase in area due to the lateral extensions while there was no volume change. Thus, the instantaneous area was determined to calculate the applied stress.

A small chip of the failed UCS sample, around 50 to 60 g was oven dried for 24 hours for moisture content. The rest of the failed UCS samples were oven dried for use in the SEM and TGA tests.

5.4.1 UCS failure mode

The common failure modes observed from the UCS were shearing, splitting, crushing, bulging, and combination of these failures. The soft and wet samples exhibit a significant vertical deformation prior to failure. The failure of the dry and rigid samples were abrupt compared to the soft and wet samples. The soft jelly-like samples were mostly the ones with lower binder content of 3 %. Some samples cured for short term period (7 days) also indicated jelly-like deformation.

The images of the different modes of failures (Fig. 5.6) and the comparison of the stiffness from the stress and strain plots is shown below (Fig. 5.7).

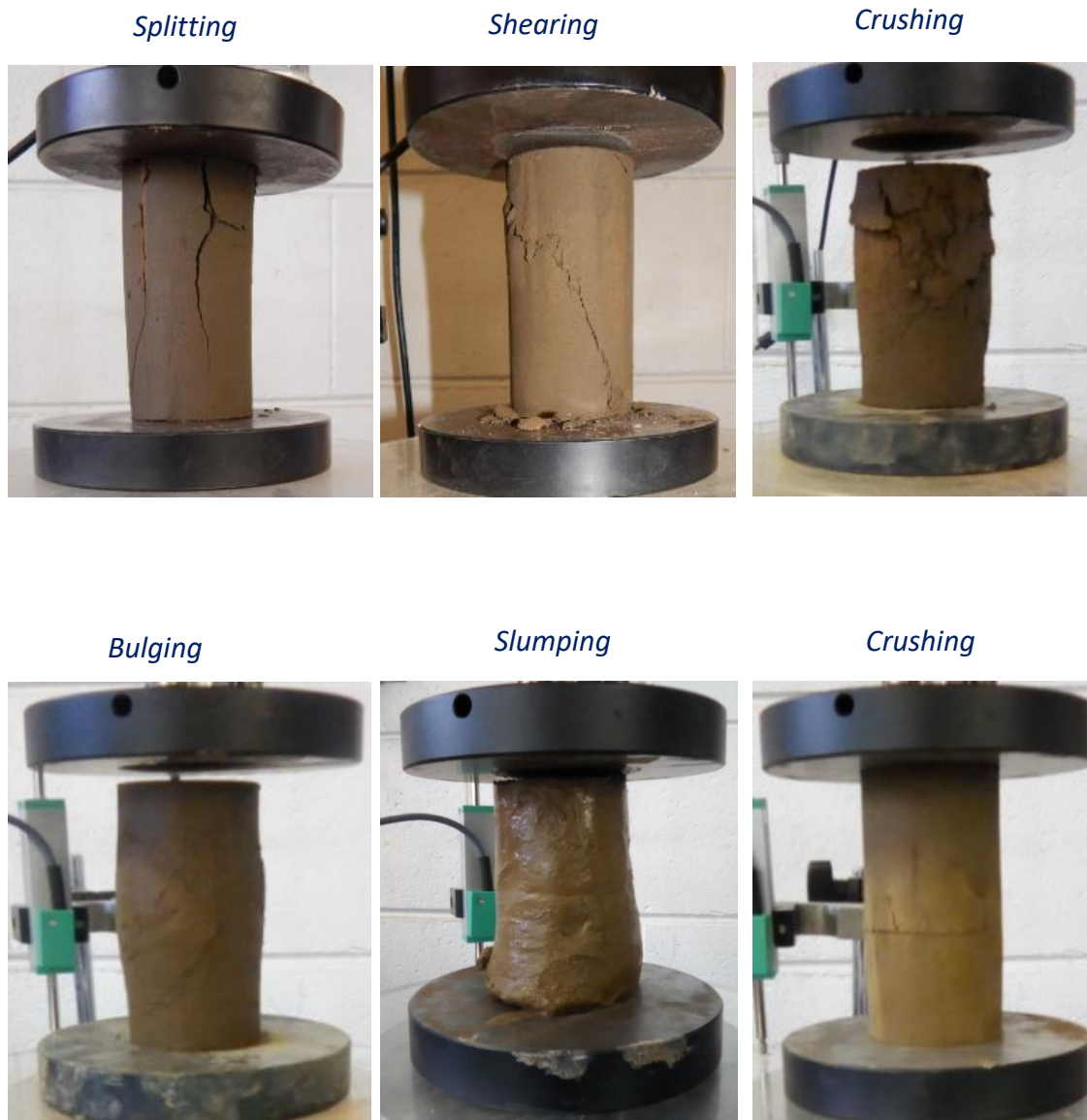


Fig. 5.6 UCS failure modes

Common failure modes observed for the competent samples were crushing and shearing while the soft samples failed through bulging and slumping. The competent samples took less time to fail and they were stiff while soft samples took longer and deformed both vertically and laterally. Thus, the Young's modulus value was high for hard and rigid samples compared to the soft samples as indicated below (Fig. 5.7) from the stress and strain plots from two uniaxial compression tests.

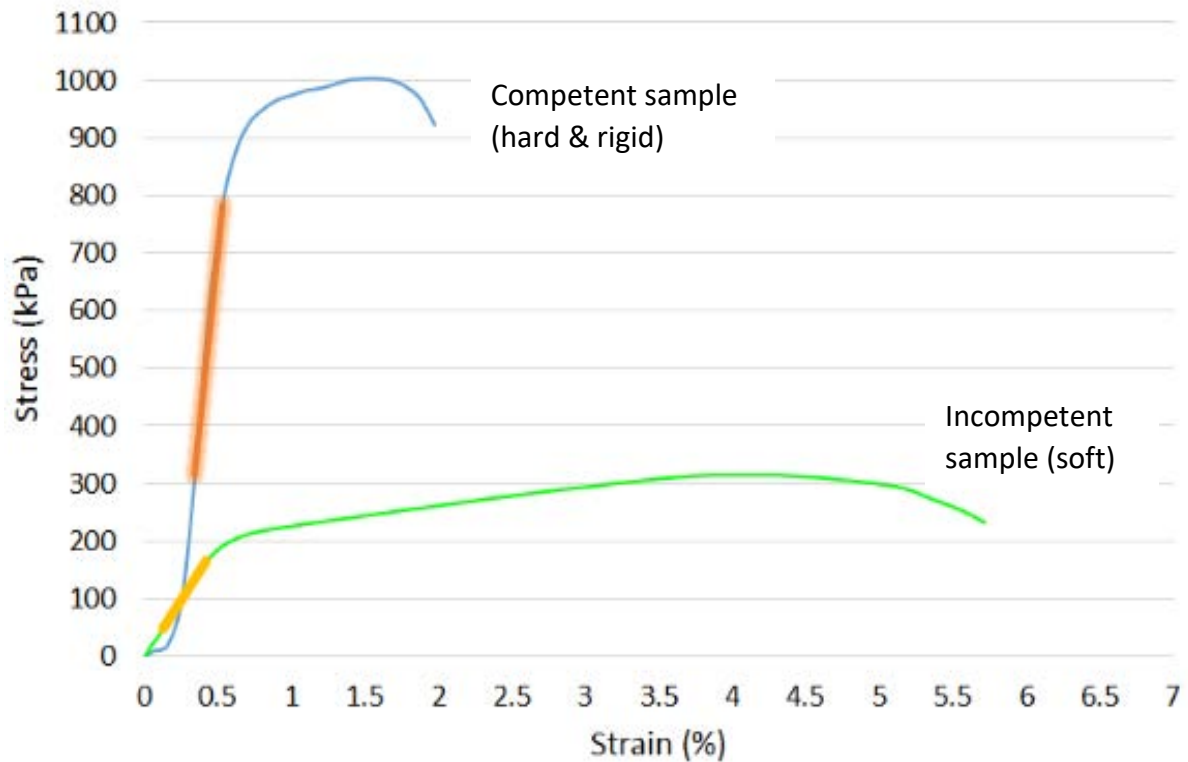
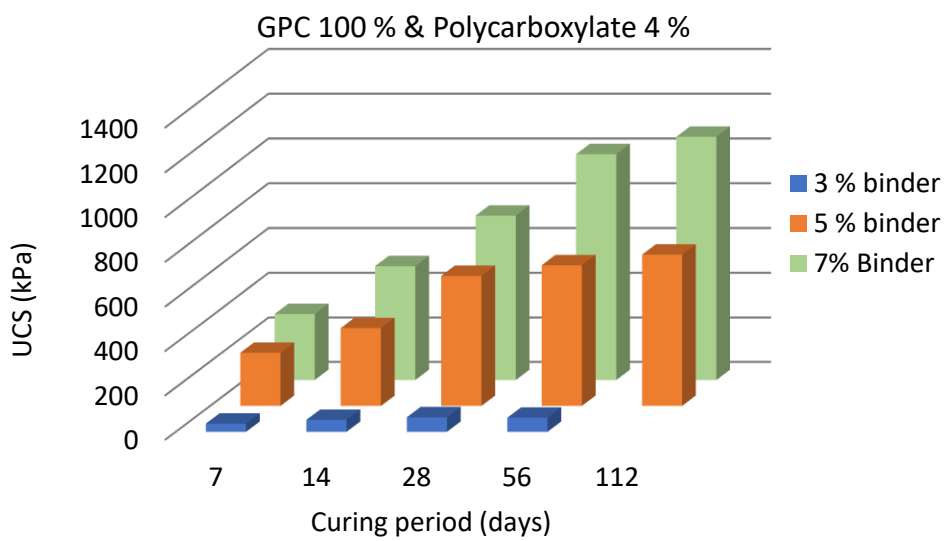
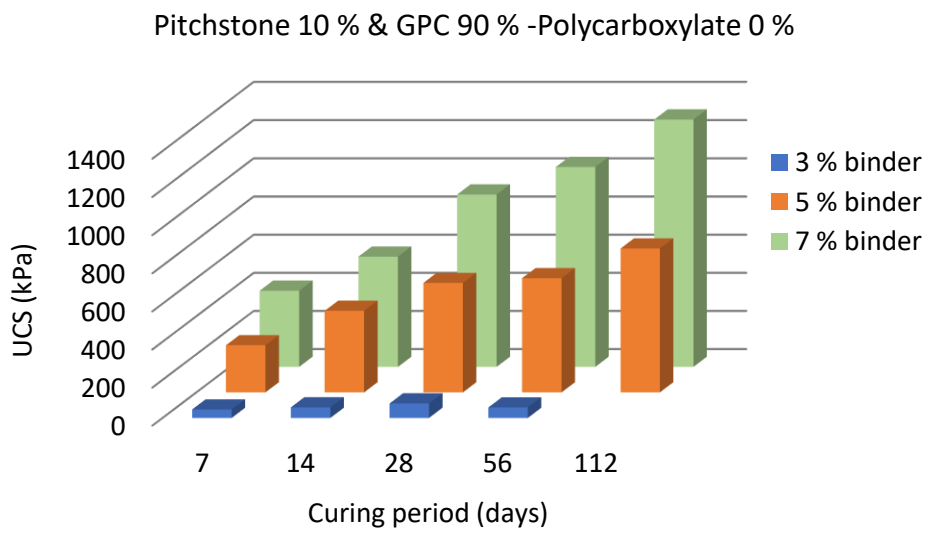
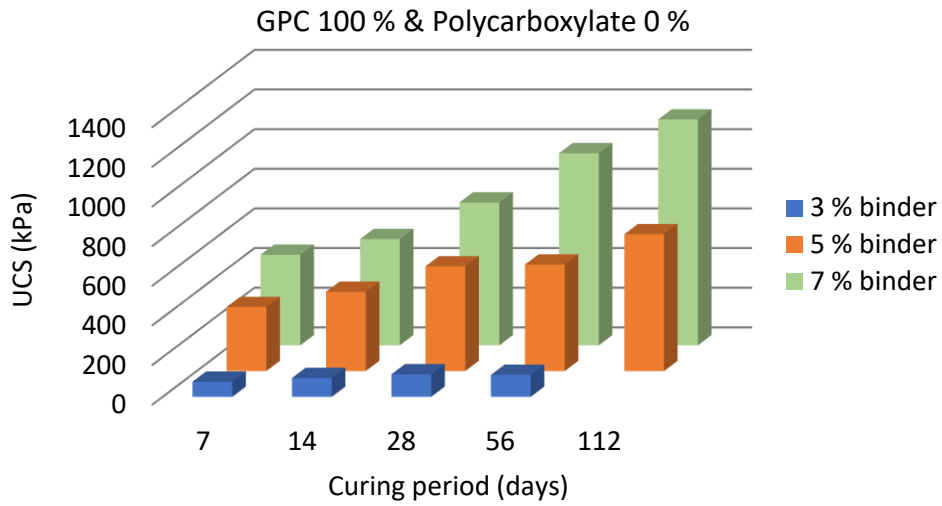


Fig. 5.7 Stress-strain and stiffness comparison

5.4.2 Effect of polycarboxylate dosage on UCS

Comparison of the influence of polycarboxylate was done on the 5 blends of binder used at different dosages from 0 %, 4 %, and 6 % at constant 74 % solid content. The results indicated no significant effect of polycarboxylate on the strength development. Although polycarboxylate significantly improved the rheology, the strength development showed no clear trend. Several graphs generated from 100 % GPC and pitchstone blends are shown below (Fig. 5.8).

The results of the UCS from the charts (Fig. 5.8) indicated that the binder dosage showed significant influence on the strength. When the binder dosage was increased, the strength also increased. Increasing the polycarboxylate dosage while maintaining the solid content (74 %) and the binder content has not increased the strength significantly over curing periods up to 112 days.



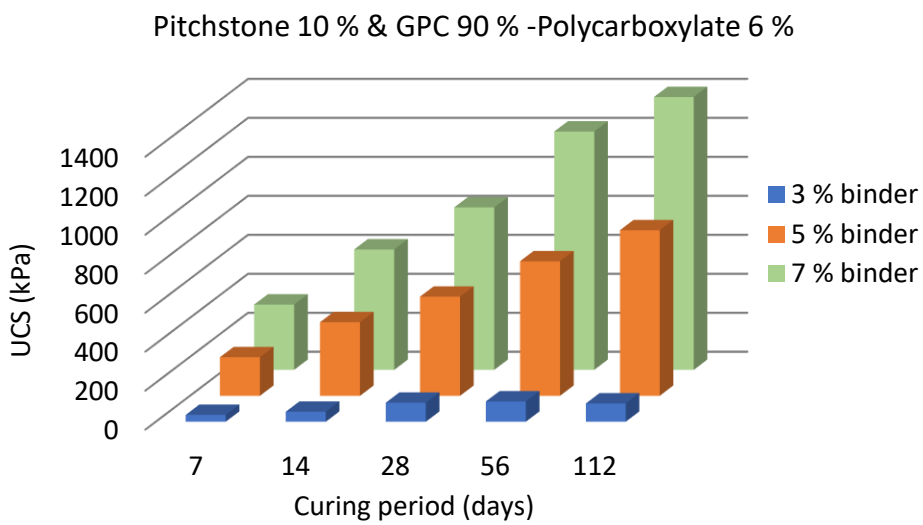
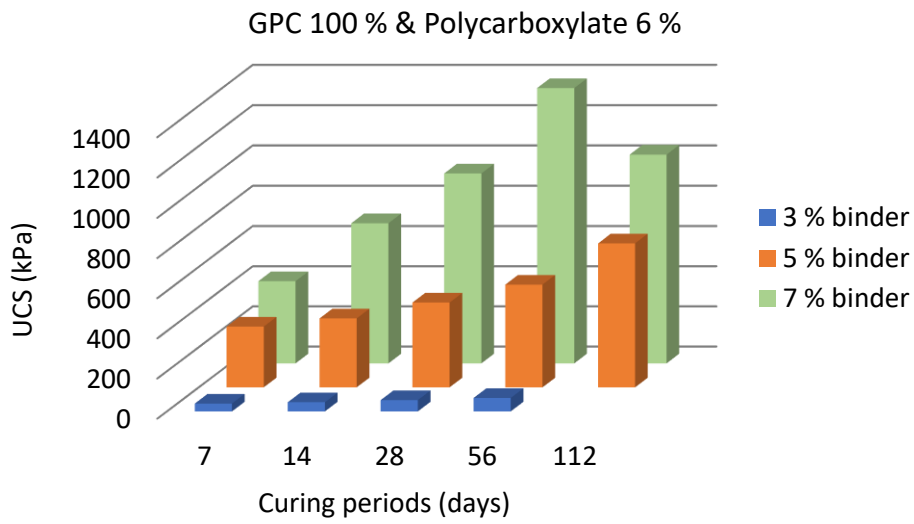
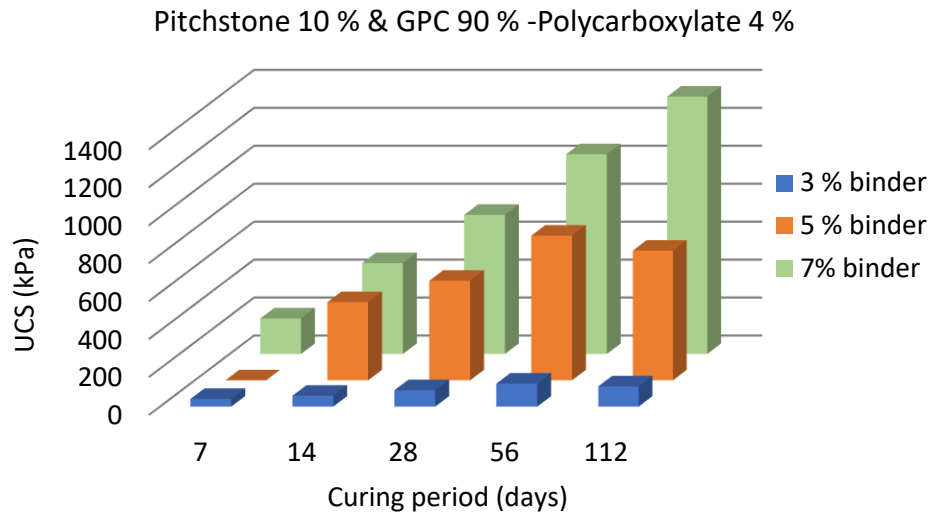


Fig. 5.8 UCS for different binders and dosages

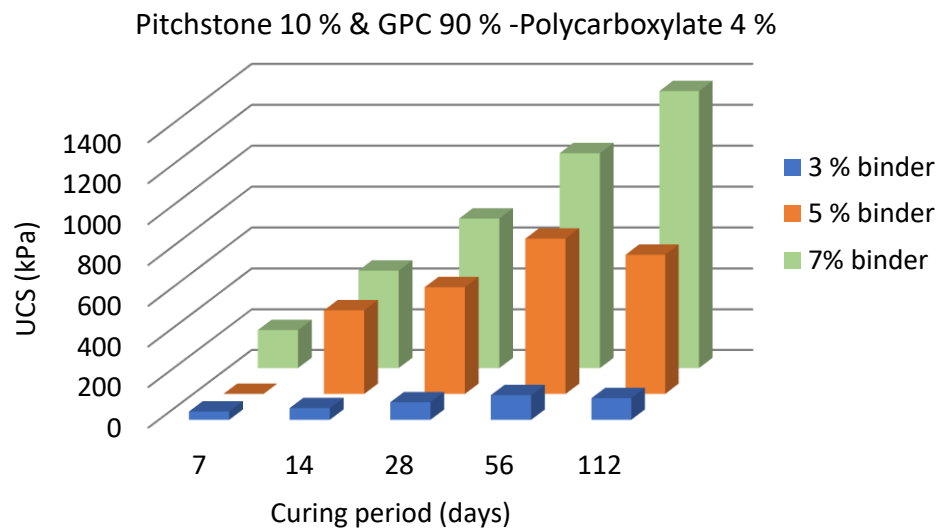
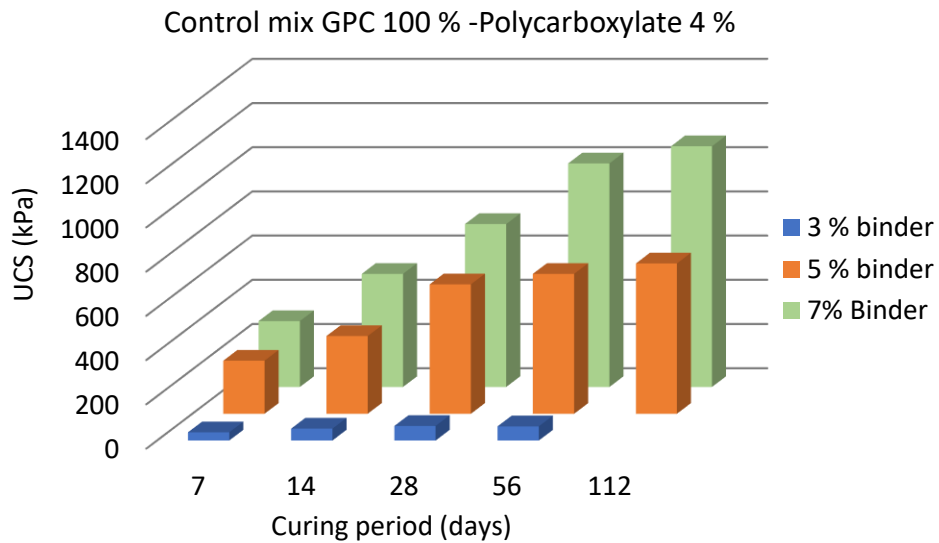
Further investigation into the effect of polycarboxylate on strength was done by sorting and tabulating the UCS test results of 21 different mixes. These 21 mixes have constant solid content of 74 %, constant binder dosage of 7 %, and varying dosages of polycarboxylate (0, 2, 4, 6, and 8 %). The UCS values and polycarboxylate dosage showed no apparent relationships as shown in Table 5.1. The results indicated that increasing the polycarboxylate dosage while maintaining the solid content does not necessarily influence the strength properties of the cemented paste fill.

Table 5.1 UCS of mixes at varying polycarboxylate dosage

Mix details								UCS (kPa)/ curing days				
Mix	Poly-Admixture (%)	Binder (%)	Portland (%)	Pitchstone (%)	Slag (%)	Flyash (%)	Solid content (%)	7 Days	14 Days	28 Days	56 Days	112 Days
Mix19	6%	7%	100%				74%	409	698	945	1,368	1,038
Mix22	2%	7%	80%	20%			74%	211	462	814	1,308	1,449
MixT26(Slg)	4%	7%	40%		60%		74%	264	818	982	1,275	1,657
Mix29	6%	7%	90%	10%			74%	335	618	834	1,223	1,416
Mix24	6%	7%	80%	20%			74%	253	526	884	1,170	1,437
Mix21	0%	7%	80%	20%			74%	249	440	791	1,154	1,285
Mix25	8%	7%	80%	20%			74%	327	573	942	1,110	1,354
MixT25(Slg)	0%	7%	40%		60%		74%	138	234	620	1,097	1,184
MixT25 (FA)	0%	7%	75%			25%	74%	284	502	904	1,065	1,199
Mix28	4%	7%	90%	10%			74%	187	478	733	1,053	1,338
Mix26	0%	7%	90%	10%			74%	400	579	904	1,048	1,297
Mix23	4%	7%	80%	20%			74%	219	531	847	1,029	1,428
Mix18	4%	7%	100%				74%	297	511	737	1,011	1,012
Mix16	0%	7%	100%				74%	457	536	721	969	1,140
Mix30	8%	7%	80%	10%			74%	239	438	740	960	1,193
Mix27	2%	7%	80%	10%			74%	305	397	658	931	1,259
Mix20	8%	7%	100%				74%	403	513	817	835	1,276
Mix17	2%	7%	100%				74%	301	474	605	824	985
MixT26(FA)	4%	7%	75%			25%	74%	-	314	452	620	1,092
MixT27(FA)	6%	7%	75%			25%	74%	81	240	405	601	1,045
MixT27(Slg)	6%	7%	40%		60%		74%	-	44	107	286	626

5.4.3 Effect of pozzolan and binder dosage on UCS

UCS strength comparisons were made for the different binder types used. The 5 charts below (Fig. 5.9) compared the UCS of the 5 blends of binder used at a constant polycarboxylate dosage of 4 % and at 74 % solid content for curing periods from 7 to 112 days.



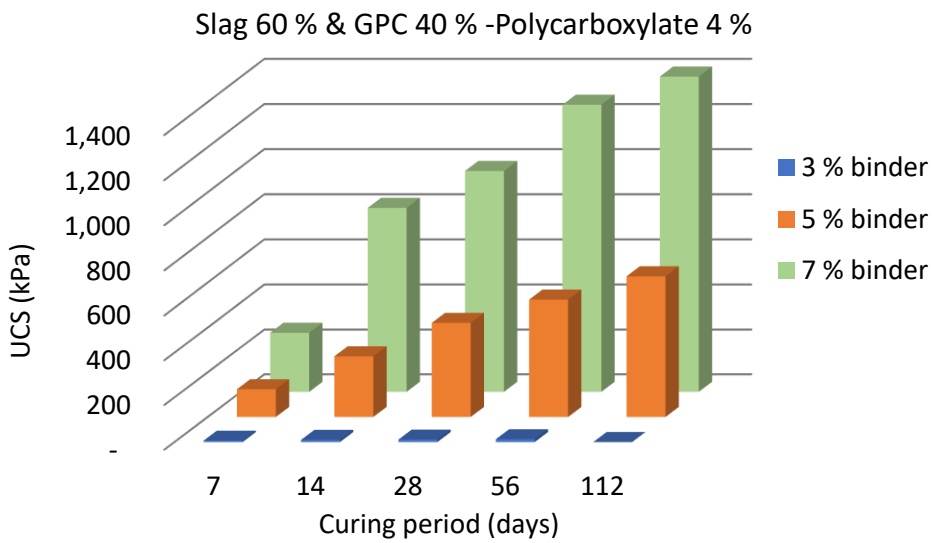
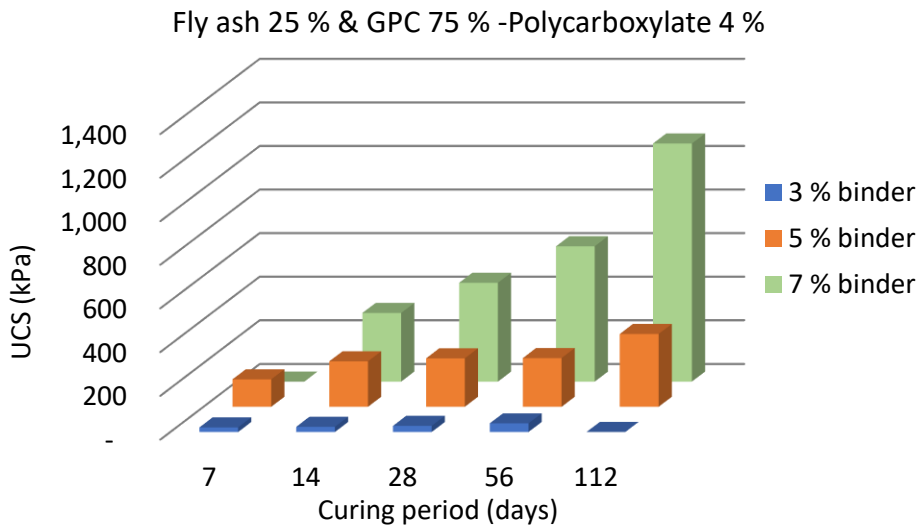
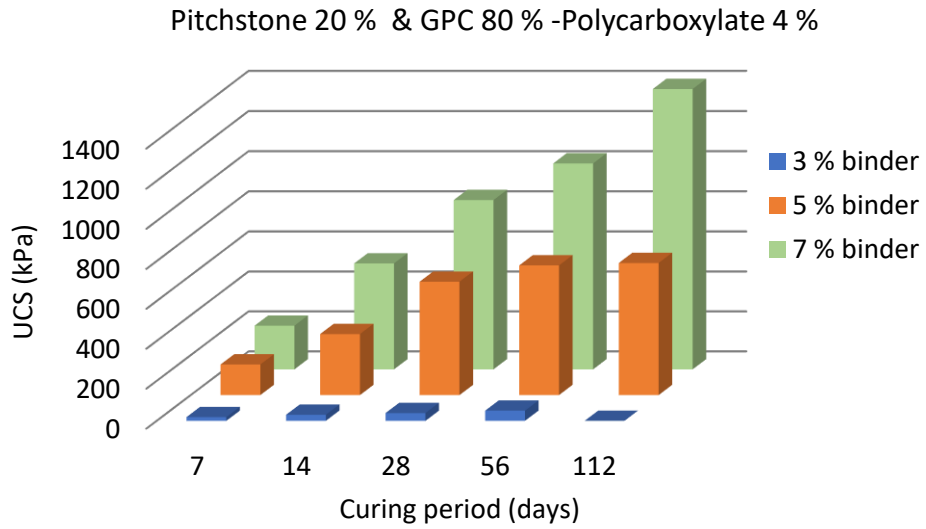


Fig. 5.9 UCS for different binder types and dosages

Results (Fig. 5.9) indicated that UCS for 5 blends of binder at lower dosage (3 %) was below 150 kPa, which was considered as incompetent and can liquefy when subjected to blasting. Binder dosage at 5 % and curing over 28 to 112 days reached 500 to 800 kPa, which can serve as competent fill for adjacent ore blasting. Binder dosage at 7 % and curing over 56 days attained strength above 1 MPa which can serve as crown, sill, or rib pillar support when mining adjacent stope. In addition, the increase in the curing time increased the strength of the CPF due to the continuation of hydration process.

The UCS results indicated that at lower binder content at 3 %, both the GPC (100 %) and the pitchstone blend could not reach the desirable strength of 1 MPa for ground support. At 5 % binder dosage, the long-term strength (28 to 112 days curing) reached around 500 to 800 kPa which served as competent fill for adjacent blasting, however, may not be desirable for crown or sill pillar support. The 7 % binder dosage attained strength beyond 1 MPa for control (GPC 100 %), as well as blended binder of pitchstone and fly ash. Pitchstone blend with GPC of 10:90 ratio indicated that it can be applicable in mine filling with strengths attained above 1 MPa, for curing days beyond 56 days. Results affirmed that the UCS value is directly related to binder dosage.

5.4.4 UCS and ground support limits

UCS limits for paste fill have been adapted in mines for different strength requirements. A minimum UCS target of 100 kPa is maintained to prevent liquefaction from blasting or seismic magnitude of 7.5 on Richter scale and is adapted from the work of Clough et al. (1989). A free-standing paste requires UCS less than 1 MPa, and for ground support requires UCS higher than 1 MPa (Belem et al., 2008).

Comparisons were made for binder dosage of 5 % and 7 %, at 74 % solid content, and curing up to 56 days. The 3 % binder dosage showed UCS value below 150 kPa and therefore was not included for this comparison. Results (Fig.

5.10 and Fig. 5.11) indicated that the strength increased with the increase in the binder dosage, thus the UCS values of 7 % binder dosage were higher than 5 % binder dosage. The strength further increased for 7 % binder dosage after 28 days curing period compared to 5 % binder dosage and this was due to the continued hydration reaction and strength development from the additional portlandite present in the higher binder dosage. In additions, the results indicated that the pozzolans attained unconfined compressive strength (UCS) comparable to 100 % GPC binder. Apart from the popular SCMs like fly ash (FA) and slag (SL), pitchstone fines (PF) of both 10 % and 20 % blend with GPC have attained meaningful strength for application in mine filling.

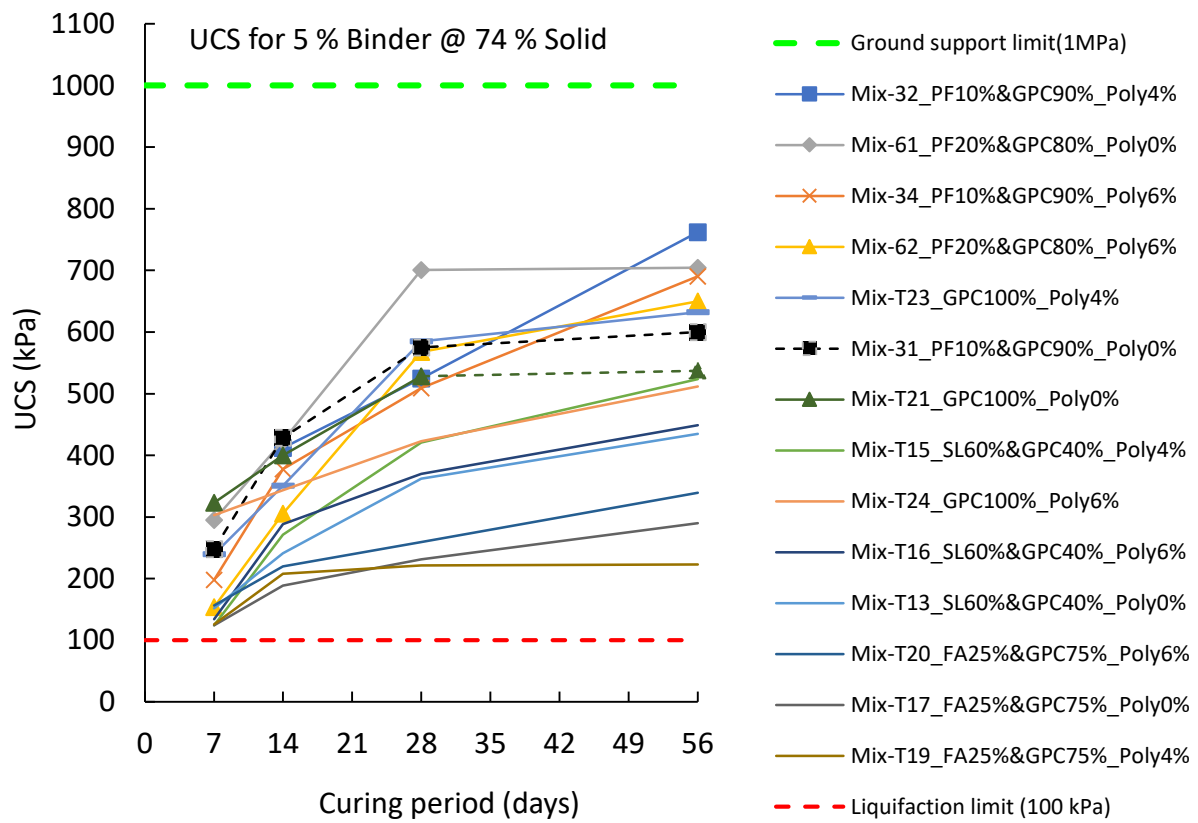


Fig. 5.10 Strength of 5 % binder mixes

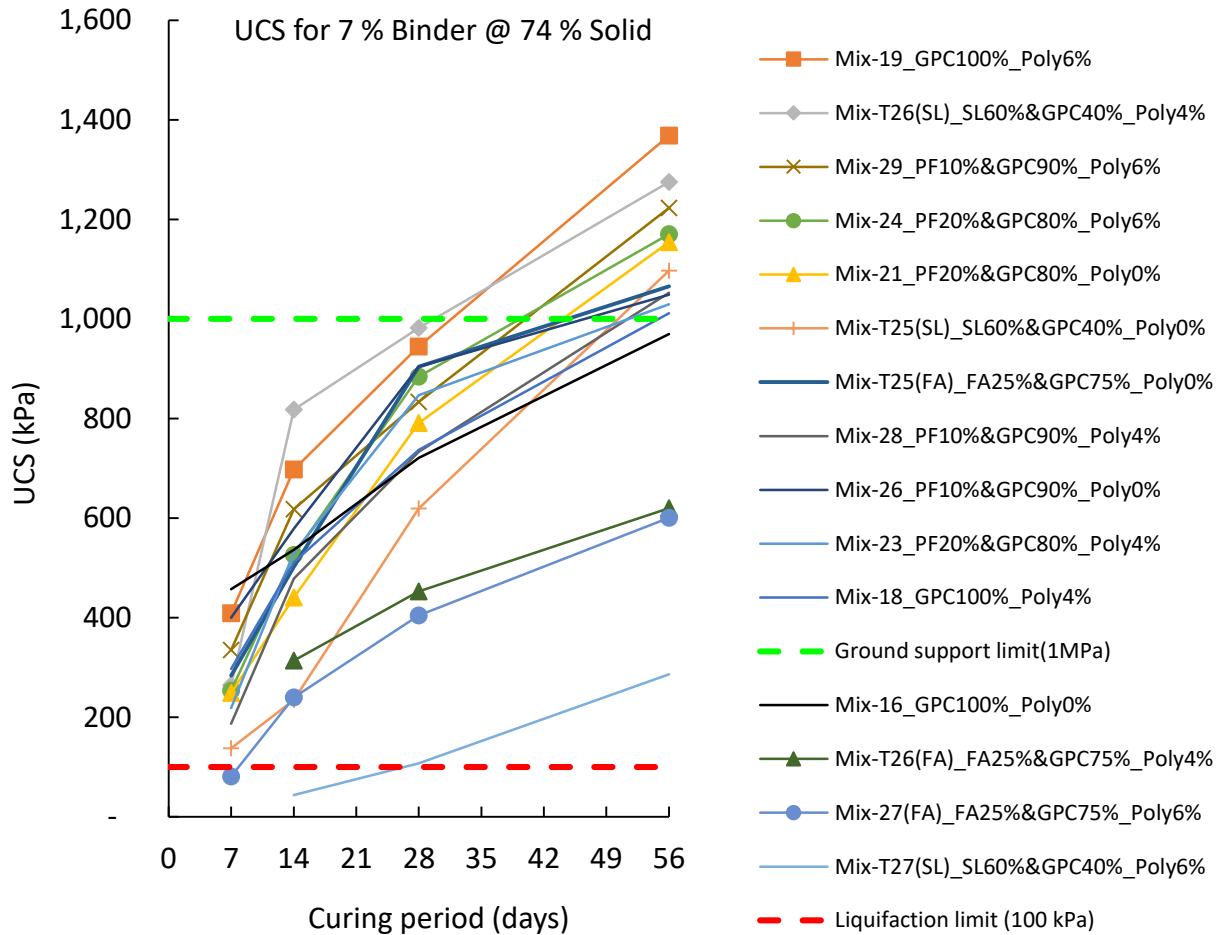


Fig. 5.11 Strength of 7 % binder mixes

5.4.5 Pozzolan and strength activity index (SAI)

Strength activity index (SAI) is a measure of reactivity of pozzolan with cement and is defined as the UCS of pozzolanic mix relative to the control mix over the same curing period and is expressed as percentage. Control mix was cast with ordinary Portland cement to compare the strength of the CPF to the other mixtures to determine the reactivity of the SCMs. ASTM C618 requires that pozzolanic materials must attain SAI above 75 % of control mix at 7 to 28 days.

SAI was compared for the 5 different binder types (Fig. 5.12) at different percentage replacement of GPC after 28 days curing period. The results indicated that the 5 binders have performed better with all the SAI values above the threshold of 75 %.

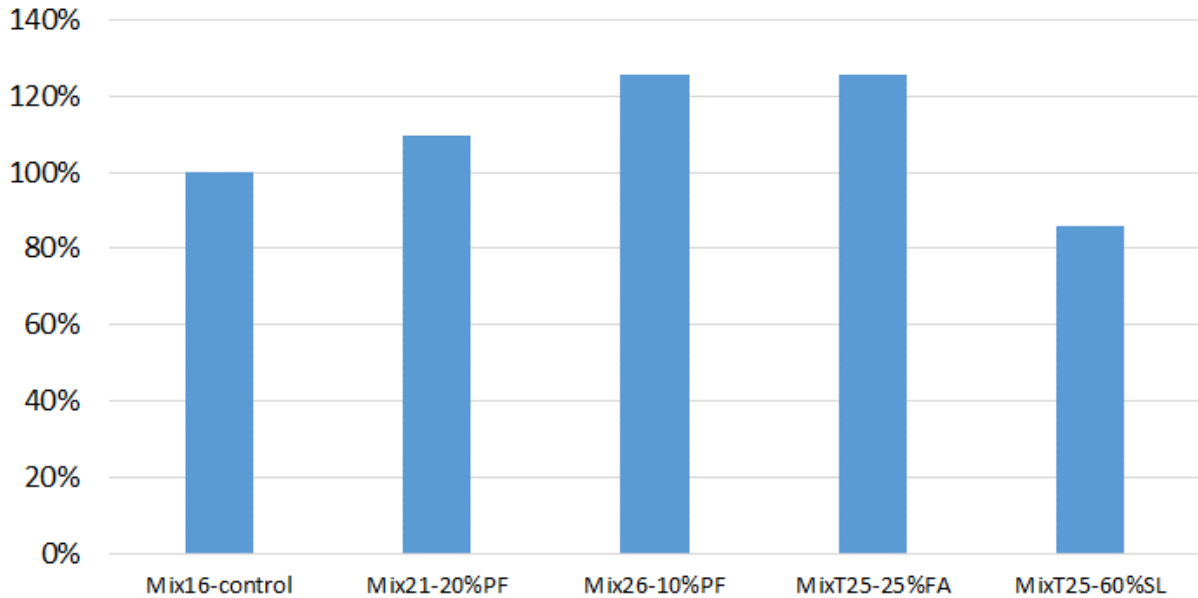


Fig. 5.12 Strength activity index (SAI) comparison after 28 days

The SAI for the 5 different binder types at different percentage replacement of GPC and over different curing periods up to 112 days were compared (Fig. 5.13). The results indicated that the 5 binders have performed better with all the SAI values above 75 % over the curing periods.

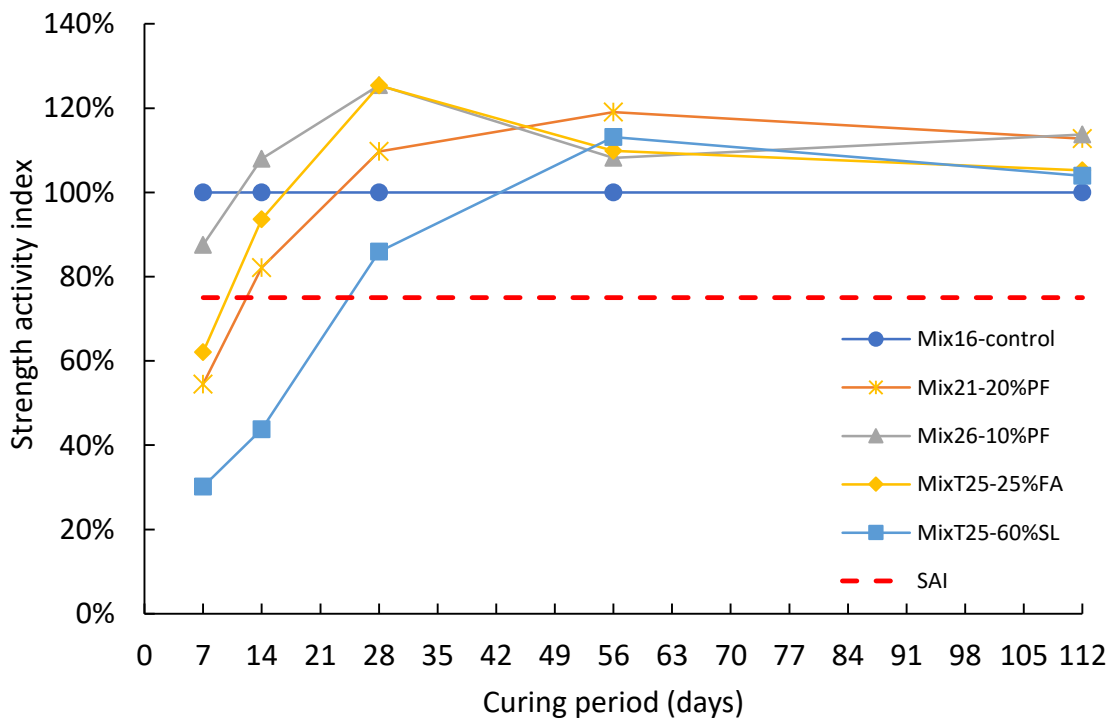


Fig. 5.13 Strength activity index (SAI) comparison over curing periods

In general, the results indicated that for all 5 binder types at 7 % binder dosage, 75 % SAI was attained at 28 days curing and in compliance with strength requirements as per ASTM C618 for concrete and paste fill application.

5.4.6 Effect of solid content on UCS

Comparison of the strength of 5 different mixes with varying solid contents (74, 75, 76, 77, and 78 %) for curing periods from 7 to 112 days is shown below (Fig. 5.14). For the 5 mixes, a constant binder dosage of 5 % was applied. The results (Fig. 5.14) indicated that the strength increased with the increase in the solid content.

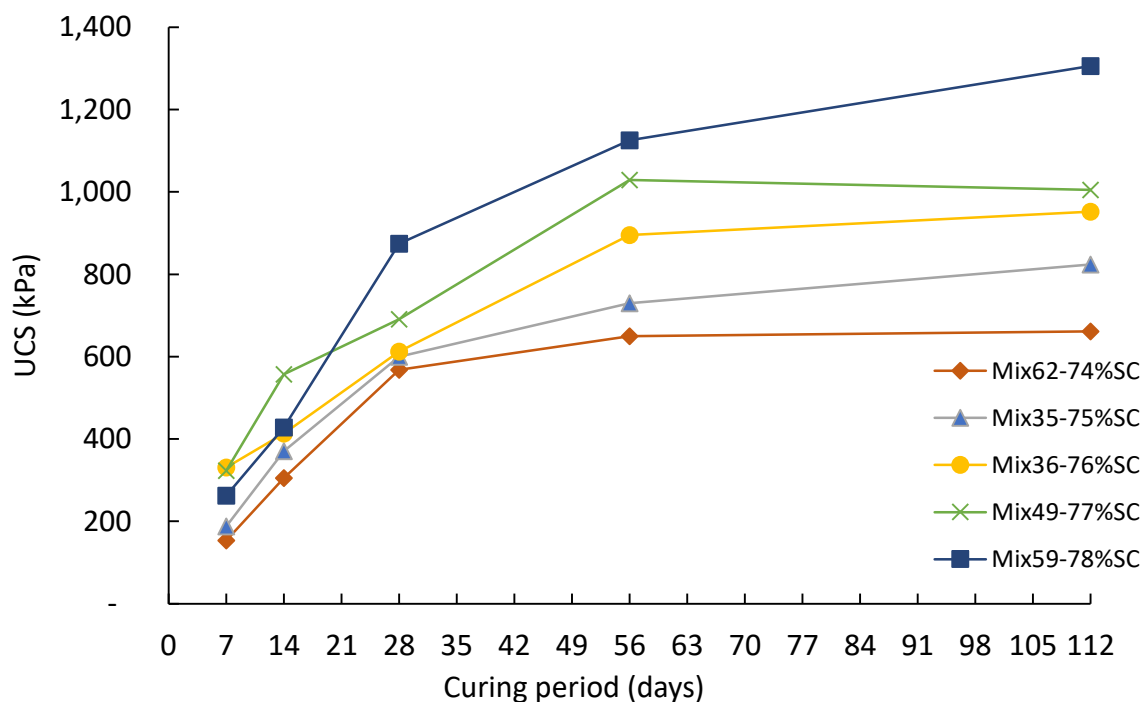


Fig. 5.14 UCS and solid content over curing periods @ 5 % binder

5.4.7 Young's modulus and UCS

UCS values were plotted against the Young's modulus for the several samples tested to establish a range where with a known UCS the stiffness can be

estimated. The results (Fig. 5.15) indicated a range of Young's modulus (E) that can be estimated for cemented paste fill. The range from the plots indicated that the boundary of E can be determined as:

- Young's modulus (minimum boundary) $E=150 * UCS$
- Young's modulus (maximum boundary) $E=250 * UCS$

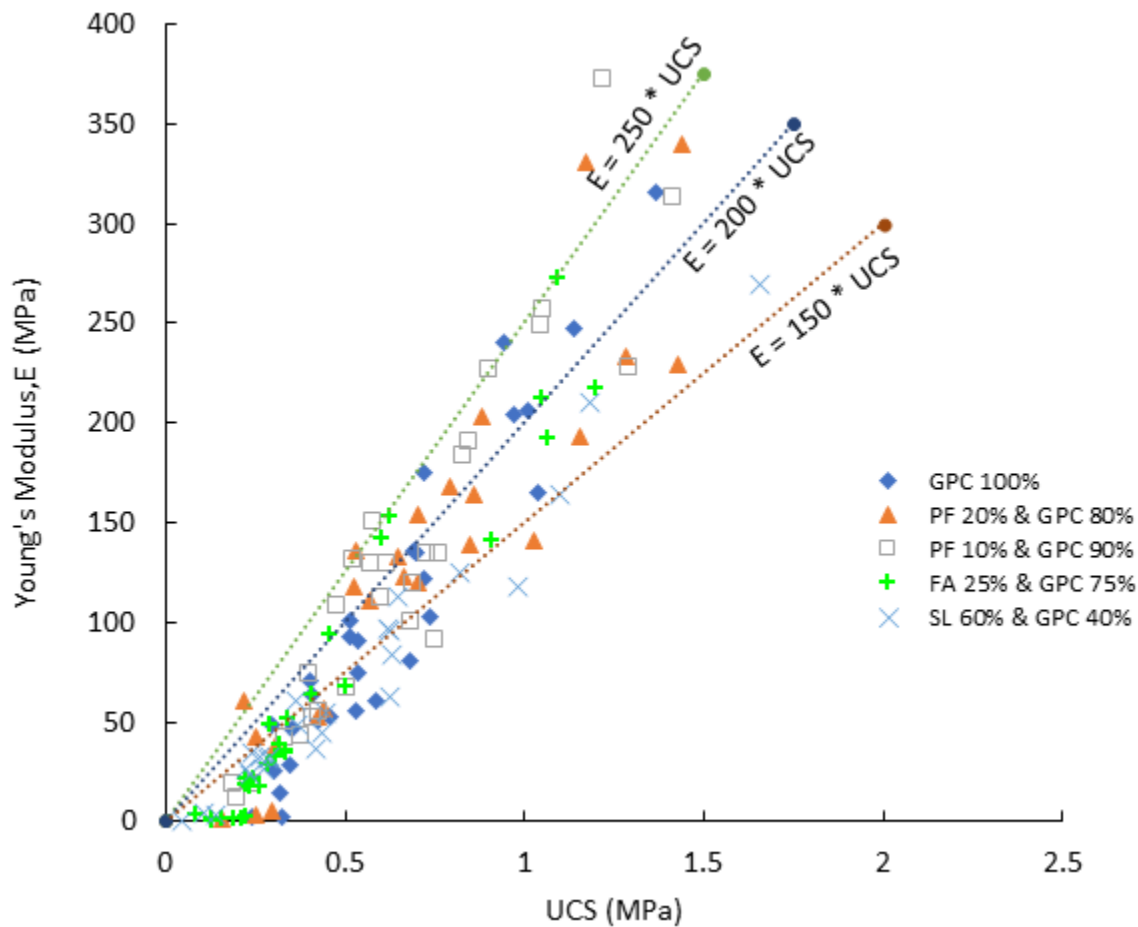


Fig. 5.15 E and UCS relations

5.5 Indirect tensile strength

Tensile strength of materials like rocks and soils are difficult to determine directly so other indirect strength tests methods are used. The indirect tensile strength (ITS) or the Brazilian test was done to determine the tensile strength of the paste fill sample. The procedure outlined in AS 1012.10 standard was used to do the

ITS test. ITS sample was trimmed to get a diameter to height ratio ranging from 1.5 to 2.5 and was tested using triaxial machine. The sample diameter was 50 mm with height trimmed to 25 mm, maintaining a ratio of 2.



Fig. 5.16 ITS specimen preparation

The sample was placed inside the bracket, secured, centralised and loaded. The guide bracket was used to prevent the sample from rolling out. The guide was removed prior to loading. The loading rate for the ITS test was set at 1 mm per minute over a duration of 5 minutes.

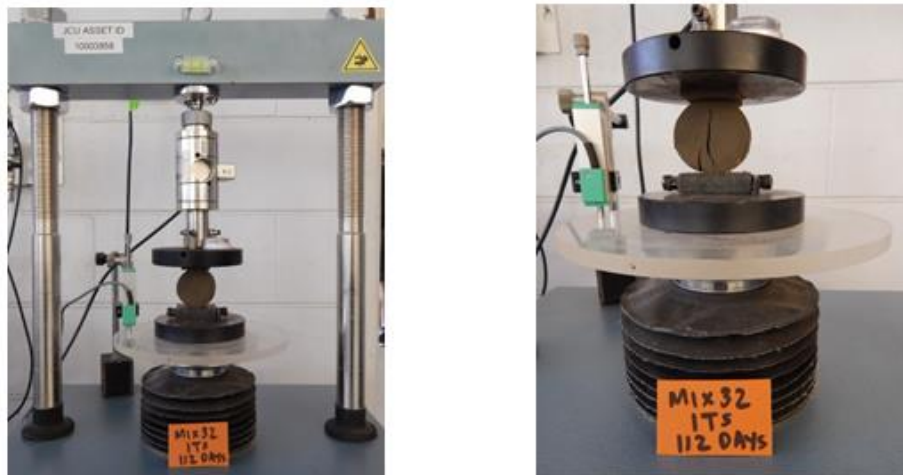


Fig. 5.17 ITS testing to failure

Load and deformation data from the triaxial data logger was analysed to determine the tensile strength (σ_t). The ITS value was calculated as:

ITS:
$$\sigma_t = \frac{2P}{\pi Dh} \quad (\text{Eqn. 5.7})$$

where P is the applied load, D is the diameter of the sample, and h is the thickness of the sample.

5.5.1 Relevance of ITS and UCS

ITS values were plotted against the UCS values for the several samples tested to establish a range where UCS can be estimated from ITS values. The results (Fig. 5.18) indicated a range of ITS value that can be estimated for cemented paste fill. The range from the plots indicate that the boundary of ITS can be determined as:

- ITS (minimum boundary) ITS = 0.125 * UCS
- ITS (maximum boundary) ITS = 0.250 * UCS

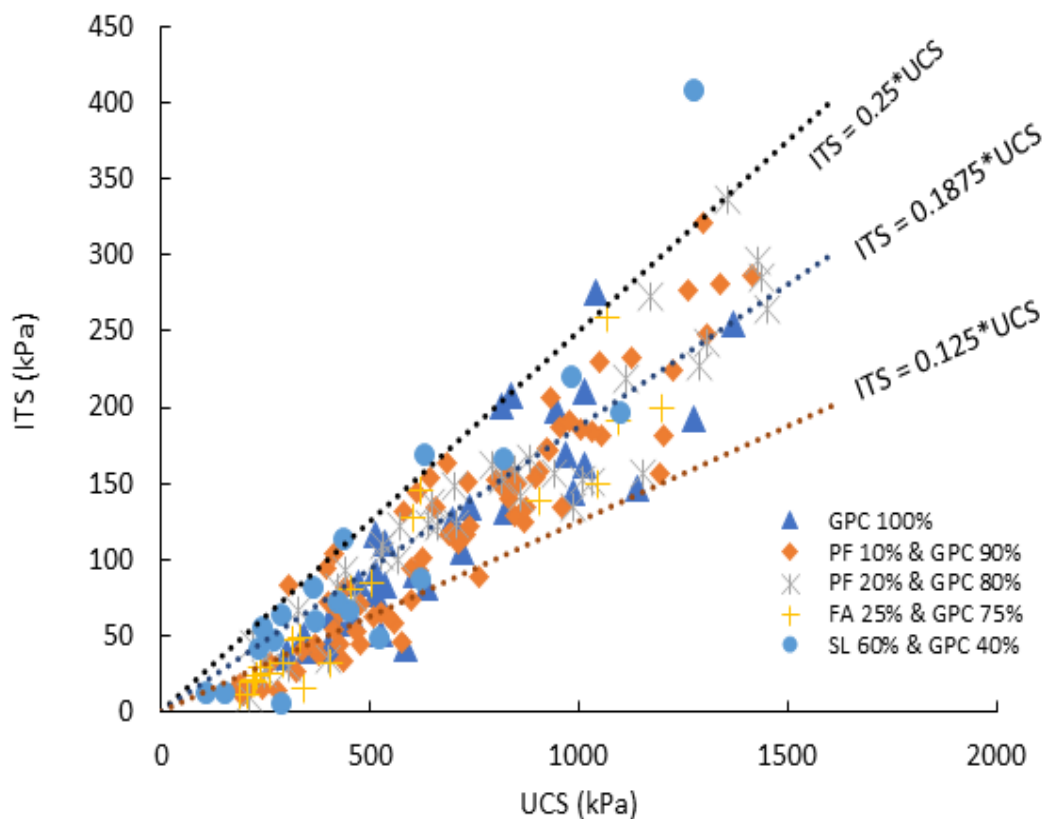


Fig. 5.18 ITS with UCS relations

5.6 Flexural Strength

The 3-point bending test was applied to determine the flexural strength of the cemented paste fill. On the testing day, the samples were removed from the humidity chamber and dimensions were measured.



Fig. 5.19 Casting and storing 3-point samples

The whole sample was tested with two points at the base with 220 mm apart, and the load was applied centrally at the top point to failure. With the 3-point bending test, only the flexural strength was determined. Stress-strain chart were not plotted for samples tested as they failed through sudden snapping at the maximum load.

Flexural strength:
$$\sigma_t = \frac{3FL}{2bh^2} \quad (\text{Eqn. 5.8})$$

Where b and h are the width and thickness of the beam, L is the distance between the contact point at the base, and F is the maximum applied load at failure.

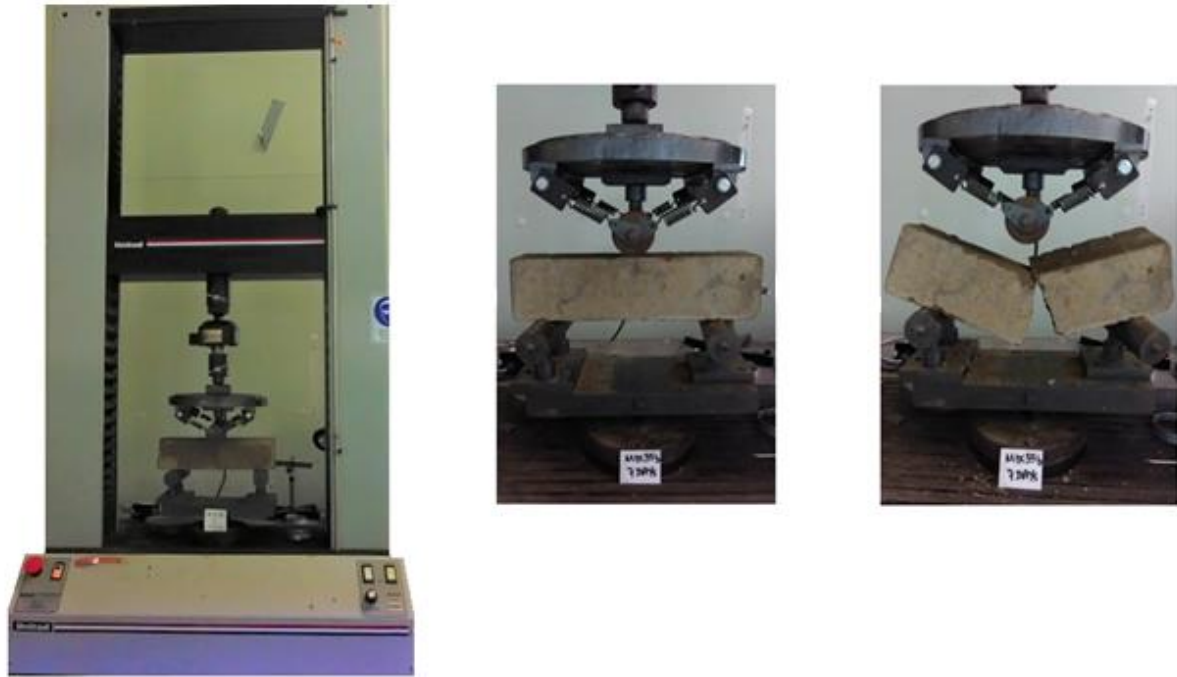


Fig. 5.20 3-Point loading to failure

5.6.1 Relevance of flexural strength and UCS

The flexural strengths determined from some of the samples tested were compared against the UCS values. Several mixes were sorted by UCS values from the small to large and flexural strength values were plotted against the UCS values of the same mix over 28 days curing. The results (Fig. 5.22) indicated that there was absence of meaningful correlation of UCS to flexural strength.

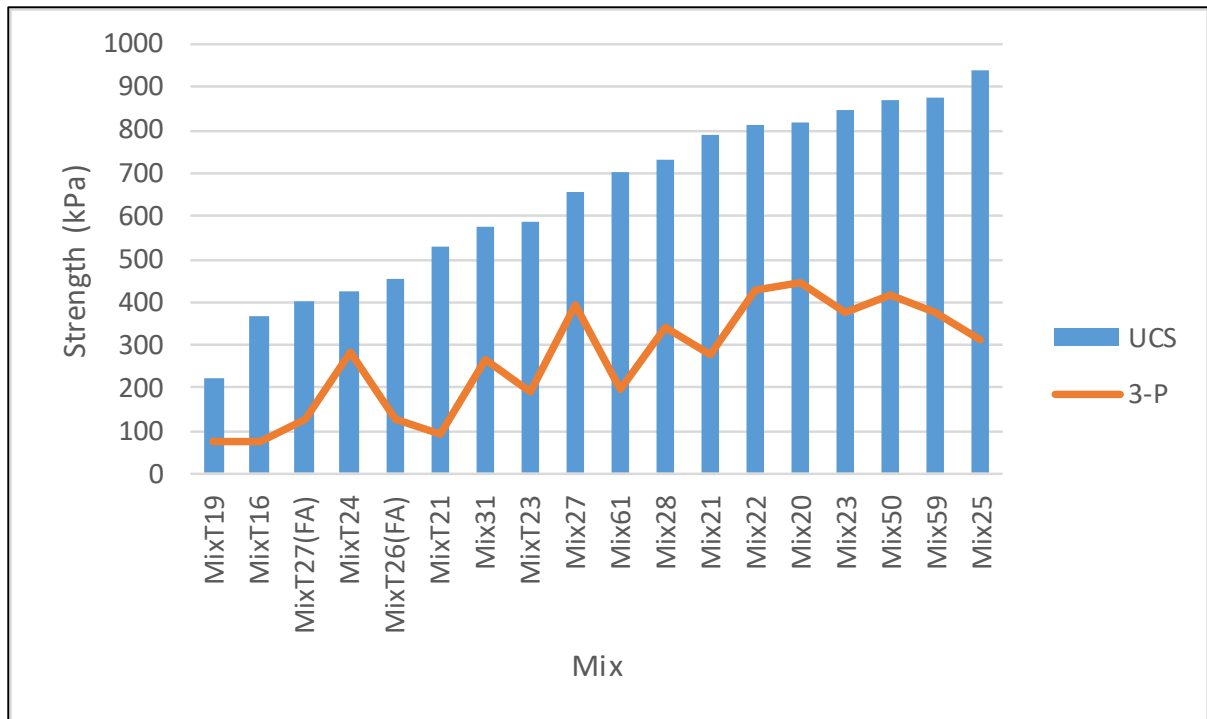


Fig. 5.21 Strength comparison of UCS and flexural @ 28 days cure

The flexural strength did not increase as expected corresponding to the increase in the UCS. Same comparison was done for 56 days curing and the results were similar, with no clear correlation established. The flexural strength was within 100 to 400 kPa and not showing correlation to either the binder dosage or the solid content.

Majority of the samples cast for the 3-point bending tests cracked due to shrinkage during the curing periods. The cracking was due to shrinkage of clay in the tailings. Several measures were taken to tighten the mould with cable ties and sticky tapes to counteract the expansion and contraction. However, that did not prevent the cracking and most of the samples were discarded.

Further test work with an improved method of casting and curing of the 3-point samples is required to observe any relationships with UCS. Using a metal mould may be an option, however in this study, it was not trialled as the number of moulds were few and not enough samples can be cast.



Fig. 5.22 Samples cracking with and without cable fasteners

5.7 Summary

The three strength parameters tested were the unconfined compressive strength (UCS), indirect tensile strength (ITS), and the flexural strength. UCS is a common strength property that most mines use to determine the strength of the paste fill. UCS values less than 100 kPa is susceptible to liquefaction when undergoing vibration from blasting activities.

Results from the tests indicated that at lower dosage of binder (3 %), the UCS value was below 150 kPa, which was considered as incompetent and can liquefy when subjected to blasting. Binder dosage at 5 % and curing over 28 to 112 days reached 500 to 800 kPa, which can serve as competent fill for adjacent ore blasting, however, may not be desirable for pillar support. Binder dosage at 7 % and curing over 56 days attained strength above 1 MPa which can serve as crown, sill, or rib pillar support when mining adjacent stope.

Strength activity index (SAI) is a measure of reactivity of pozzolan with cement and is defined as the UCS of pozzolanic mix relative to the control mix over the same curing period and is expressed as percentage. ASTM C618 requires that pozzolanic materials must attain SAI above 75 % of control mix at 7 to 28 days. Results indicated that for all 5 binder types at 7 % binder dosage, 75 % SAI was

attained at 28 days curing and in compliance with strength requirements as per ASTM C618 for concrete and paste fill application.

Plots of UCS and Young's modulus (E) of different mixes of cemented paste fill were done and a range of values were established indicating E ranged from $E=150 * UCS$ to $250 * UCS$. Moreover, plots of ITS and UCS were done and the range of values indicated ITS ranges from $ITS = 0.125 * UCS$ to $0.25 * UCS$. Plots of values of flexural strength to UCS were done, however, no clear trend was established due to majority of the samples for 3-point load tests were defective.

Comparison of the influence of polycarboxylate was done on the 5 binder types used at different dosages from 0 %, 4 % and 6 % at constant 74 % solid content. The results indicated no significant effect of polycarboxylate on the strength development. Although polycarboxylate significantly improved the rheology, the strength development showed no clear trend.

6. Microstructure development

6.1 Introduction

Microstructure of the cemented paste (CPF) is influenced by the development of the hydration products such as ettringite, portlandite (CH), and calcium silicate (C-S-H). Hydration products and evolution of microstructures was studied using scanning electron micrograph (SEM) and thermogravimetry analysis (TGA).

SEM was done to observe the growth of hydration products at range of curing days from 7 days, 14 days, and 28 days. TGA was done on mixes of 7 % binder dosage to measure the amount of portlandite present at range of curing periods 7 days, 14 days, 28 days, and 56 days. The decrease in the amount of portlandite over curing periods indicates the growth of calcium silicates which further increases the strength of the CPF. Thermogravimetry analysis (TGA) was done on the oven dried and grounded CPF. Thermal analyser instruments were used in an inert (nitrogen) environment to measure the mass changes over increase temperature. The phase change indicates the presence of the different compounds.

6.2 Scanning electron micrograph

Scanning electron micrograph (SEM) analysis was done on very small fractured CPF specimens from the UCS testing.

6.2.1 Samples preparation for SEM

Isopropanol infiltration and oven drying was performed on samples to expel free water. Preparation of the samples for SEM is outlined below.

- i) Chips were extracted from the failed samples from UCS test and were dried in oven for 24 hours.

- ii) The oven dried samples were removed and were fully submerged into isopropanol solution in a small container for 24 hours.
- iii) Samples were removed from isopropanol bath and oven dried at low temperature (40 to 60 °C) for 24 hours.
- iv) Samples were packed in a sealed plastic bag and stored.
- v) To do SEM, the samples were taken to analytical laboratory for preparation. The samples preparation involved carbon coating one side of plate.
- vi) Specimens were loaded into the machine Hitachi SU5000. Electron beams were directed to the specimen to produce image with high magnification and resolution.
- vii) Images were captured at different magnifications (5 μm , 10 μm , 20 μm , 50 μm and 100 μm).

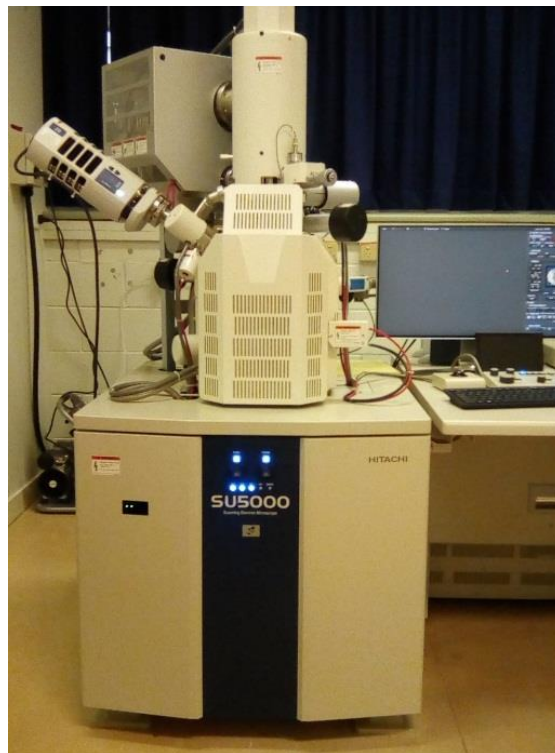


Fig. 6.1 SEM machine Hitachi SU5000 for scanning specimen

SEM films were captured and examined to understand the formation of hydration products like portlandite (CH), calcium silicate (C-S-H), ettringite and how the strength was affected. In addition, porosity and distribution of voids were studied using the SEM images. Pore space distribution in CPF is influenced by curing time, binder type, and solid content (Xu et al., 2018).

6.2.2 SEM of George Fisher mine tailings

SEM of George Fisher Mine tailings were done at different magnification to use as a baseline to compare the growth of hydration crystals and precipitates. The SEM image below (Fig. 6.2) indicated the microscopic grain shape at 5 μm and 10 μm scales.

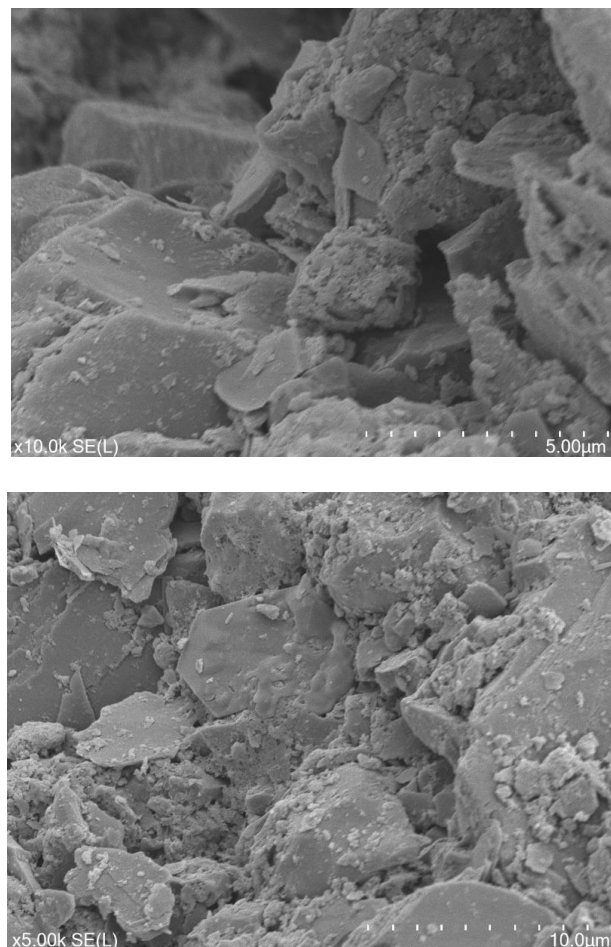


Fig. 6.2 SEM of tailings at 5 μm and 10 μm scales

The micrograph of the mine tailings indicated that the fines (< 75 µm) of the tailings were mostly clay given the flaky and flat morphology of the grains.

6.2.3 Microstructure development comparison

Microstructure developments for several mixes with higher strength were compared. Samples with lower strength crumbled during preparation and shanks could not be easily produced to make a good comparison. Ideally SEM in early curing days and up to 28 days was preferred to view the growth of hydration products (crystals and precipitates) and days beyond 28 days may have fully developed crystals and difficult to discern.

Selected mixes of 7 % and 5 % binder dosage were used to show the changes in the crystal morphology of the specimens over the curing periods as well as the influence of binder dosage on the growth of hydration products.

i) Microstructure development of control mix 16

Mix 16 was a control mix of 7 % binder dosage, consisting 100 % GPC with no pozzolans and plasticizer added. The SEM images were compared for 7 days, 14 days, and 28 days to understand the development of hydration products over curing periods.

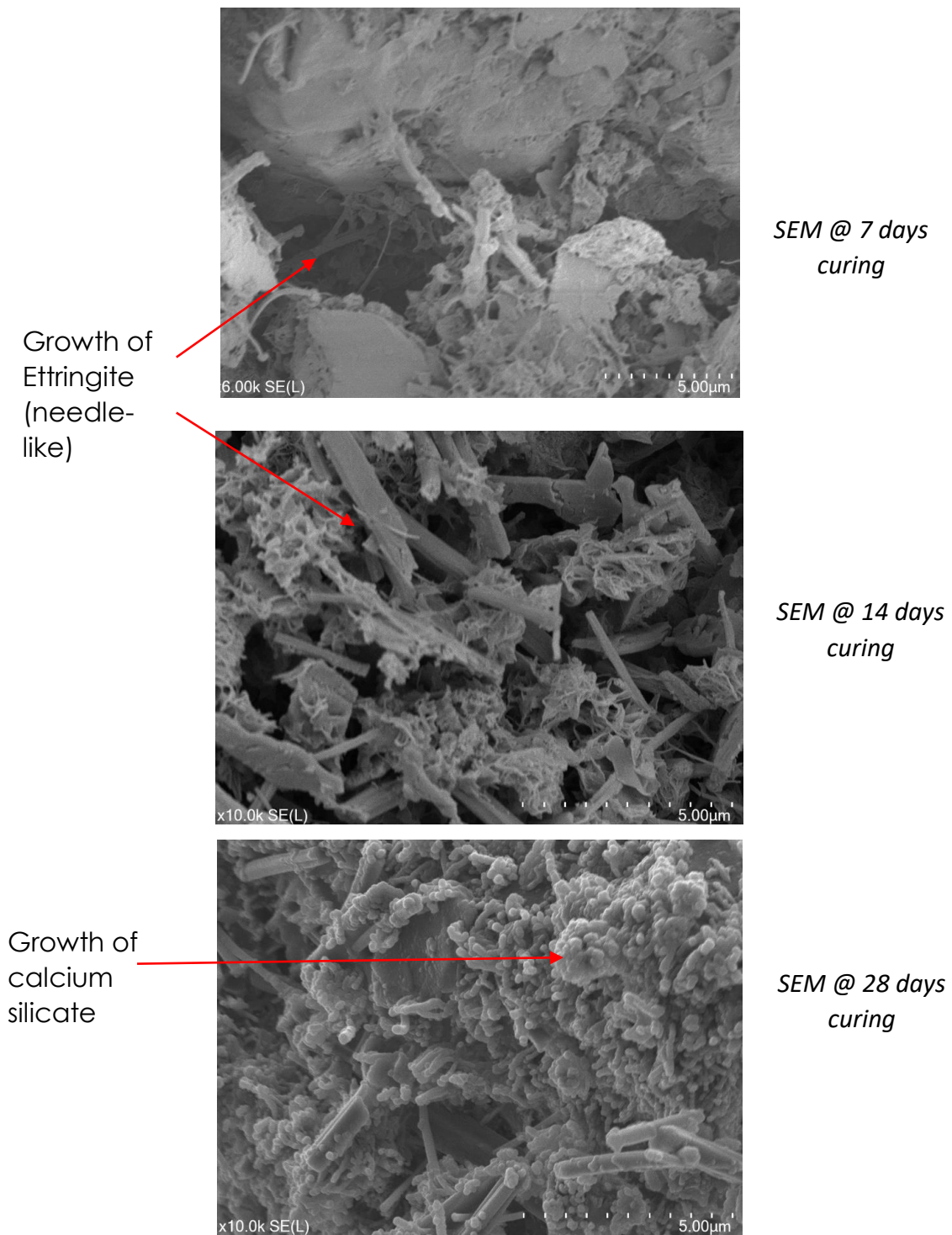


Fig. 6.3 Comparison of SEMs of mix 16

The SEM of mix 16 (Fig. 6.3) showed that during the early curing periods (7 to 14 days), ettringite minerals were developed, and at later curing periods (> 28 days), calcium silicates were developed. The growth of calcium silicates occupied voids at longer curing periods. Similar trend of growth of hydration

products were observed for other mixes that were analysed as shown below (Fig. 6.4, Fig. 6.5, and Fig.6.6).

ii) Microstructure development of control mix 19

Mix 19 has the same amount of ingredients as control mix 16, however, polycarboxylate dosage of 6 % was added to study its influence on the growth of hydration products over curing periods.

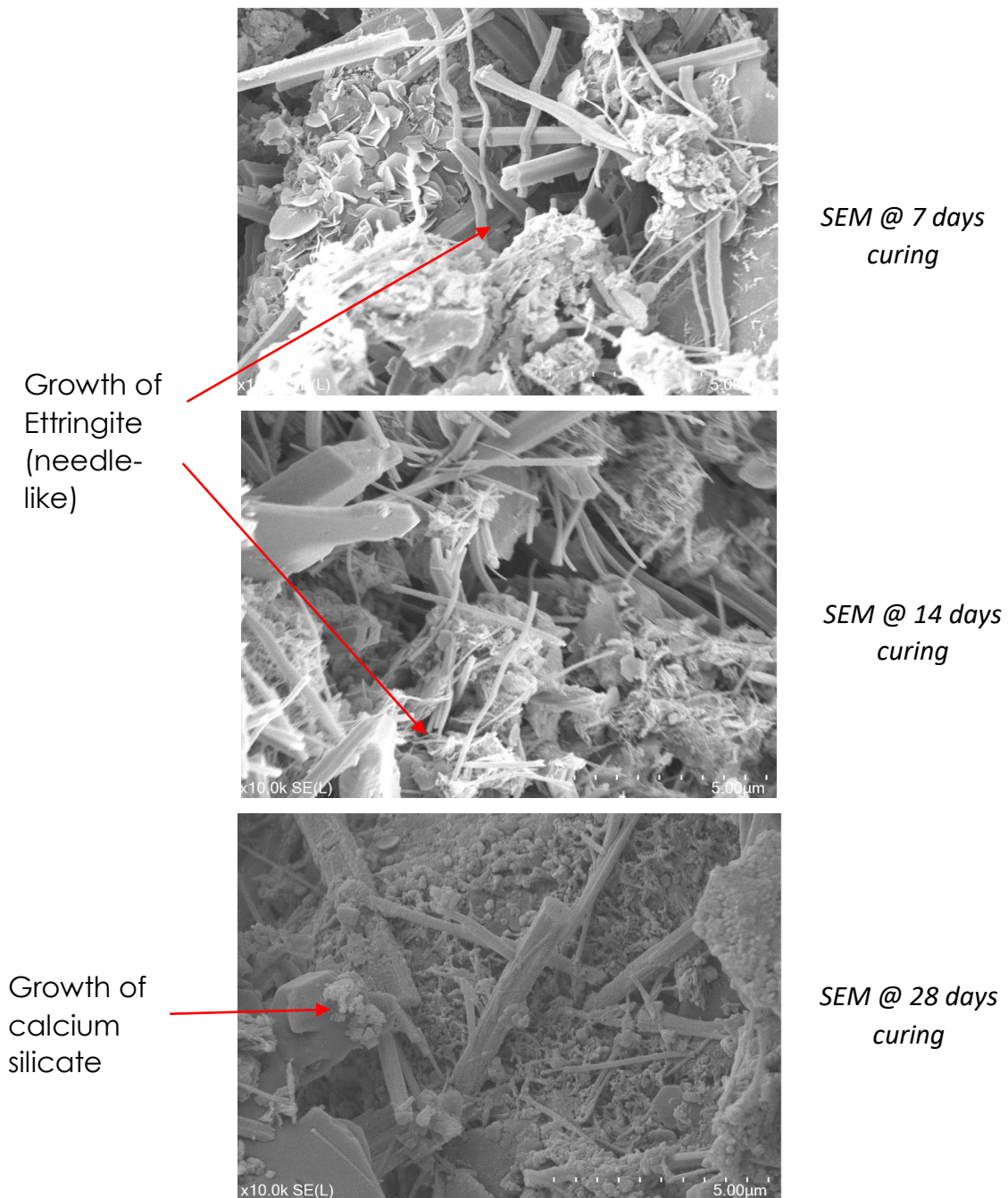


Fig. 6.4 Comparison of SEMs of mix 19

iii) Microstructure development of control mix 24

Mix 24 has 7 % binder in the ratio of 20:80 pitchstone to Portland cement respectively. A dosage of 6 % polycarboxylate plasticizer was added to study its influence on the development of the hydration products.

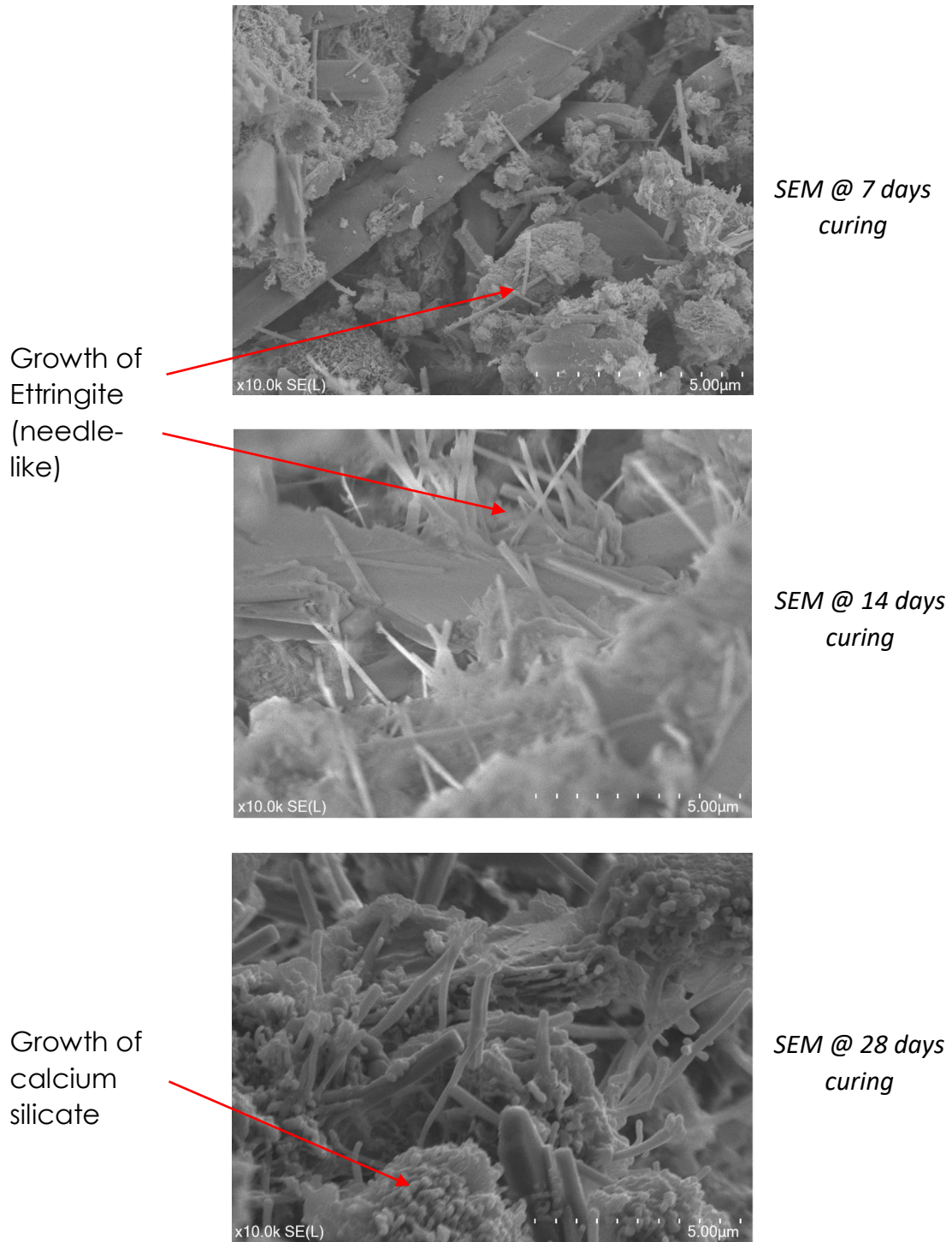


Fig. 6.5 Comparison of SEMs of mix 24

iv) Microstructure development of control mix 29

Mix 29 has 7 % binder in the ratio of 10:90 pitchstone to Portland cement respectively. A dosage of 6 % polycarboxylate plasticizer was added to study its influence on microstructure development.

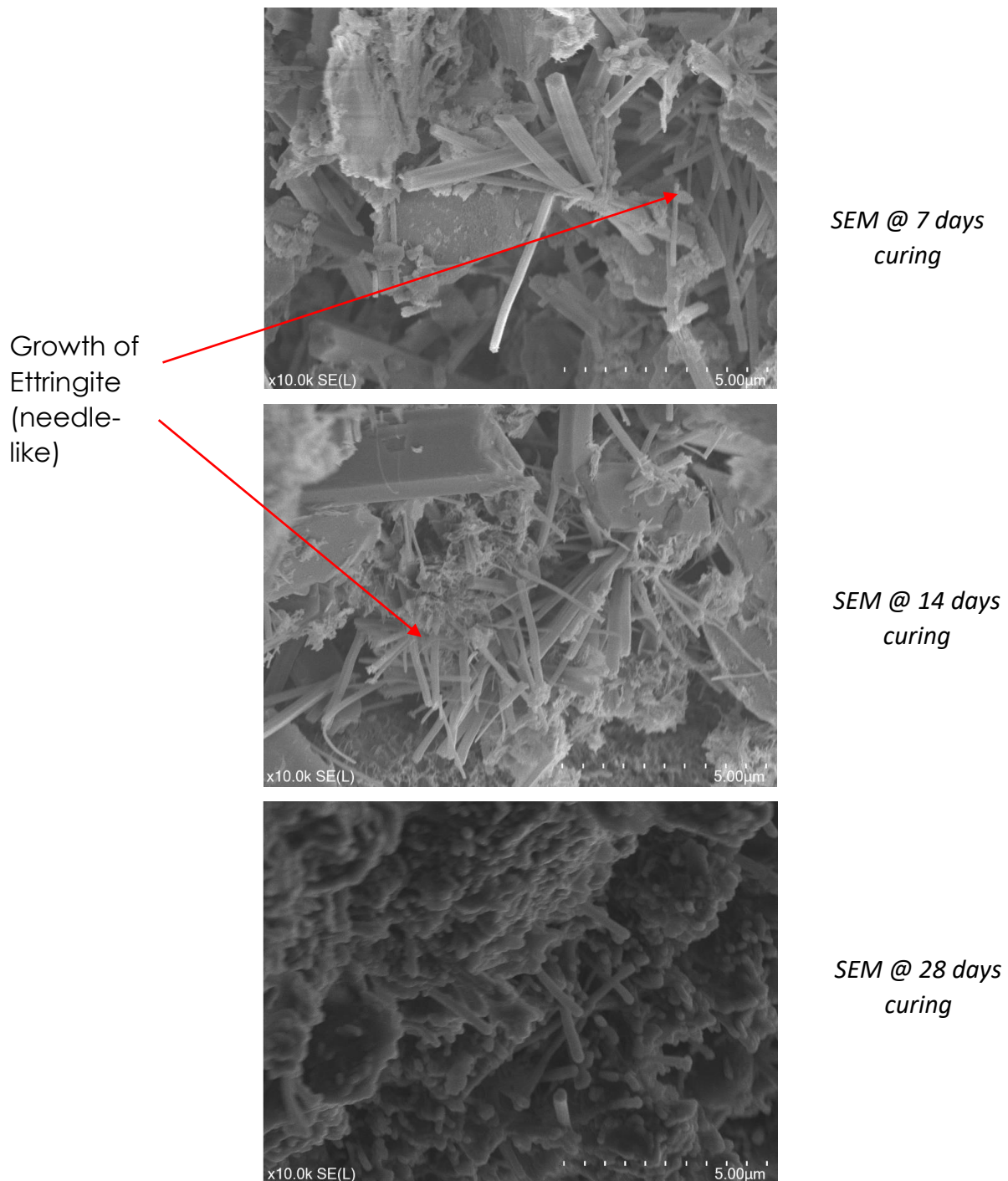


Fig. 6.6 Comparison of SEMs of mix 29

v) Microstructure development of control mix 39

Mix 39 has 5 % binder in the ratio of 10:90 pitchstone to Portland cement respectively. A dosage of 6 % polycarboxylate plasticizer was added. The solid content was 76 %. SEM of the mix 39 with low binder dosage (5 %) was done to compare the other preceding mixes on the influence of binder dosage on the growth of the hydration products over curing periods.

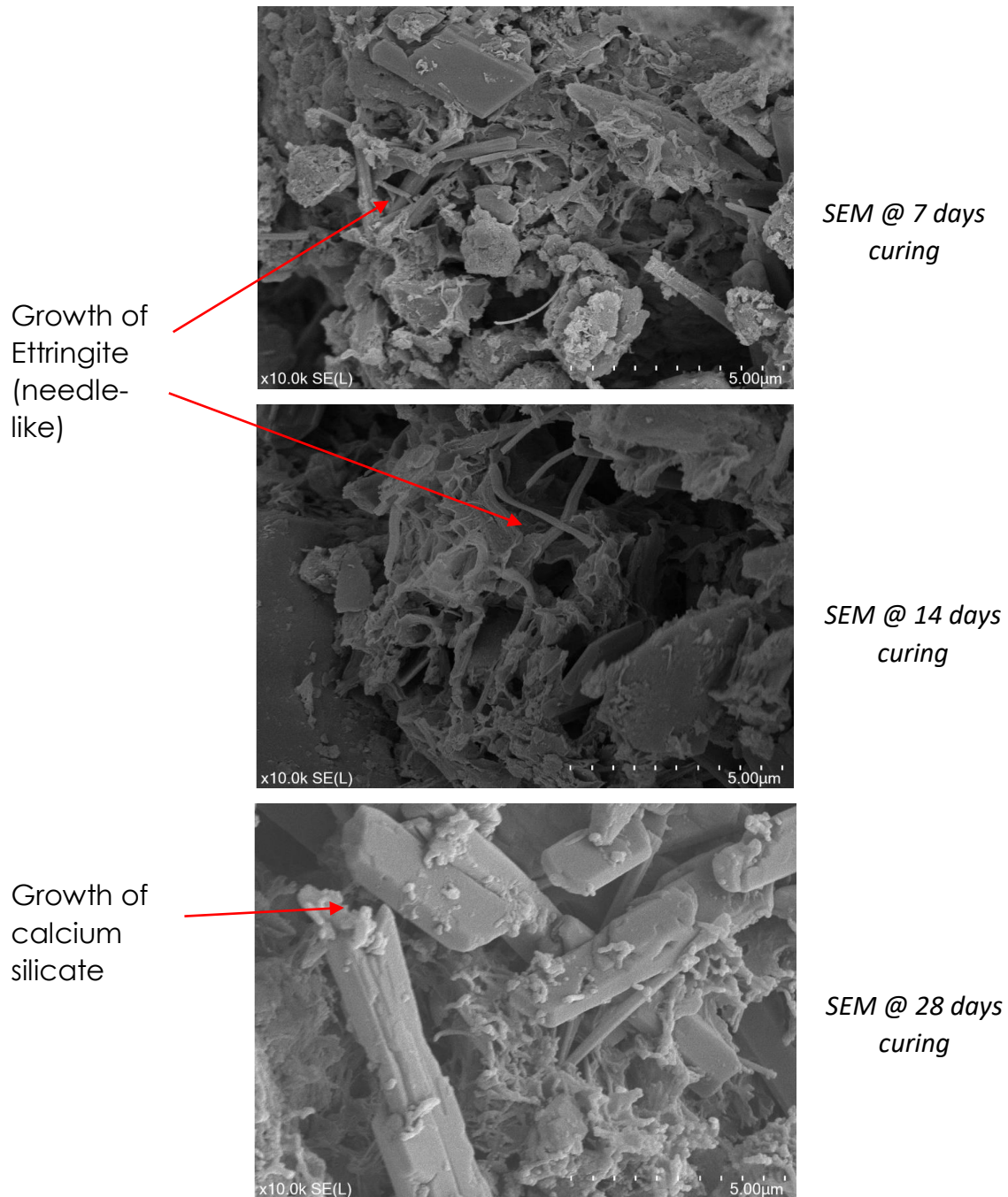


Fig. 6.7 Comparison of SEMs of mix 39

The results (Fig. 6.3 to Fig. 6.6) indicated that the microstructure development at the earlier stages from 7 to 14 days has presence of ettringite (needle like) while at longer periods, the growth of calcium silicates (C-S-H) was prominent. The development of C-S-H reduced the existence of voids. Comparison of the SEM of binder dosage indicated significant difference in the growth of crystals and existence of voids. With less binder dosage (Fig. 6.7), the growth of crystal was less compared to 7 % binder dosage (Fig. 6.3 to Fig. 6.6).

SEM observations indicated that the strength increased with the growth of calcium silicates (C-S-H). Regardless of the binder type, the longer the curing period (> 28 days), the C-S-H growth reduced the voids, made the cemented paste fill denser, and increased the strength.

6.3 TGA and DTG analysis

Thermogravimetry analysis (TGA) and derivative thermal gravimetric (DTG) analysis were done by measuring the change in mass of sample over a constant heating rate of 20 degrees per minute to maximum of 600 °C. TGA and DTG analysis were performed on the small specimens (3 to 10 mg) to determine the phase change of hydration product (calcium hydroxide) over different curing periods. In addition, TGA and DTG were performed on tailings as an additional test to identify the presence of minerals to compliment the XRD data.

The TA SDT 650 (Discovery) was used for the TGA analysis. A desktop computer and the Trios software were used to process the real time data. TGA set up is shown below (Fig. 6.8).



Fig. 6.8 TA SDT 650 (Discovery) model set up for TGA

6.3.1 Sample preparation for TGA and DTG

TGA were done on specimens of mixes with higher cement content of 7 % binder dosage. Binder amount used in the mixes were very low compared to concrete mixes, therefore binder dosages of 3 % and 5 % were not used in the TGA test as they may not show significant peaks and may be difficult to discern.

The early stages of preparation were mainly focused on drying and expelling the free water present in the samples using isopropanol.

- i) Several specimens were extracted from the UCS sample (tested and crushed sample) and oven dried for 24 hours at 105 °C.
- ii) The specimens were submerged into isopropanol bath for 24 hours. The specimens were removed from isopropanol bath and put into oven at 40 °C and removed after 24 hours.
- iii) The samples were finely grounded and packed in a plastic bag or container prior to the TGA test
- iv) Prior to loading the sample into the oven, two crucibles were placed on the scale inside the TGA machine and tared. One crucible remained in the balance while the other one was loaded with the specimen.

- v) Specimen mass ranging from 3 to 10 mg was placed in one crucible and placed in the balance in TGA machine.
- vi) The temperature rate was set at 10 °C per minute and the test was running for an hour.
- vii) The software, Trios was used to record all the test data.
- viii) The oven was closed, and testing began. After 1.5 hours, the test was completed, and the results were saved or copied.
- ix) The crucible with the load was removed and next sample was loaded.



Fig. 6.9 Specimen preparation for TGA and DTG

6.3.2 TGA of portlandite and tailings

A mix was done using pure lime (calcium oxide) and water to produce calcium hydroxide. The mixture was cured for 7 days, submerged into isopropanol bath and oven dried. TGA and DTG analysis were done on the specimen and the range of temperature that calcium hydroxide changed phase was from 350 to 450 degrees as shown below (Fig.6.10).

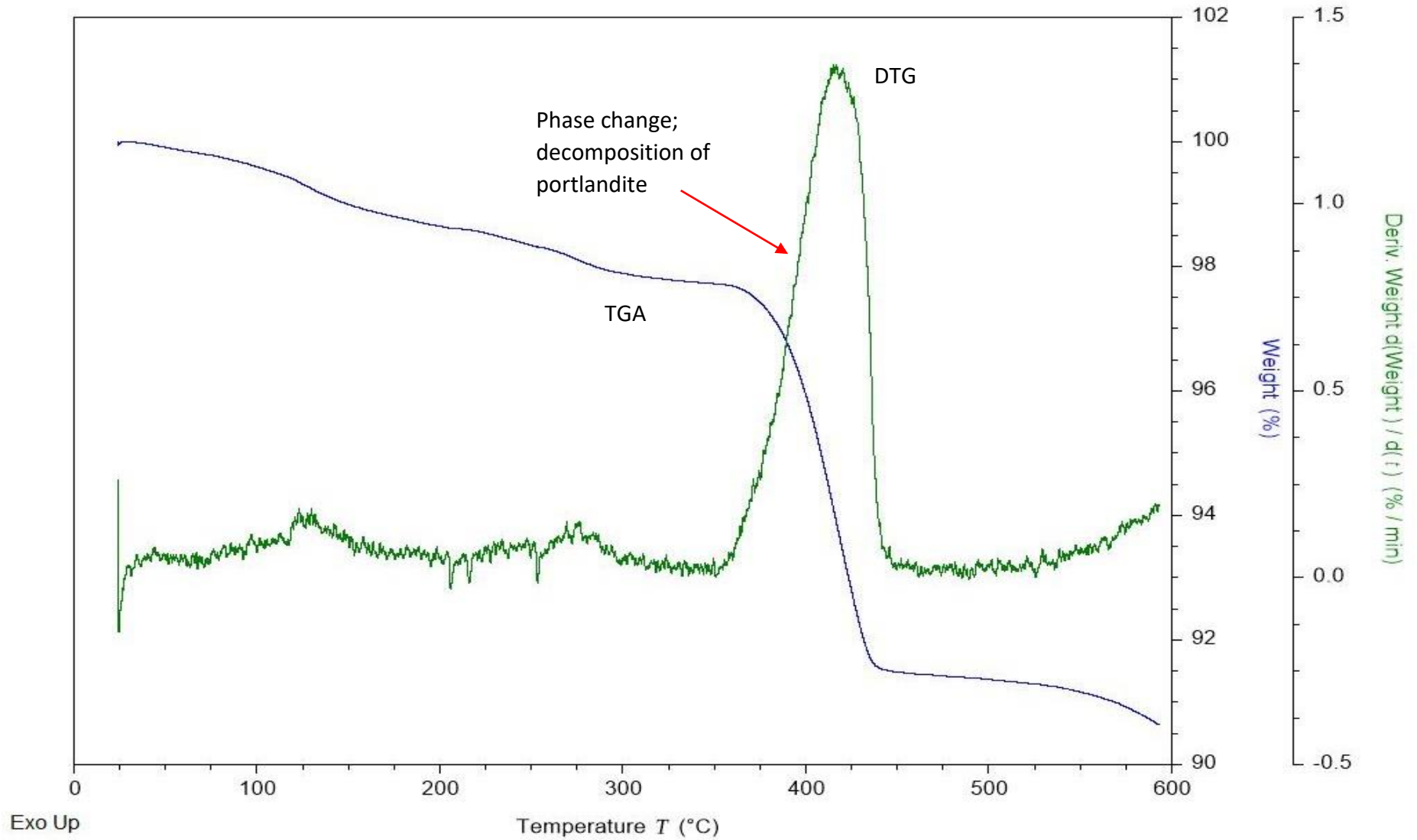


Fig. 6.10 TGA and DTG done on specimen of calcium hydroxide

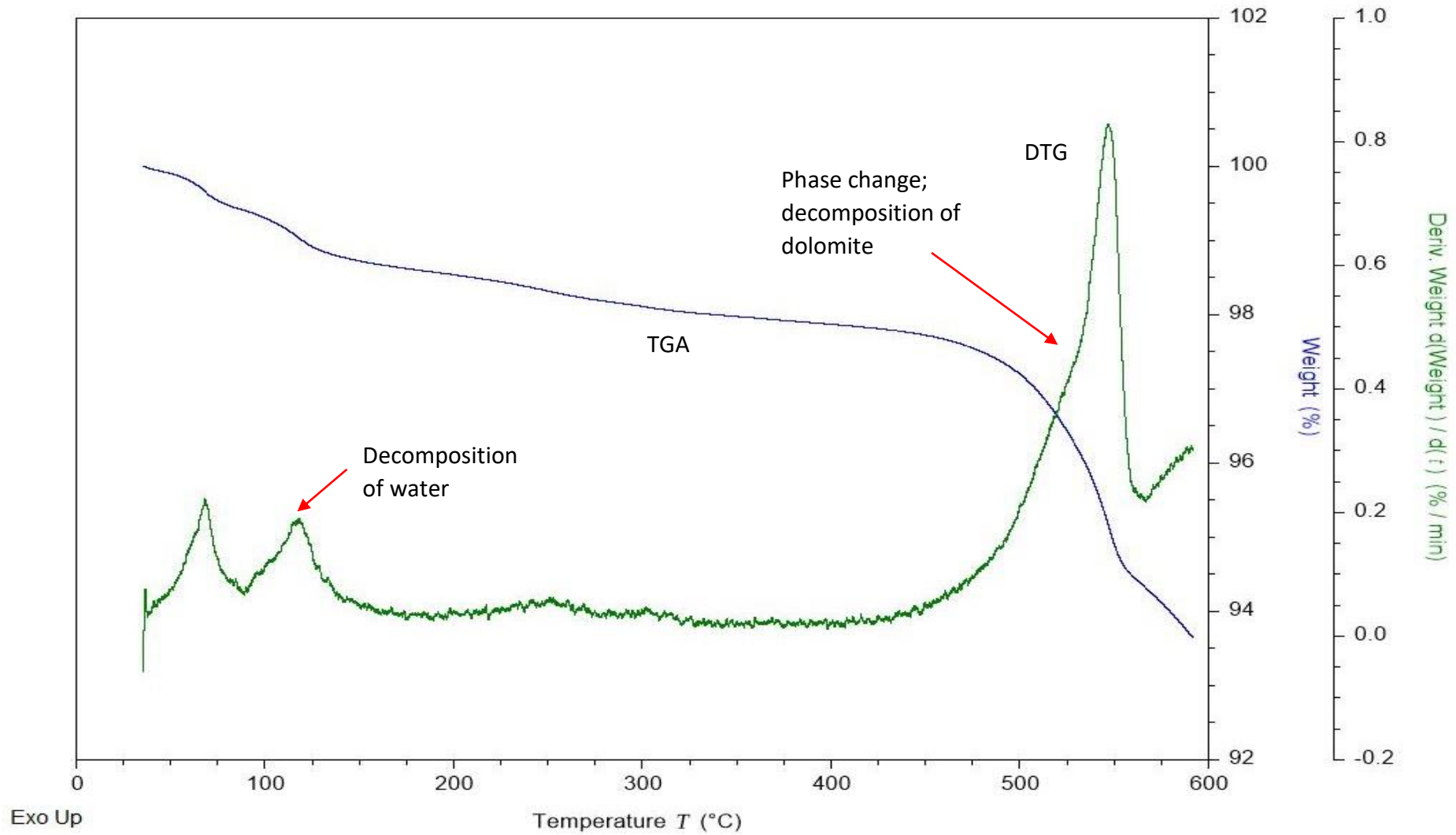


Fig. 6.11 TGA and DTG of GFM tailings

In addition, TGA was done on several powdered specimen of pure tailings without binder to determine the presence of calcareous and dolomitic minerals. The results (Fig. 6.11) showed phase change of dolomite present in the GFM tailings. Three other specimens were tested and all showed similar results.

TGA analysis of the George Fisher Mine (GFM) tailings used in the study confirmed the mineralisation of GFM. The ore is hosted in pyritic shale and calcareous siltstone and high content of lime or calcium carbonate is expected from the TGA. The TGA and DTG analysis of the GFM tailings indicated that it contained significant amount of amorphous (non-crystalline) carbonate and thus decarbonate within the temperature range of 455 to 560 °C. Calcite are crystalline and decarbonate at temperature above 600 °C while amorphous calcium carbonate decarbonate at temperatures 400 to 600 °C (Scrivener, 2017) and the results confirmed the mineralogical study (XRF).

From the TGA analysis done on the calcium hydroxide and the tailings, the temperature range to determine the de-hydroxylation of portlandite was within 350 to 450 °C and these temperature range was used consistently for all the specimen analysed.

6.3.3 Effect of pozzolans on portlandite

TGA is an analytical technique done on cemented samples to evaluate the content of portlandite over curing periods and reactivity of the supplementary cementitious materials (SCMs). De-hydroxylation of calcium hydroxide occurred around 350 to 445 °C and corresponded with the range reported in other literatures (400 to 500 °C). The weight loss of water during the heating process was used to determine the corresponding amount of portlandite present using the molecular masses (Scrivener, 2017).

$$\begin{aligned} \text{Ca (OH)}_2 &= \text{WL}_{\text{Ca(OH)}_2} \times (m_{\text{Ca(OH)}_2} / m_{\text{H}_2\text{O}}) \\ &= \text{WL} * 74/18 \end{aligned} \quad (\text{Eqn. 6.1})$$

where WL is weight loss, and m is molecular mass. Where WL is weight loss, and m is molecular mass.

The molecular mass of portlandite ($m_{\text{Ca(OH)}_2} = 74 \text{ g/mol}$, and water $m_{\text{H}_2\text{O}} = 18 \text{ g/mol}$). The amount of portlandite present over curing periods for the 6 different mixes undergoing TGA is shown below (Fig. 6.12).

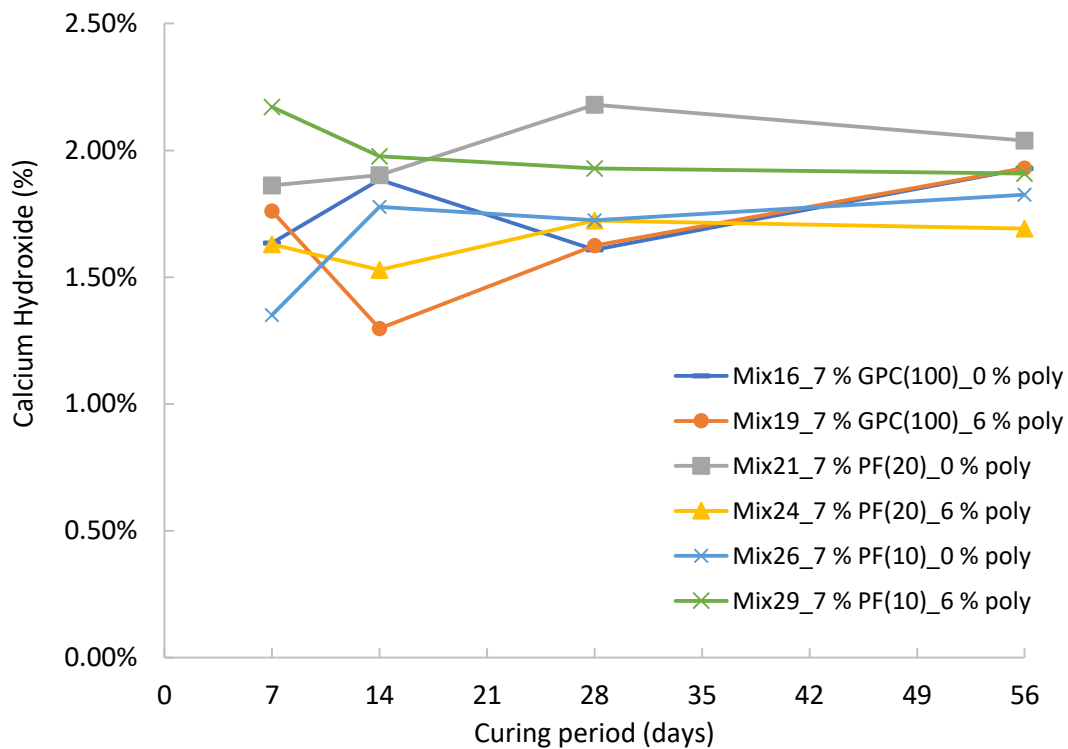


Fig. 6.12 TGA of calcium hydroxide over curing days

There was no clear trend of reduction of calcium hydroxide over longer curing periods for the 6 mixes (Fig. 6.12). The absence of the trend can be due to either the small amount of binder dosage (7 %) used which was much lower than dosage used in concrete or the small mass of specimen (3 to 7 mg) used for the TGA. The mix was thoroughly stirred and was homogenous prior to

casting the samples, thus, the absence of trend was attributed to the sample size and binder dosage.

6.3.4 TGA and DTG plots comparison

From the 7 mixes that TGA was done, the control mix 16 (using GPC 100 %) and the mix 21 (using pitchstone fines as blend) were used for comparisons of the phase changes from the 7 to 28 days curing periods. Control mix 16 consist of 7 % binder, 100 % GPC, 74 % solid content, and 0 % polycarboxylate. Mix 21 consist of 7 % binder, 80 % GPC and 20 % pitchstone fines, 74 % solid content, and 6 % polycarboxylate plasticizer dosage. TGA and DTG plots for the phase change and decomposition of the minerals present in the two mixes are all shown below (Fig. 6.13, Fig. 6.14, and Fig. 6.15).

TGA and DTG results generally showed the presence of the portlandite (from cement hydration), water, and calcareous minerals present in the tailings. Phase change of water occurred around 0 to 120 °C. Decomposition of portlandite occurred around 400 to 500 °C and dolomite occurred around 455 to 560 °C. The plots showed that the decomposition of portlandite (calcium hydroxide) and calcareous minerals occurred within a similar range of temperatures. The portlandite peak was minimum due to the insignificant amount present compared to the calcareous minerals (dolomite) present in the tailings.

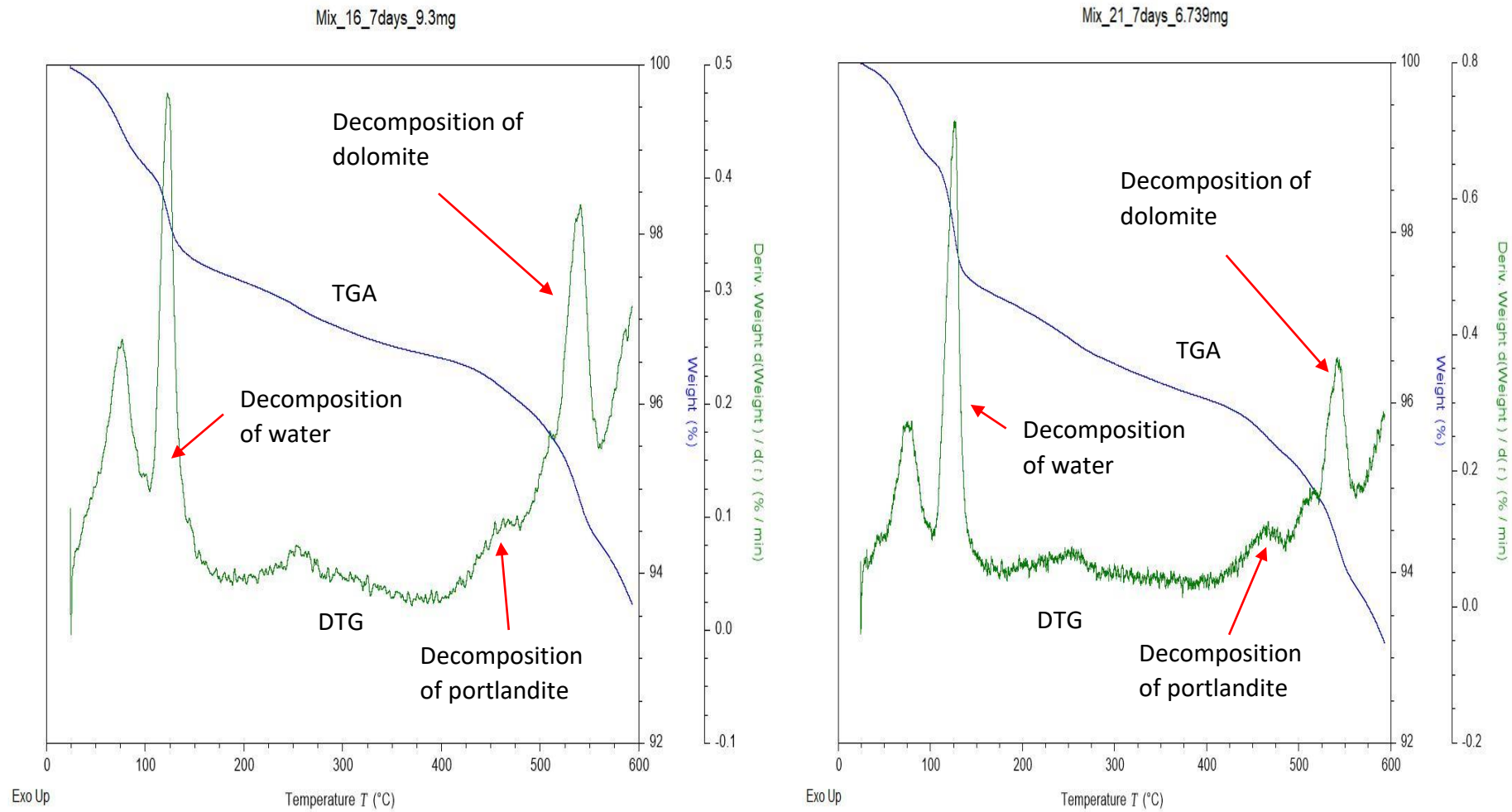


Fig. 6.13 TGA and DTG of control mix 16 and mix 21 @ 7 days cure

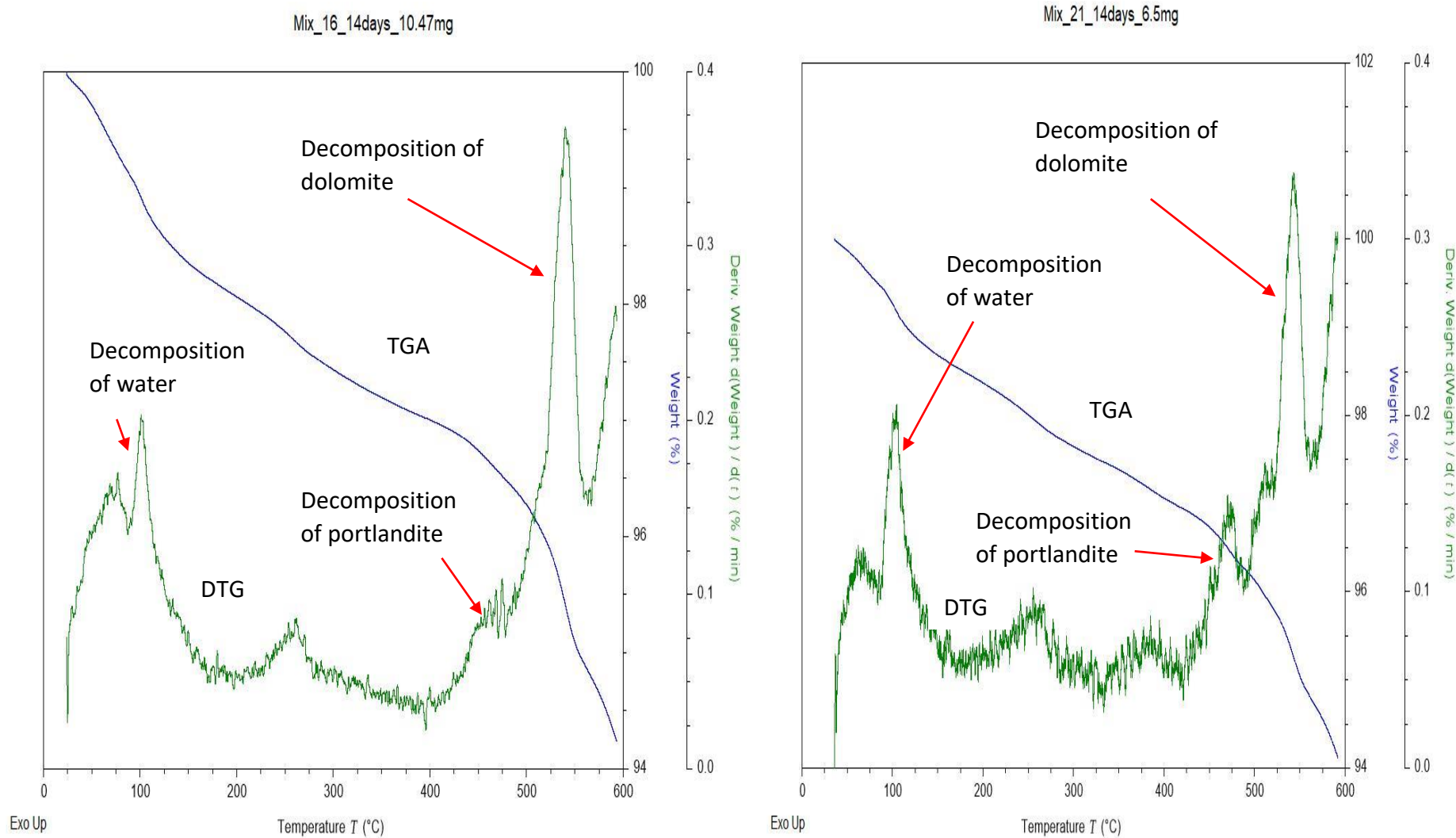


Fig. 6.14 TGA and DTG of control mix 16 and mix 21 @ 14 days cure

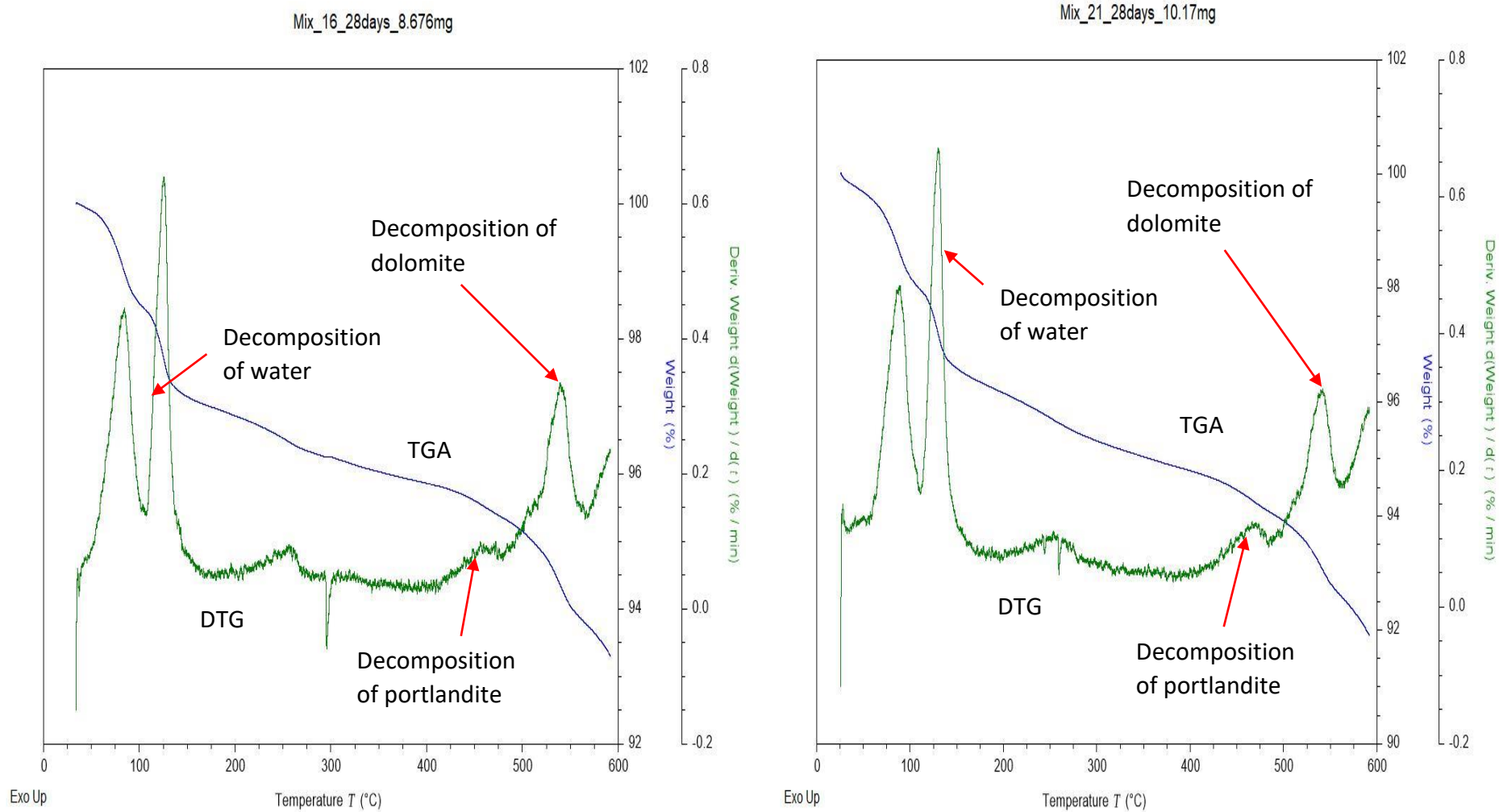


Fig. 6.15 TGA and DTG of control mix 16 and mix 21 @ 28 days cure

6.3.5 Relevance of UCS and TGA

From the TGA and DTG tests completed, the results were inconclusive due to the lack of general trend and thus UCS value could not be correlated to the amount of Portlandite present.

6.4 Summary

The development of hydration products were studied using thermogravimetry analysis (TGA) and scanning electron micrograph (SEM). TGA was done to determine the amount of portlandite present over different curing periods. The decrease in the amount of portlandite indicated the formation of additional calcium silicate through the reaction of calcium (released from portlandite) with silica (released from pozzolans). SEM was done to observe the growth of hydration product over curing periods. The growth of calcium silicate increased the strength of cemented paste fill (CPF).

SEM analysis indicated that the ettringite (needle-like) mineral was formed in the early stages of hydration (7 to 14 days) while the calcium silicate was formed at later stages (>14 days). The growth of calcium silicates occupied most of the voids, thus making the CPF dense and strong. In addition, the binder dosage influenced the growth of the hydration crystals. At high binder dosage (7 %), more crystals were developed which contributed to the strength development compared to the low binder content.

TGA and DTG done on the calcium hydroxide specimen indicated the decomposition range to be within 350 to 450 degrees, which affirmed the temperature range that other literatures reported. TGA and DTG analysis of the GFM tailings indicated the presence of amorphous calcareous minerals (carbonates). The tailings indicated phase change within the temperature range of 455 to 560 °C, which the dolomite present in the tailings decomposed. The decomposition of portlandite and calcareous minerals occurred within a similar range of temperatures.

7. Rheology

7.1 Introduction

Knowing the rheological properties of cemented paste fill is necessary to design the pump and reticulation systems for efficient transportation and disposal of cemented paste fill (CPF) into the open stopes. Rheology study of the CPF slurry involved the measurement of slump, yield stress, viscosity, and the bulk density. Rheology tests were performed on the fresh slurry mix. Slump is a measure of the degree of wetness, workability, and consistency of the batch. Yield stress is a measure of the resistance of slurry to plastic deformation that initiates flow at very low shear rate. Viscosity is a measure of the resistance of the paste slurry to flow at different shear rates.

7.2 Preparation for yield stress and viscosity measurements

Yield stress and viscosity measurements were done using the Brookfield DV3T Rheometer. The steps involved in the test work are outlined below:

- i) 1 kg of oven dried tailings was used and the other ingredients such as water, binder dosage, and admixture were determined using equations 3.1 to 3.4 in chapter 3.
- ii) An electrical drill with a vane spindle was used to thoroughly mix the ingredients placed in a bucket.
- iii) The paste mix was then scooped to fill a 250 mL glass beaker.
- iv) The beaker was tapped at the base to expel any entrapped air in the paste. The beaker was positioned directly under the DV3T Rheometer prior to measurement.
- v) Two vane spindles were used, either the V73 or the V75. The criteria to use which spindle was depended on the torque. When the V73 spindle registered out of range torque ($> 100\%$), the smaller V75

spindle was used. Vice versa, when the V75 spindle registered low torque ($< 10\%$), the V73 spindle was used. The targeted torque range was between 10 to 100 %. The dimensions of V75 are 0.803 cm width by 1.61 cm height and was used for yield stress ranging from 80 to 800 Pa. The dimensions of V73 are 1.267 cm width by 2.535 cm height and was used for yield stress ranging from 20 to 200 Pa.

- vi) When the appropriate spindle was selected, the yield stress was measured first. The run speed range targeted were within 0.05 to 1.0 RPM. Run speed selected for the yield stress measurement were 0.05, 0.25 and 0.5 RPM.
- vii) The spindle was cleaned after each test to remove the solids that coagulated around the spindle that can cause slippage and thus reduce torque.
- viii) Brookfield guidelines were used to set the parameters for the yield stress and viscosity measurements.
- ix) After the yield stress measurements, the same mix was used for the viscosity measurements. Viscosity was measured at several run speeds from 1 to 200 RPM. The selected run speed for the viscosity measurements were 1, 2, 5, 20, 100, and 200 RPM.
- x) The electronic data was recorded and transferred into a USB that was plugged into the rheometer and were analysed for yield stress and viscosity.



Fig. 7.1 Preparation of yield stress and viscosity measurements

Tables 7.1 and 7.2 below summarise the parameters entered into the DV3T-HA Brookfield rheometer to measure the yield stress and the viscosity.

Table 7.1 Yield stress parameters

Parameter	Value
Spindle	V73 or V75
Immersion	Primary
Pre-shear speed (rpm)	5
Pre-shear time (min)	1
Zero speed (rpm)	0.01 - 0.5
Wait time (sec)	30
Run speed (rpm)	0.05 - 0.5
Torque reduction (%)	100

Table 7.2 Viscosity parameters

Parameter	Value
Spindle	V73 or V75
Immersion	Primary
Zero speed (rpm)	0.01 - 0.5
Wait time (sec)	30
Run speed (rpm)	0.5 - 200
Torque reduction (%)	100

7.3 Yield stress measurements

Yield shear stress of a fluid is the in-situ stress that is overcome before the fluid flows. Newtonian fluids exhibit a linear correlation between the applied shear stress and the shear rate, while Bingham fluids like paste have yield stress that must be overcome to establish flow. Yield shear stress was determined directly from the DV3T HA Rheometer when the maximum torque has been reached. The run speed of the vane spindle was below 1 RPM to prevent errors from inertia (Ouattara et al., 2017). Unlike the previous models of Brookfield viscometer, yield shear stress was recorded directly in $\text{dyne}\cdot\text{cm}^{-2}$ and was converted to pascals (Pa) for data analysis.

Typical yield stress of CPF is around 250 Pa while the operating yield stress is site specific and can range from 50 to 500 Pa depending on the pumping, reficulation system, and paste properties (Sivakugan et al., 2015). The rheological model of a Bingham fluid is expressed as:

Shear stress:
$$\tau = \tau_0 + \eta\dot{\gamma}$$
 (Eqn. 7.1)

where τ is the shear stress, τ_0 is the yield stress, η is the plastic viscosity and $\dot{\gamma}$ is the shear rate.

Yield shear stress of paste slurry was determined using ASTM D2573 standard. Yield stress measurements showed variations in the values due to the spring torque range of the Brookfield rheometer used. The DV3T-HA used measured yield stress ranging from 20 to 200 Pa using V73 vane spindle. Most of the paste fill slurry have yield stress ranging from 100 to 800 Pa, and thus the DV3T-HA rheometer was not suitable for thick fluids such as the cemented paste.

7.3.1 Effect of solid content on yield stress

Research show that the solid content and yield stress are interdependent. When the solid content was increased, the yield stress also increased. Similar study was done previously, and the yield stress ranged from 80 to 200 Pa for many of the mixes with constant solid content of 74 % (Niroshan et al., 2018). Another study indicated a yield stress of 50 Pa for a mix with 75 % solid content (Hallal et al., 2010).

Results from the measurements have not clearly indicated the relation of the solid content with the yield stress due to the limitation of the rheometer used. The DV3T-HA Brookfield rheometer used measured yield stress ranging from 80 to 200 Pa using the V73 spindle. With the thick fluids such as cemented paste fill, the measurements done on majority of the mixes varied significantly and less meaningful data were gathered to analyse the effect of solid content on

the yield stress. However, some of the data showed general trend where the increase in the solid content showed an increase in the yield stress.

The results (Table 7.3) from this study indicated the range of values of yield stress measured for the various solid contents.

Table 7.3 Solid content and yield stress range

Solid content (%)	Yield stress range (Pa)	Average yield stress (Pa)
74	25 - 180	103
75	115 - 180	148
76	135 - 315	225
77	190 - 270	230
78	400	400

The average values of the minimum and maximum yield stress values (Table 7.3) indicated an exponential relationship of solid content with yield stress. At lower solid content of 74 %, the average yield stress was around 100 Pa and increased significantly to 400 Pa for a solid content of 78 %. Further test work with the appropriate rheometer torque range is required to establish the relationship in an exponential manner.

7.3.2 Effect of polycarboxylate dosage and binder on yield stress

Polycarboxylate plasticizer is an admixture that reduces the yield stress and increases the slump. Comparisons were made with several binder and polycarboxylate dosages on 74 % solid content mixes as shown below (Fig. 7.2).

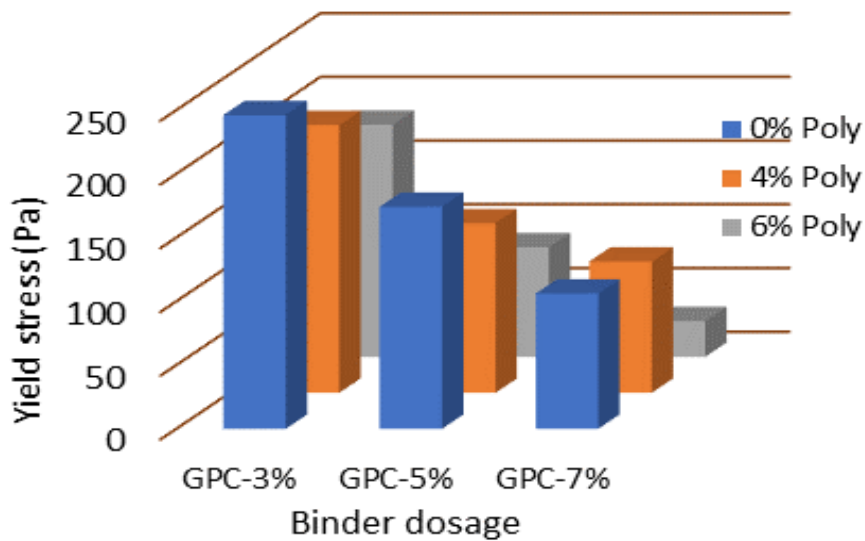


Fig. 7.2 Yield stress @ varying binder and polycarboxylate dosages

The mass of polycarboxylate plasticizer added was calculated based on the mass of the binder (Eqn. 3.4). The polycarboxylate dosage was dependent on the binder content. The higher the binder content, the higher the amount of polycarboxylate. Thus, at binder dosages of 3 % and 5 %, the polycarboxylate quantity was less compared to the 7 % binder at the same dosage rate of polycarboxylate.

Results (Fig. 7.2) indicated that polycarboxylate plasticizer reduced the yield stress with increased dosage of binder. Plasticizer had a significant effect on the yield stress of mix with 7 % GPC compared to 3 % and 5 % binder dosage.

Effect of binder dosage was observed but there was no significant relationship that can be established. The results were not clear to establish a trend for the binder dosage with yield stress for mixes with no polycarboxylate plasticizer added. However, there were indication of a decrease in the yield stress when the binder dosage was increased from 5 % to 7 %. That can indicate that the increase in binder has lubricated the mix and that has reduced the yield stress as observed in the 5 binder types used in the study.

Table 7.4 Polycarboxylate dosage on rheological properties

	Mix21	Mix22	Mix23	Mix24	Mix25
	Ingredients				
PC-Admixture (%)	0%	2%	4%	6%	8%
Binder (%)	7%	7%	7%	7%	7%
Portland (%)	80%	80%	80%	80%	80%
Pitchstone (%)	20%	20%	20%	20%	20%
Slag (%)					
Flyash (%)					
Solid content (%)	74%	74%	74%	74%	74%
	Rheology				
Slump (mm)	140	210	235	278	285
Spread (mm)	240	340	400	670	runny
Paste/Cake	cake/paste	paste	paste	paste	paste
Yield stress (Pa)	106	79	40	54	58

Polycarboxylate dosage have impacted on the yield stress of the CPF slurry as indicated in Table 7.4 above. At solid content of 74 % and with 0 % polycarboxylate dosage the average yield stress was around 100 Pa. However, as the polycarboxylate dosage was increased (4 to 8 %), the yield stress decreased significantly from 100 Pa to as low as 40 Pa.

7.3.3 Effect of rheometer and spindle on yield stress

Yield stress and viscosity measurements are significantly affected by the type of rheometer and the vane spindle used. In this study, the digital Brookfield DV3T HA Rheometer was used. The range of the DVT3 HA using the vane spindle V73 was up to 200 Pa (2000 dyne/cm²). Any yield stress beyond the maximum was outside the range and the value was not registered. This has been an issue as paste fill mix with solid content above 75 % were out of range. To rectify this problem, a V75 vane spindle was purchased which had maximum yield stress range of 800 Pa (8000 dyne/cm²). Although, the V75 used on the DV3T HA gave results, the yield stress values were inconsistent when yield

stress values were above the 200 Pa. That situation has been common in many of the tests done. To get a better result for thick fluids such as paste, a rheometer with higher torque range will be more suitable to be used with V73 vane spindle.

7.3.4 Relevance of UCS and yield stress

Optimum mix of CPF should attain strength that can withstand blasting and flow through pipelines. Based on general practice, UCS of 1000 kPa and yield stress of 150 Pa were used as limits to identify optimum mixes.

Binder content of 7 % was used for comparison of different binder types as majority of the mixes that used 3% and 5 % binder dosage did not reach UCS value above the threshold of 1 MPa. Comparisons were made for 56 days cure for 7 % binder dosage as shown below (Fig. 7.3). Results indicated that majority of the mixes reached 1 MPa and above except 3 mixes of fly ash and slag blend with 4 to 6 % polycarboxylate dosage. Interestingly all the mixes with pitchstone fines were within the optimum mix zone.

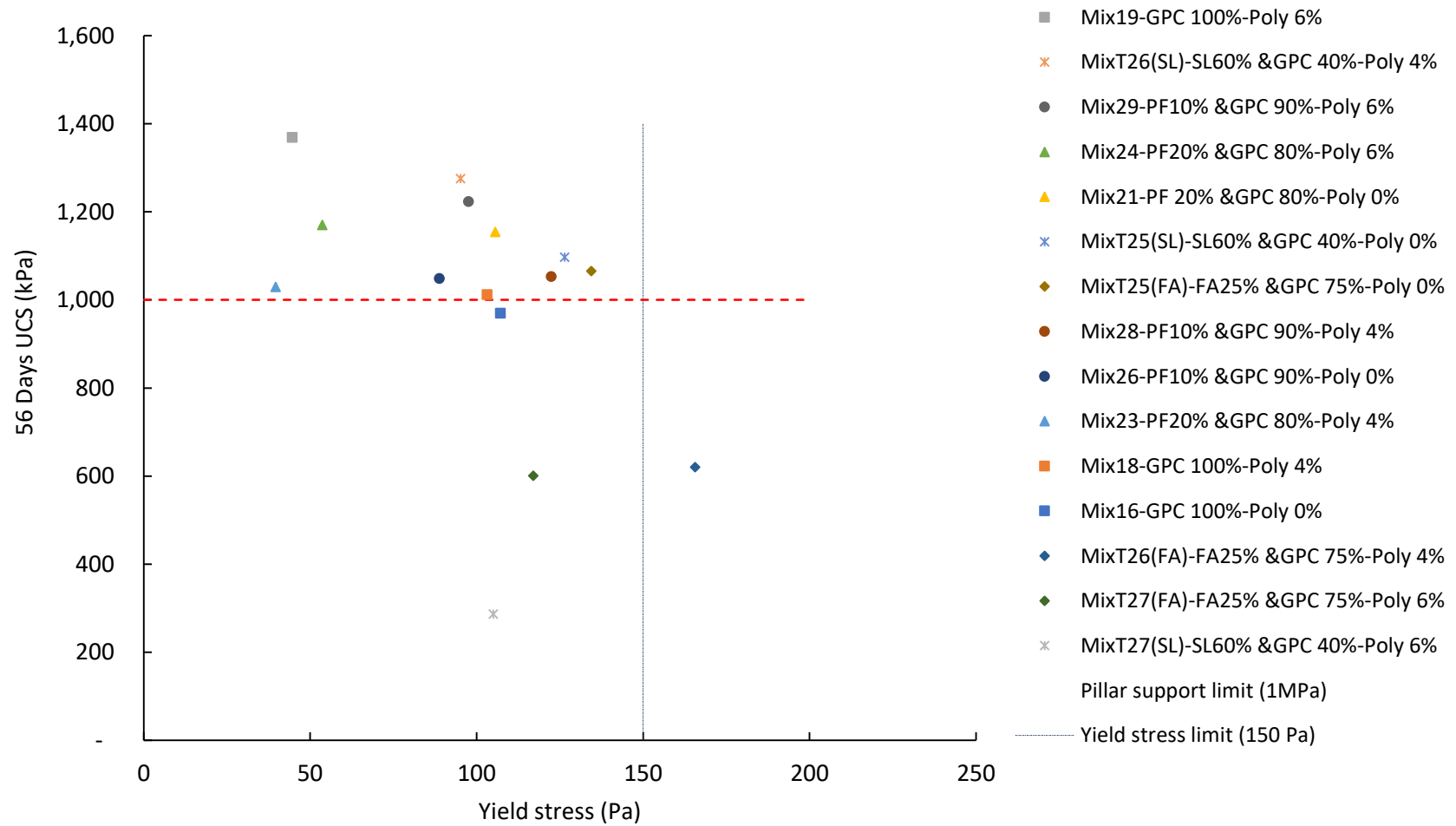


Fig. 7.3 Yield stress and 56 days UCS @ 7 % binder dosage

7.3.5 Effect of solid content on viscosity

Viscosity (η) is defined as the internal frictional resistance between two layers within a fluid's flow regime. Increasing the solid content enables more tailings to be disposed but makes it difficult for slurry to flow without pipe blockages. The viscosity of the cemented paste fill slurry at different solid contents were measure and plotted below (Fig. 7.4).

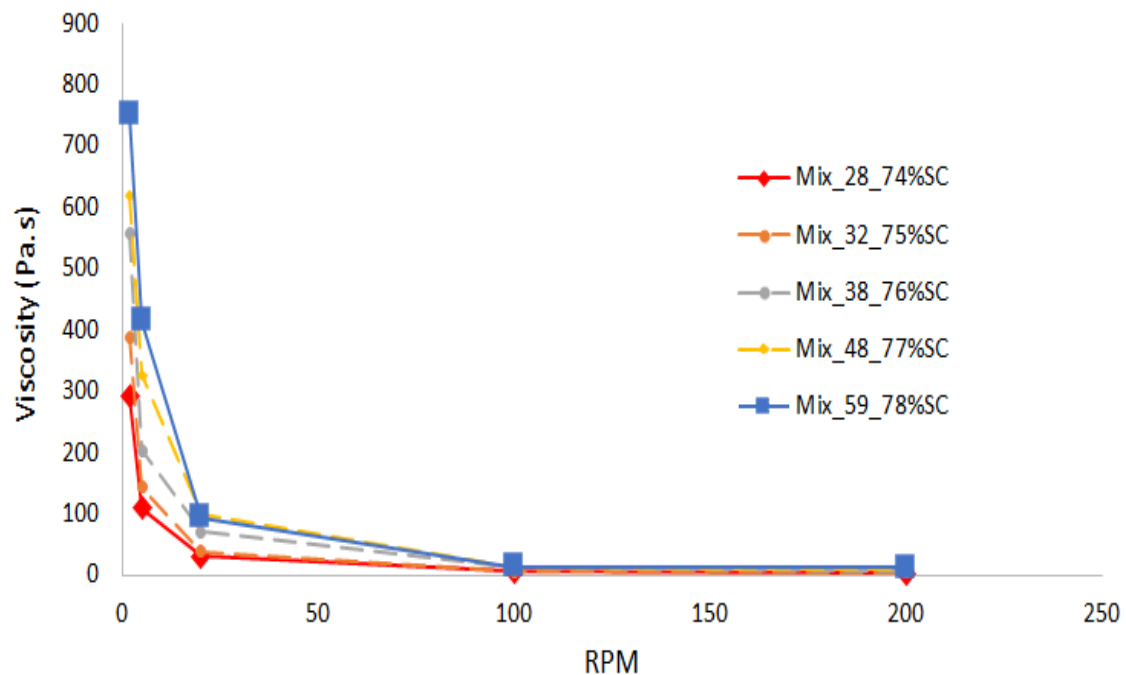


Fig. 7.4 Viscosity relations to different solid contents

Results (Fig. 7.4) indicated that as the solid content was increased, the viscosity also increased at low RPM. Regardless of the solid content, at run speed above 100 RPM, viscosity approached zero for all solid contents. At higher RPM, the coagulated particles were deflocculated, which resulted in the low viscosity.

7.3.6 Effect of polycarboxylate on viscosity

At 74 % solid content, four mixes with 2 % and 8 % polycarboxylate dosages were compared. Polycarboxylate dosages of 4 and 6 % were omitted given

the close cluster of values, thus only the minimum (2 %) and maximum (8 %) dosage were used to compare the 4 different mixes. Results (Fig. 7.5) indicated that at lower RPM (RPM < 5), the viscosity was low for the 2 mixes (mix 25 and mix 30) with high (8 %) polycarboxylate dosage compared to mixes (mix 22 and mix 27) with 2 % polycarboxylate dosage. In addition, at higher run speed (RPM > 100), the viscosities approached zero with no significant difference in the viscosity values.

Results (Fig. 7.4 and Fig. 7.5) affirmed that cemented paste fill is a non-Newtonian pseudoplastic fluid which displayed a decreasing viscosity with increasing shear rate.

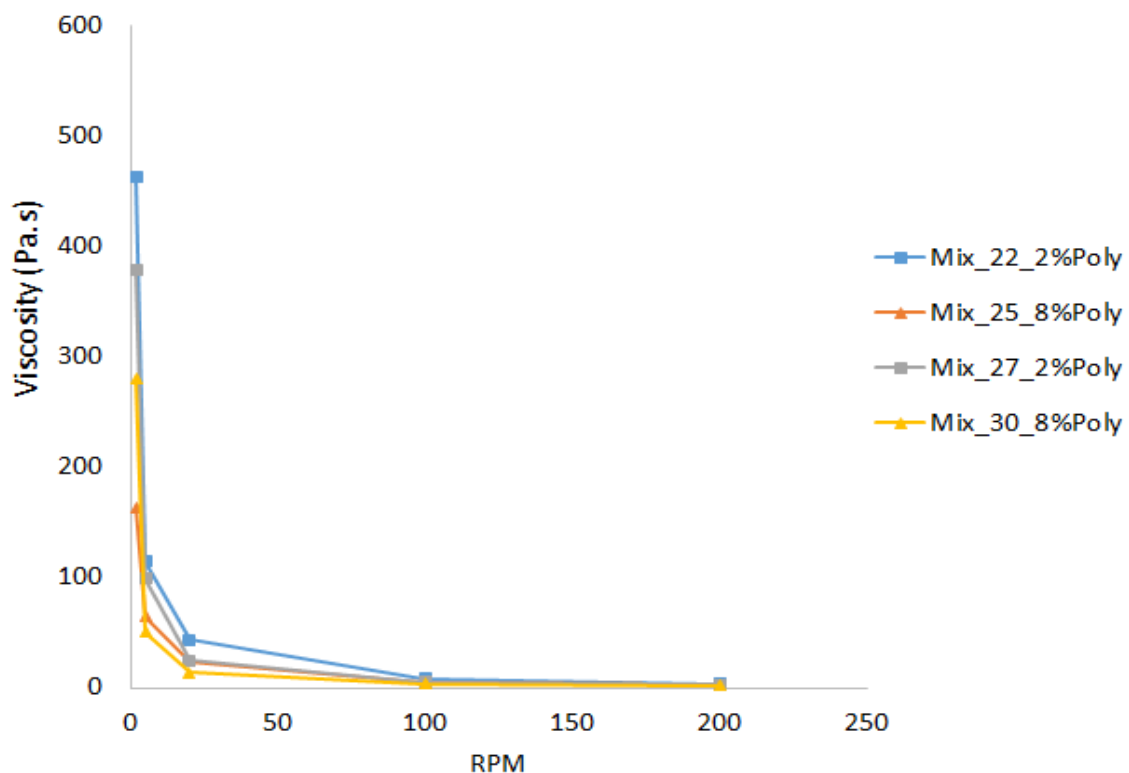


Fig. 7.5 Viscosity relations to polycarboxylate dosage

7.3.7 Effect of time on viscosity

One of the CPF mixes (mix 63) was analysed for the effect of time on the viscosity at a constant run speed (RPM). Generally, the viscosity decreased as

time elapsed as shown below (Fig. 7.6). The results indicated that the cemented paste fill is a thixotropic fluid where the viscosity decreases as time elapses at a constant shear rate. The viscosity tests have indicated that cemented paste fill is a non-Newtonian pseudoplastic and thixotropic fluid.

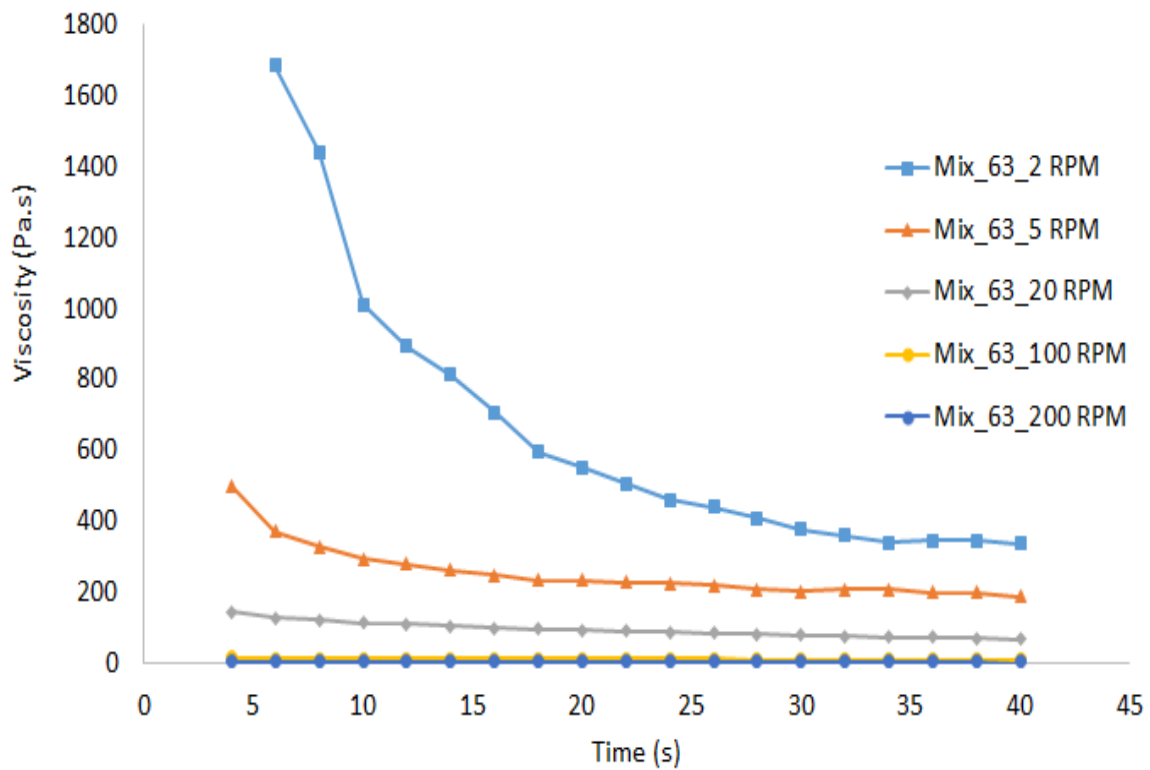


Fig. 7.6 Viscosity relations to time Mix 63 @ 76 % solids

7.4 Slump measurement

Slump test was done using standard truncated cone of 100 mm top diameter, 200 mm bottom diameter, 300 mm height and as per ASTM C143 procedures (Fig. 7.7). Slump test was done on the fresh mix of the cemented paste fill (CPF) to determine the workability and consistency of batch. Slump value indicate whether the mix exist as either a slurry, paste, or cake. The spread distance from the slump indicate the ease of outward flow of the slurry.



Fig. 7.7 Slump test of cemented paste fill

Slump test was done during the preparation of the mixes prior to the casting of samples for the UCS, ITS, and 3-Point tests. Tailings mass of 9 to 10 kg were used for each mix and the amount was adequate to completely fill the standard slump cone. After the slump test, the mix was dumped back into the bucket, stirred for a while, and cast into moulds for the strength tests.

7.4.1 Effect of polycarboxylate and solid content on slump

Slump value decreases when the solid content increases. In order to improve the slump of the slurry at higher solid content, admixtures are used. The admixture polycarboxylate was applied on mixes with several solid contents (74, 75, 76, 77, and 78 %) to study its impact on the slump and the results are shown below (Fig. 7.8).

Results indicated that the polycarboxylate plasticizer had a significant effect on the slump and spread of the slurry. When the dosage of polycarboxylate was increased, the slump height and spread distance increased significantly.

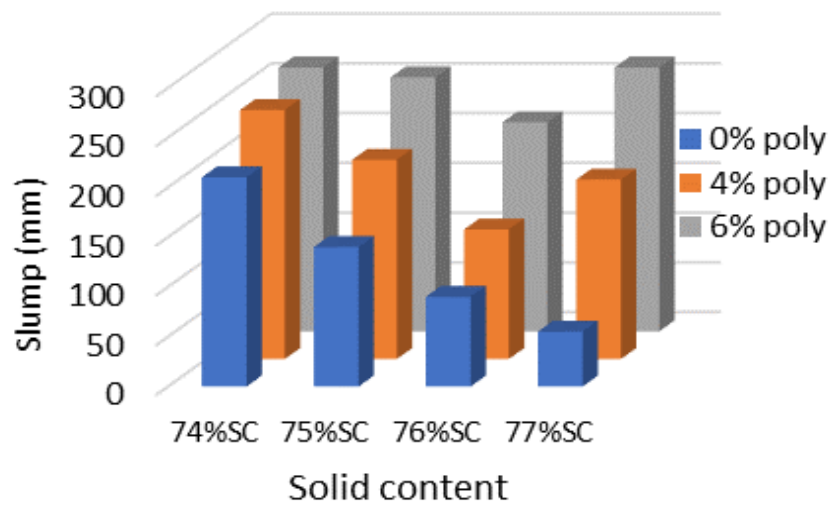


Fig. 7.8 Polycarboxylate, slump and solid content

Slump value was low (55 mm) at high solid content of 77 % and 0 % dosage of polycarboxylate. However, as the polycarboxylate dosage was increased to 6 %, the slump increased to 250 mm, which was optimum for paste filling. Slump height increased significantly for mixes with high solid content (76 to 77 %) when the polycarboxylate dosage increased (6 to 8 %).

Slump and the solid content of cemented paste fill (CPF) are interdependent. Slump increased (> 200 mm) at lower solid content (74 %), while at higher solid content (77 %), the slump decreased (< 60 mm) without the addition of polycarboxylate (0 %). Polycarboxylate requirement at lower solid content (74 %) was minimum to attain an optimum slump. A lower dosage of polycarboxylate (2 to 4 %) was adequate to attain the desired slump (> 200 mm) for a mix with 74 % solid content. At high solid content (77 %) and with increased dosage of polycarboxylate, the paste transformed from cake to slurry as clearly illustrated below (Fig. 7.9). Polycarboxylate has proven to improve the workability of the slurry to maintain an optimal slump (> 200 mm) at higher solid content.

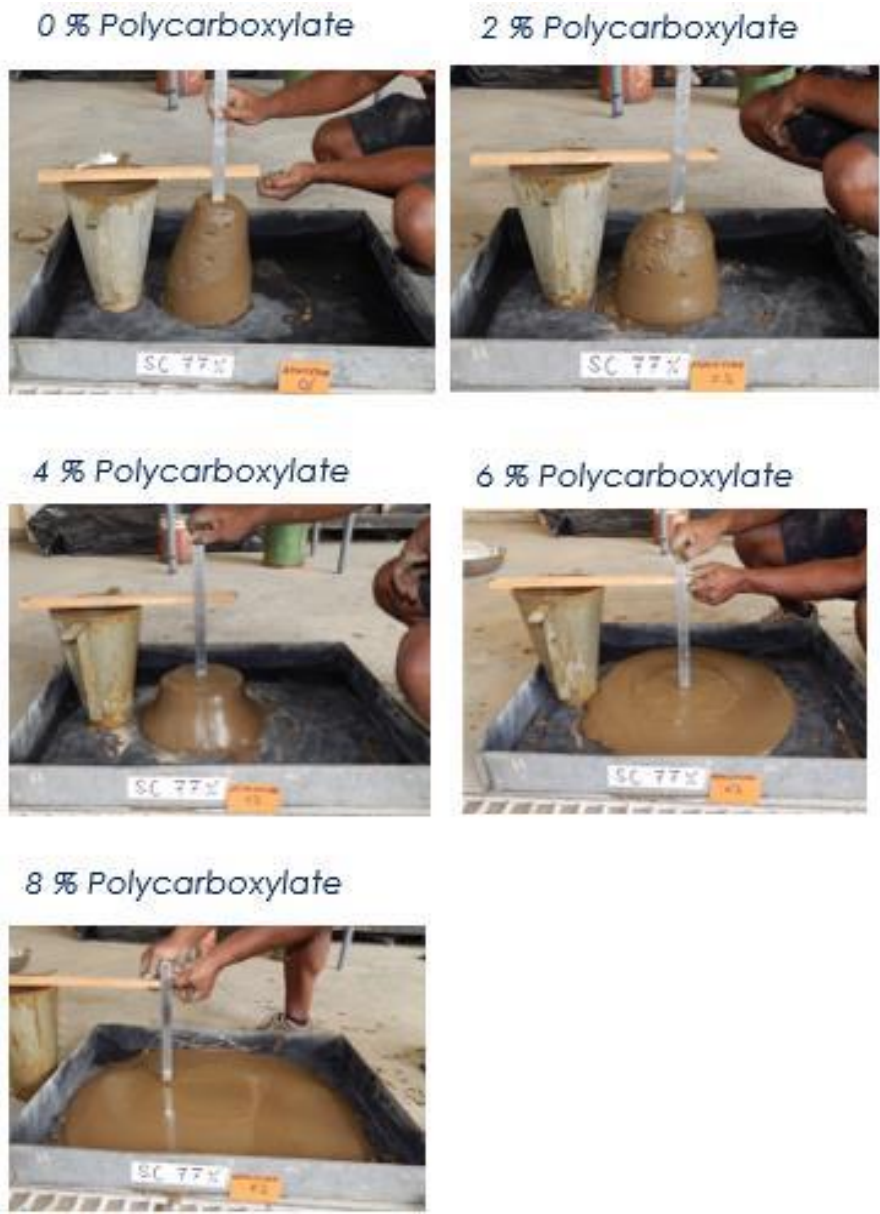


Fig. 7.9 Effect of polycarboxylate dosage on slump of 77 % solid

Slump requirement is site specific for different mines depending on the pumping and reticulation system. In most cases, slump greater than 200 mm is preferred for transportation via reticulation over longer distances. Slump usually range from 235 to 275 mm for most mines and a slump of 150 to 250 mm is optimum for pumping through reticulation lines (Sivakugan et al., 2015; Belem et al., 2008).

7.4.2 Relevance of yield stress and slump

Slump cone test is the quickest and conventional mode of relating slump to yield stress. High slump indicates an ease of flow of the slurry with low yield stress value. Poor slump value indicates that the mix is caking with high yield stress and is not optimal for pumping and transporting over long distance for mine filling.

The slump and yield stress measurements of some of the mixes were plotted as shown below (Fig. 7.10). The chart indicated a nearly linear relationship between the slump (S) and the yield stress. The chart affirmed the general rule of thumb where a slump of 235 to 275 mm corresponded to a yield stress value of 100 Pa. The relationship established can be used to estimate the yield stress from slump measurements.

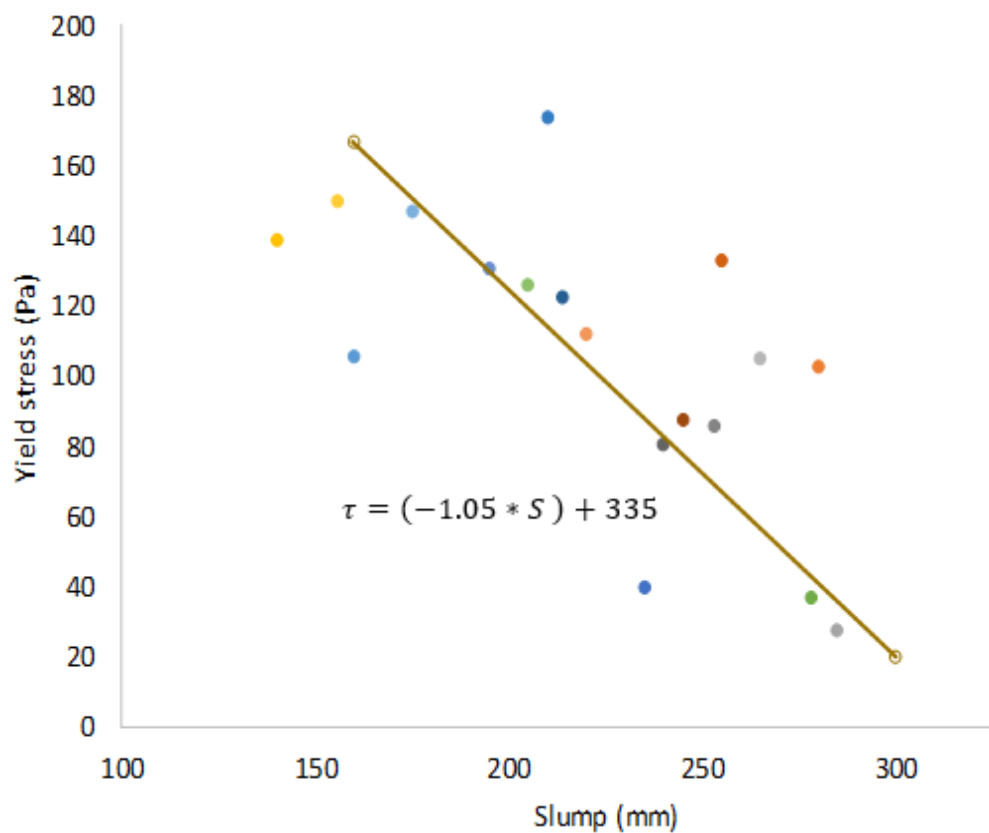


Fig. 7.10 Relation of yield stress and slump

Mines can operate at yield stress ranging from 50 to 500 Pa depending on the capacity of the positive displacement pumps. In most mines, the range of yield stress values from 50 to 125 Pa and slump values from 200 to 260 mm are ideal for paste filling.

7.5 Bulk density measurement of paste fill slurry

Bulk density of paste fill slurry is easy to measure for quality control purposes. Variations in the bulk density is minimised to maintain the consistency of the paste fill slurry discharged into underground voids. Bulk density varies depending on the mineralogy of the tailings, solid content, and fluidity of the mix. Bulk density of the CPF was determined using cup method as per ASTM D2216 procedure and is expressed as;

$$\text{Bulk density (kg/m}^3\text{)} \quad Y_b = \frac{W_b}{V_b} \quad (\text{Eqn. 7.2})$$

where Y_b is the bulk unit weight, W_b is total weight of in situ sample (water + void + solids), V_b is the total volume of sample.

Bulk density was determined using a metal mould of 50 mm diameter, 100 mm height and 1008 g mass. The mould was filled with the CPF to the brim, the top was levelled, the mass was recorded, and the bulk density was determined. There was no application of vibration or compaction to the CPF. The bulk density determined was regarded as a pour bulk density.

Bulk density determined from several mixes throughout the research showed minor variations. The wet bulk density determined ranged from 1.9 to 1.96 kg/m³ from several mixes with 74 % solid content. The bulk density of solid contents higher than 75 % were difficult to determine due to caking. When the samples were scooped into the mould, it was difficult to even out and completely fill the mould. If compaction was applied, the mould would have

filled up better, but in this study no compaction was done and thus the bulk density was not performed for mixes with high solid content.

7.6 Summary

Rheological properties of the cemented paste fill (CPF) is critical for the slurry transportation via reticulation over long distances. Slump, yield stress, viscosity, and bulk density were measured for different solid contents, binder dosages, and polycarboxylate dosages.

The solid content significantly affected the slump and yield stress. When the solid content was increased, the yield stress increased, and the slump distance decreased. With the application of polycarboxylate, the yield stress decreased significantly from 100 Pa to as low as 40 Pa and the slump increased from caking to runny slurry. Polycarboxylate has proven to improve the workability of the slurry to maintain an optimal slump (> 200 mm) at higher solid content.

The binder type and binder dosage had no significant influence on the rheological properties. The bulk density measured ranged from 1.9 to 1.96 kg/m³ for mixes with 74 % solid content.

The slump and the yield stress have a linear relationship. Range of yield stress values from 50 to 125 Pa and slump values from 200 to 260 mm are ideal for paste filling in most mines.

8 Summary, conclusion, and recommendation

8.1 Summary and key findings

The results from this study affirmed the many other studies done on the potential of using pozzolanic materials to partially replace general Portland cement (GPC) and using polycarboxylate admixture to improve rheology. There are many variables that influence the rheology, hydration process, microstructure growth, and strength development of cemented paste fill such as the binder dosage, solid content, physio-chemical properties of mill tailings, chemistry of water, pozzolan type, and admixture type and dosage.

In this research, the focus was mostly on the physio-chemical properties of tailings, binder type and dosages, polycarboxylate dosage, solid contents, and how these factors influence the strength and rheological properties of the cemented paste fill. The mill tailings used were from George Fisher Mine (GFM) in Mt Isa. The binders used were slag blend (60 % slag and 40 % GPC), fly ash blend (25 % fly ash and 75 % GPC), pitchstone blend (10 % pitchstone and 90 % GPC, and 20 % pitchstone and 80 % GPC). The binder dosages were 3 %, 5 %, and 7 %. The polycarboxylate dosages were 2 %, 4 %, 6 %, and 8 % of the mass of binder. Majority of the mixes were done with 74 % solid content with few other mixes were done with solid content of 75 %, 76 %, 77 %, and 78 %.

The key findings from the extensive laboratory test work are summarized under four main topics which are the physio-chemical properties of tailings, rheological properties of paste slurry, microstructure growth, and strength development.

i) Mill tailings

- Particle size distribution (PSD) of the George Fisher Mine (GFM) mill tailings contained 5 % by mass of particles less than 20 μm which has less fines than the rule of thumb threshold of 15 %. Fines retain water

better due to their large surface area and have lubricating effect which minimises the pressure loss due to friction along reticulation lines. GFM tailings with less fines will require either higher water to solids ratio or increased dosage of polycarboxylate plasticizer. The preferred option to maintain workability is to increase the dosage of polycarboxylate due to the reason that high water content will reduce the strength of the cemented paste fill (CPF).

- Uniformity coefficient (C_u) and coefficient of curvature (C_c) determined were 6.5 and 1.0 respectively. Tailings with C_u ranging from 5 to 10 contain lesser spread of grain sizes which indicates a poorly graded tailing. GFM Tailings with C_u of 6.5 is within the range from 5 to 10 that contained lesser spread of grain sizes and indicated a poorly graded tailing. GFM tailings with lower C_u will require either additional binder dosage to attain the similar strength to a well graded tailing due to the presence of voids or addition of micro silicates or micro limestone as fillers. Further study is required to understand feasibility of using other options without increasing the cost of the operation.
- Specific gravity was measured to be 2.77 which is also the particle density of the tailings (2.8 g/cc). Specific gravity values are spread out due to the mineralogy of the ore mined and can range from 2.8 to 4.4 for heavier minerals. GFM ore has high content of silica (40.74 %) and calcareous minerals (18.4 %), therefore the specific gravity is at the lower range.
- Bulk density of the solid tailings without any form of vibration or compaction was measured to be within the range of 1300 to 1480 kg/m³. The bulk densities measured were similar to the range of bulk densities of soil due to the high content of silica and calcareous minerals present in the GFM tailings. Silica and carbonates are common minerals that make up the earth's crust.

- Scanning electron micrograph (SEM) analysis done on the tailings indicated that the grain shape of the ultra-fines ($< 75 \mu\text{m}$) were bulky and flaky. The grain shape reflected the crushing and grinding process involved in the extraction process of the GFM ore.
- X-ray diffraction (XRD) analysis was done on the GFM tailings and the dominant minerals in the composition of the tailings were silica (40.74 %), iron oxide (19.11 %), sulphite (12.65 %), dolomite (18.4 %), and other lesser content of metal oxides. The high silica (SiO_2) content is from shale, a sedimentary rock. The sulphite (SO_3) and iron oxide (FeO_3) are from the mineral pyrite (FeS_2). The dolomite is from the calcareous siltstones. The tailings also contained sphalerite (ZnO) which is the mineral that contained zinc, and galena (PbO) which is the mineral that contained lead.
- Thermogravimetry analysis (TGA) was done on the GFM tailings and the phase change occurred within the temperature range of 450 to 550 °C. The phase change may likely indicate the decomposition of dolomite. Further investigation is required to understand better the phase changes.

ii) Slurry rheology

- Slump and the solid content of cemented paste fill (CPF) are interdependent. At lower solid content (74 %), the slump increased ($> 200 \text{ mm}$), while at higher solid content (77 %), the slump decreased ($< 55 \text{ mm}$). Slump requirement is site specific for different mines depending on the pumping and reticulation system. In most cases, slump greater than 200 mm is preferred.
- Slump, spread, and dosage of polycarboxylate plasticizer are interdependent. Maintaining a constant solid content and increasing the polycarboxylate dosage resulted in the increase of slump distance. At higher solid content (77 %) where the slump was around 55 mm, the

addition of 4 % polycarboxylate dosage increased the slump to 150 mm, and further addition of 6 % polycarboxylate dosage increased the slump to 250 mm. Polycarboxylate significantly improved the workability with the increase in dosages.

- Polycarboxylate requirement at lower solid content was minimum. A lower dosage of polycarboxylate plasticizer (2 %) was adequate in attaining the desired slump (260 mm) for a mix with 74% solid content.
- Yield stress measurements showed variations in the values due to the spring torque range of the Brookfield rheometer used. The DV3T-HA used measures yield stress ranging from 20 to 200 Pa using V73 vane spindle. Most of the paste fill slurry have yield stress ranging from 100 to 800 Pa, and thus the DV3T-HA rheometer was not suitable for thick fluids such as the cemented paste.
- Yield stress measured on average indicated an exponential relation with the solid content. However, further test work with a suitable rheometer is required to affirm the relationship. At lower solid content of 74 %, the average yield stress was around 100 Pa and increased significantly to 400 Pa for a solid content of 78 %.
- Polycarboxylate dosage has a significant impact on the yield stress of the CPF slurry. At solid content of 74 % and with 0 % polycarboxylate dosage, the average yield stress was around 100 Pa. However, as the polycarboxylate dosage was increased (4 to 8 %), the yield stress significantly decreased from 100 Pa to as low as 40 Pa.
- Yield stress and slump were not impacted by the binder type and the binder dosage in any significant way.

iii) Strength

- Common failure modes observed from the UCS test samples were splitting, shearing, crushing, slumping, and bulging. Competent samples

failed through splitting and shearing, while the incompetent (soft) samples failed through bulging and slumping.

- Polycarboxylate dosage has no significant influence on the strength. Increasing the polycarboxylate dosage while maintaining the solid content and the binder content has not increased the strength significantly over periods up to 112 days.
- Binder dosage significantly affects the unconfined compressive strength (UCS) and indirect tensile strength (ITS) of the CPF. At 74 % solid content, binder dosage of 3 % attained less than 150 kPa, binder dosage of 5 % attained 200 to 600 kPa, while binder dosage at 7 % attained strength of 1 MPa after 28 days curing period.
- Blended binder influences the long-term strength depending on their reactivity and percentage replacement of cement. Pozzolans mostly replace cement up to 30 % and still maintain a comparable strength to the control mix. Any high replacement of cement depends on the reactivity of the pozzolan.
- Pitchstone fines can replace cement up to 20 % and still attain a comparable strength to the control mix. Increasing binder content (5 to 7 %) and replacing the cement with pitchstone fines up to 20 % affirmed the potential of pitchstone fines application in mine filling.
- Pitchstone fines at higher solid content (76 to 77 %) and 5 % binder dosage reached 1 MPa with addition of polycarboxylate dosage of 6 to 8 % which indicated an optimum mix that reduced the binder dosage and increased the solid content.
- Strength activity index (SAI) of the pozzolans (slag, fly ash, pitchstone fines) used in this research attained values above the 75 % threshold after 28 days curing and can be used in concrete and paste filling.

- Solid content significantly affects the strength over curing periods. High solid content (78 %) at binder dosage of 5 % has attained strength greater than 1 MPa after 28 days curing.
- Range of Young's modulus (E) for CPF can be estimated from known UCS value. The range of E were from $E = 150 * UCS$ to $250 * UCS$.
- Range of indirect tensile strength (ITS) for CPF can be estimated from known UCS value. The range of ITS were from $ITS = 0.125 * UCS$ to $0.25 * UCS$.

iv) Microstructure

- Scanning electron micrograph (SEM) images showed that at early curing days, ettringites (needle like crystals) were formed and calcium silicates were formed after 7 days.
- Growth of calcium silicates occupied the voids and increased the strength of the CPF over time.
- Thermogravimetry analysis (TGA) of pure calcium hydroxide (portlandite) showed a phase change at the temperatures range of 350 to 450 degrees.
- TGA analysis of the several mixes cured for 7, 14, and 28 days indicated no clear trend of the phase change of the de-hydroxylation of calcium hydroxide. That may be due to the small dosage of binder (7 %) and the small mass of specimen (3 to 7 mg).

8.2 Conclusion

The overall goal of this research was to optimise the cemented paste fill (CPF). Optimisation involves attaining the desired strength and rheological properties of CPF at minimum cost to the mining operation and the natural environment. The major cost driver in a paste fill operation is cement and therefore pozzolans

were trialled in this study to partially replace cement to save cost. Cemented paste fill is a slurry with high solids that are transported over long distances which can undergo pressure loss to friction, and compounded with hydration reaction happening, there is potential of clogging the reticulation system. Therefore, polycarboxylate plasticizer was trialled in this study to improve the workability and retard setting.

Results from the strength tests indicated that the pozzolans used attained strength activity index (SAI) well above the threshold of 75 % compared to the control mix. The pozzolans used complied with the strength requirements as per ASTM C618 standard and can be utilised in concrete and paste filling. Apart from common pozzolans such as slag and fly ash, pitchstone fines, a natural volcanic rock has attained comparable strength and has the potential to be used in paste filling in the mines.

Results from the rheological measurements indicated that the polycarboxylate had significant influence on the workability of the cemented paste slurry. As the dosage of the polycarboxylate increased, the slump increased, and the yield stress decreased. Moreover, the use of polycarboxylate reduced the requirement of water which reduced the water to cement ratio and increased the strength. Even when polycarboxylate was added to high solid content like 78 %, the slump increased significantly. High performance plasticizer (superplasticiser) like polycarboxylate is a common admixture used in paste filling in mines and this study affirmed that it is an effective admixture to maintain workability of paste slurry when used in paste filling in the mines.

8.3 Recommendations for future research

Throughout the research, there were some tests methods and equipment used that were not ideal to produce data that can be meaningfully analysed. In addition, there were other necessary test work that were not completed due to time factor and those can be captured for further research. This section

outlines the recommendations for continuous improvement for future studies of cemented paste fill.

i) *Improvements to method and equipment*

- Majority of the samples cast for the 3-point bending test were defective and were discarded. Incomplete data were gathered from the few tests done which could not be used in any meaningful way. For future studies, two improvements are recommended. Firstly, use a rigid metal rectangular prism instead of using wooden moulds. The lack of rigidity and confinement resulted in cracking of most of the samples due to the swelling and shrinking of clay minerals in the mix during the hardening process. Secondly, an ideal humidity condition has to be determined to cure the samples to prevent the sudden drying of samples that can trigger cracking.
- The rheometer used for the yield stress measurement was not suitable for thickened fluids such as cemented paste fill. Brookfield rheometer model DV3T-HA with a spring torque of 1.44 mN was used. Maximum yield stress that the DV3T-HA measures using the recommended V75 vane spindle ranges from 20 to 200 Pa. Most of the paste fill slurry have yield stress ranging from 100 to 800 Pa. Many of the yield stress measurements were out of range when the torque value surpassed 100 %. A smaller sized V75 vane spindle was used instead with DV3T-HA which has a yield stress range from 80 to 800 Pa. However, the yield stress values measured from the two different spindles with the same rheometer DV3T-HA, were significantly different. A suitable rheometer with a higher spring torque such as the DV3T-HB is recommended for future yield stress measurements. The Brookfield rheometer DV3T-HB has a spring torque of 5.75 mN and with the recommended spindle V73, the yield stress it can measure ranges from 80 to 800 Pa and is suitable for cemented paste slurry.

- Thermogravimetry (TGA) analysis technique applied to measure the content of portlandite over different curing periods of the cemented paste fill showed inconsistent results. Portlandite content is generally expected to reduce as curing period increases, however that trend was not observed from the cemented paste specimens tested. The likely explanation would be that the cement dosage for the paste was 7 % which was much lower than cement dosage (30 %) used in concrete. The small specimen sizes ranging from 3 to 7 mg made it difficult to measure the portlandite content. A suitable specimen size of 10 to 20 mg is recommended for the thermogravimetry analysis. Furthermore, for each mix, three different test runs is recommended to determine a more representative result.

ii) ***Further investigations***

- Investigate the rheological and strength properties of mix at higher solid contents (75 to 85 %) by increasing the dosage of polycarboxylate plasticizer and while maintaining a minimum binder dosage between 3 to 5 %. This investigation will lead into increasing the rate of tailings disposal into underground voids, quick turnover of stopes, less cement usage, and reduction in mining costs.
- Investigate the strength properties of other natural pozzolans apart from pitchstone such as volcanic tuff, pumice, serpentine, obsidian, volcanic ash, and other volcanic rocks that contain reactive silica. This investigation will lead into opening up opportunities for commercialisation of industrial minerals, partial replacement of cement, reduction of greenhouse gas emissions, and reduction in mining costs.
- Investigate the long-term strength and durability of the blended binders at different dosage of binder and polycarboxylate. The long-term curing can be from 56 days, 112 days, 168 days, 224 days, or up to a year. This

investigation will lead into determining the increase in strength over time due to the pozzolanic reaction and its durability and resistance to sulfate attack or attack from other destructive chemical reactions.

- Investigate the rheological properties (slump, yield stress, and viscosity) of fresh cemented paste slurry of different binder and polycarboxylate dosages at different time intervals such as 1 minute, 5 minutes, 10 minutes, 30 minutes, 60 minutes, 2 hours and so forth. This investigation will lead into determining the setting time which is important in the design of paste fill that can maintain its workability along long distances without clogging the pipelines.
- Investigate the other types of plasticizers apart from polycarboxylate to determine their effectiveness in workability and strength development. This investigation will lead into determining the plasticizer that produces the optimum workability at minimum dosage and cost.
- Investigate the application of fillers especially on tailings that contain less fines. The rule of thumb threshold is to maintain a minimum of 15 % of tailings to contain fines less than 20 μm . This study will lead into determining the filler type that can increase the strength of CPF at minimum cost for tailings with less fines (< 15 % of 20 μm).

Reference

- Ababneh, A., & Matalaka, F. (2018). "Potential use of Jordanian volcanic tuffs as supplementary cementitious materials." *Case Studies in Construction Materials*, 8,193-202.
- American Concrete Institute, (2001). "Use of raw or processed natural pozzolans in concrete (ACI232.1R-00)." *ACI Committee*, 232.
- ASTM C143 Standard Test Method for Slump of Hydraulic-Cement Concrete, ASTM International.
- ASTM C150 Standard Specification for Portland Cement, ASTM International.
- ASTM C494 Standard Specification for Chemical Admixtures for Concrete, ASTM International.
- ASTM C618 Standard specification for coal fly ash and raw or calcined natural pozzolan for use in concrete, ASTM International.
- ASTM D854 Standard Test Methods for Specific Gravity of Soil Solids by Water Pycnometer, ASTM International.
- ASTM D2166 Standard Test Method for Unconfined Compressive Strength of Cohesive Soil, ASTM International.
- ASTM D2216 Standard Test Methods for Laboratory Determination of Water (Moisture) Content of Soil and Rock by Mass, ASTM International.
- ASTM D2573 Standard Test Method for Field Vane Shear Test in Saturated Fine-Grained Soils, ASTM International.
- ASTM D6913 Standard Test Methods for Particle-Size Distribution (Gradation) of Soils Using Sieve Analysis, ASTM International.
- Australian Standards AS 1012.3.1 (2014) Methods of testing concrete - Determination of properties related to the consistency of concrete - Slump test.

Australian Standards AS 1012.10 (2000) Methods of testing concrete - Determination of indirect tensile strength of concrete cylinders (Basil or splitting test)

Australian Standards AS 1289.3.2.1 (2009) Methods of testing soils for engineering purposes - Soil classification tests - Determination of the plastic limit of a soil.

Australian Standards AS 1289.3.4.1 (2008) Methods of testing soils for engineering purposes - Soil classification tests - Determination of the linear shrinkage of a soil.

Australian Standards AS 1289.3.5.1 (2006) Methods of testing soils for engineering purposes - Soil classification tests - Determination of the soil particle density of a soil.

Australian Standards AS 1289.3.6.1 (2009) Methods of testing soils for engineering purposes - Soil classification tests - Determination of the particle size distribution of a soil - Standard method of analysis by sieving.

Australian Standards AS 1289.6.4.1 (2016) Methods of testing soils for engineering purposes - Soil strength and consolidation tests - Determination of compressive strength of a soil - Compressive strength of a specimen tested in undrained triaxial compression without measurement of pore water pressure.

Australian Standards AS 1289.3.6.3 Methods of testing soils for engineering purposes - Soil classification tests - Determination of the particle size distribution of a soil - Standard method of fine analysis using a hydrometer.

Australian Standards AS 1289.3.1.1 Methods of testing soils for engineering purposes - Soil classification tests - Determination of the liquid limit of a soil - Four-point Casagrande method.

- Australian Standards AS1289.3.9.1 Methods of testing soils for engineering purposes - Soil classification tests -Determination of the cone liquid limit of a soil.
- Barcelo, L., Kline, J., Walenta, G., and Gartner, E. (2014). "Cement and carbon emissions." *Journal of Materials and Structures*, 47(6), 1055-1065.
- Barger, G. M., Hulshizer, A. J., Popovics, S., Call, B. M., Jaber, T. M., Prusinski, J., and Cook, J. E. (2001). "Use of Raw or Processed Natural Pozzolans in Concrete." *ACI Committee*, 232
- Belem, T., & Benzaazoua, M. (2008). "Design and Application of Underground Mine Paste Backfill Technology." *Journal of Geotechnical and Geological Engineering*, 26(2), 147-174.
- Belem, T., El Aatar, O., Bussiere, B., and Benzaazoua, M (2016). "Gravity driven 1-D consolidation of cemented paste fill in 3 m high columns". *Journal of Innovative Infrastructure Solutions*, 1 (37).
- Berodier, E., Gibson, L. R., Burns, E., Roberts, L., and Cheung, J. (2018). "Robust production of sustainable concrete through the use of admixtures and in-transit concrete management systems." *Journal of Cement and Concrete Composites*, 101, 52-66.
- Boger, D., Scales, P., Sofra, F., Jewell, R. J., and Fourie, A. B. (2006). "Paste and Thickened Tailings: A Guide." *Australian Centre for Geomechanics*, Nedlands, W.A.
- Bougara, A., Lynsdale, C., and Milestone, N. B. (2018). "The influence of slag properties, mix parameters, and curing temperature on hydration and strength development of slag (cement blends)." *Journal of Construction and Building Materials*, 187, 339-347.
- Bullard, J. W., Jennings, H. M., Livingston, R. A., Nonat, A., Scherer, G. W., Schweitzer, J. S., Scrivener, K. L., and Thomas, J. J. (2011). "Mechanisms of cement hydration." *Journal of Cement and Concrete Research*, 41(12), 1208-1223.

- Celik, K., Jackson, M.D., Meral, C., Emwas, A.H., Mehta, P.K., and Monteiro, P.J.M., (2014). "High-volume natural volcanic pozzolan and limestone powder as partial replacement for portland cement in self-compacting and sustainable concrete." *Journal of Cement and Concrete Composites*, 45, 136 - 147.
- Cheung, J., Roberts, L., & Liu, J. (2017). "Admixtures and sustainability." *Cement and Concrete Research*." 114, 79-89.
- Cihangir, F., Ercikdi, B., Kesimal, A., Turan, A., and Deveci, H. (2012). "Utilisation of alkali-activated blast furnace slag in paste backfill of high-sulphide mill tailings: Effect of binder type and dosage." *Journal of Minerals Engineering*, 30, 33-43.
- Clough, G W; Sitar, N; Bachus, R C J. (1989). "Cemented sands under static loading." *Journal of Geotechnical Engineering Division, ASCE* 1981, 107(6), 799-817.
- Deng, X., Klein, B., Tong, L., and de Wit, B. (2018). "Experimental study on the rheological behaviour of ultra-fine cemented backfill." *Journal of Construction and Building Materials*, 158, 985-994.
- Fall, M., Benzaazoua, M., and Ouellet, S. (2005). "Experimental characterization of the influence of tailings fineness and density on the quality of cemented paste backfill." *Journal of Minerals Engineering*, 18(1), 41-44.
- Fan, Z. P., Zhang, Z. H., He, Q., Cai, M. Q., and Shi, C. (2014). "Effects of naphthalene-based super plasticizer on the performances of whole tailings backfill materials." *Journal of Applied Mechanics and Materials*, Trans Tech Publications Ltd, Zurich, 962-965.
- Grice, A. G. (1998). "Fill Research at Mount Isa Mines Limited." *Proceeding of the 4th International Symposium on Mining with Backfill*.
- Hallal, A., Kadri, E.H., Ezziane, K., Kadri, A., Khelaf, H. (2010). "Combined effect of mineral admixtures with superplasticizers on the fluidity of the blended cement paste". *Construction and Building Materials*, 24 (8), 1418-1423.

- Henderson, A., and Revell, M. (2005). "Basic Mine Fill Materials. Handbook on Mine Fill." *Australian Centre for Geomechanics, Nedlands, W.A*, 13-20.
- Juimo Tchamdjou, W.H., Cherradi, T., Abidi, M.L., Pereira de oliveira, L.A., (2017). "Influence of different amounts of natural pozzolan from volcanic scoria on the rheological properties of portland cement pastes." *Proceedings from Materials and Energy*, 139, 696-702.
- Kesimal, A., Ercikdi, B., and Yilmaz, E. (2003). "The effect of desliming by sedimentation on paste backfill performance." *Journal of Minerals Engineering*, 16(10), 1009-1011.
- Kuganathan, K.(2005). "Rock Fill in Mine Fill: Handbook on Mine Fill." *Australian Centre for Geomechanics, Nedlands, W.A*, 101-115.
- Li, L. (2013). "Generalized solution for mining backfill design." *International Journal of Geomechanics*, 14(3), 04014006.
- Liu, X. F., Peng, J. H., Zhang, J. X., Chen, M. Z., & Dong, Q. (2013). "Effect of Polycarboxylic acid plasticizer on characteristics of [alpha]-calcium sulfate hemihydrate." *Journal of Applied Mechanics and Materials*, 423-426, 1085.
- Mangane, M. B. C., Argane, R., Trauchessec, R., Lecomte, A., and Benzaazoua, M. (2018). "Influence of superplasticizers on mechanical properties and workability of cemented paste backfill." *Journal of Minerals Engineering*, 116, 3-14.
- Mitchell, R. J., (1991). "Sill mat evaluation using centrifuge models." *Journal of Mining Science and Technology*, 13(3), 301-313.
- Nagrockiene, D., Pundiene, I., and Kicaite, A. (2013). "The effect of cement type and plasticizer addition on concrete properties". *Construction and Building Materials*, 45, 324331.
- Nasir, O., and Fall, M. (2010). "Coupling binder hydration, temperature and compressive strength development of underground cemented paste

- backfill at early ages." *Tunnelling and Underground Space Technology incorporating Trenchless Technology Research*, 25(1), 9-20.
- Niroshan, N., Sivakugan, N., and Veenstra, R. L. (2017). "Laboratory study on strength development in cemented paste backfills." *Journal of Materials in Civil Engineering*, 29(7), 4017027.
- Niroshan, N., Sivakugan, N., and Veenstra, R. L. (2018). "Flow characteristics of cemented paste backfill." *Journal of Geotechnical and Geological Engineering*. 36, 2261-2272.
- Niroshan, N., Yin, L., Sivakugan, N., and Veenstra, R. L. (2018). "Relevance of SEM to long-term mechanical properties of cemented paste backfill." *Journal of Geotechnical and Geological Engineering*, 36(4), 2171-2187.
- Nochaiya, T., Wongkeo, W., and Chaipanich, A. (2010). "Utilization of fly ash with silica fume and properties of Portland cement-fly ash-silica fume concrete." *Journal of Fuel*, 89(3), 768-774.
- Panchal, S., Deb, D., and Sreenivas, T. (2018). "Variability in rheology of cemented paste backfill with hydration age, binder and superplasticizer dosages." *Journal of Advanced Powder Technology*, 29(9), 2211-2220.
- Pirapakaran, K., Sivakugan, N. and Rankine, R. (2007). "Investigations into strength of Cannington paste fill mixed with blended cements." *10th Australia New Zealand Conference on Geomechanics*, Brisbane, 144-149.
- Ouattara, D., Yahia, A., Mbonimpa, M., and Belem, T. (2017). "Effects of superplasticizer on rheological properties of cemented paste backfills." *International Journal of Mineral Processing*, 161, 28-40.
- Ray, A., Sriravindrarajah, R., Guerbois, J. P., Thomas, P. S., Border, S., Ray, H. N., and Joyce, P. (2007). "Evaluation of waste perlite fines in the production of construction materials." *Journal of Thermal Analysis and Calorimetry*, 88(1), 279-283.

- Schneider, M., Romer, M., Tschudin, M., and Bolio, H. (2011). "Sustainable cement production—present and future." *Journal of Cement and Concrete Research*, 41(7), 642-650.
- Scrivener, K., Snellings, R., Lothenbach, B. (2017). "A Practical Guide to Microstructure Analysis of Cementitious Materials." *CRC Press Taylor and Francis Group*, 177-202.
- Sivakugan, N., Rankine, K., and Rankine, R. (2005). "Geotechnical aspects of hydraulic filling of underground mine stopes in Australia." *Elsevier Geo-Engineering Book Series*, 3, 513-538.
- Sivakugan, N., Rankine, R. M., Rankine, K. J., and Rankine, K. S. (2006). "Geotechnical considerations in mine backfilling in Australia." *Journal of Cleaner Production*, 14(12), 1168-1175.
- Sivakugan, N., Veenstra, R., and Naguleswaran, N. (2015). "Underground mine backfilling in Australia using paste fills and hydraulic fills." *International Journal of Geosynthetics and Ground Engineering*, 1(2), 18.
- Tuladhar, R., Sexton, A., and Joyce, P. (2013). "Durability of concrete with pitchstone fines as a partial cement replacement." *Concrete Institute of Australia's Biennial National Conference*.
- Tuladhar, R., Smith, M., Pandey, G. R., and Joyce, P. (2011). "Use of pitchstone fine as a partial replacement of portland cement for sustainable concrete." *Proceedings of 2011 International Concrete Sustainability Conference*, Boston, USA.
- Vessalas, K., Thomas, P. S., Ray, A. S., Guerbois, J. P., Joyce, P., and Haggman, J. (2009). "Pozzolanic reactivity of the supplementary cementitious material pitchstone fines by thermogravimetric analysis." *Journal of Thermal Analysis and Calorimetry*, 97(1), 71.
- Walker, R. and Pavía, S. (2011). "Physical properties and reactivity of pozzolans, and their influence on the properties of lime–pozzolan pastes." *Journal of Materials and Structures*, 44(6), 1139-1150.

Wang, X. Y., and Park, K. B. (2015). "Analysis of compressive strength development of concrete containing high volume fly ash." *Journal of Construction and Building Materials*, 98, 810-819.

Wu, A. X., Ruan, Z.-e., Wang, Y. M., Yin, S.-h., Wang, S. Y., Wang, Y., and Wang, J. D. (2018). "Simulation of long-distance pipeline transportation properties of whole-tailings paste with high sliming." *Journal of Central South University*, 25(1), 141-150.

Www.marketrealist.com, "Room and pillar method."

Www.cdn.britannica.com, "Over-hand cut and fill method."

Www.docplayer.net, "Block caving method."

Www.sec.gov, "Primary-secondary transverse method."

Www.benp.com, "Paste fill discharge."

Yu, B., Zeng, Z., Ren, Q., Chen, Y., Liang, M., and Zou, H. (2016). "Study on the performance of polycarboxylate-based superplasticizers synthesized by reversible addition-fragmentation chain transfer (RAFT) polymerization." *Journal of Molecular Structure*, 1120, 171-179.

Appendix A: Example of UCS data record sheet (Mix39)

UCS Test Data Sheet														
Sample	Ave diameter (mm)	Ave Length (mm)	Mass (g)	Curing days	L:D ratio	Area (m ²)	Bulk volume (cm ³)	Bulk density (t/m ³)	UCS (kPa)	Failure strain (%)	Young's modulus (kPa)	Moisture (%)	Area (m ²) corrected	UCS (kPa) corrected
1	50	101	405	7	2.02	0.00196	198.21	2.05	243.45	7.06	12869	28.78	0.00211	226.25
2	50	101	407	7	2.02	0.00196	198.21	2.05	231.11	5.90	18763	29.77	0.00209	217.49
3	50	101	406	7	2.02	0.00196	198.21	2.05	275.65	7.48	14125	29.68	0.00212	255.04
4	50	101	405	14	2.02	0.00196	198.21	2.04	480.42	4.17	103518	29.81	0.00205	460.41
5	50	101	403	14	2.02	0.00196	198.21	2.03	496.09	4.83	68489	13.36	0.00206	472.11
6	50	101	404	14	2.02	0.00196	198.21	2.04	509.59	4.92	82108	28.12	0.00206	484.52
7	50	101	401	28	2.02	0.00196	198.21	2.02	623.13	2.61	130421	13.49	0.00202	606.88
8	50	101	406	28	2.02	0.00196	198.21	2.05	591.80	2.61	152669	29.60	0.00202	576.38
9	50	101	408	56	2.02	0.00196	198.21	2.06	857.98	1.40	183843	30.00	0.00199	845.99
10	50	97	383	56	1.94	0.00196	190.36	2.01	811.30	2.17	75416	29.35	0.00201	793.68
11	50	101	407	112	2.02	0.00196	198.21	2.05	927.94	1.04	220923	30.12	0.00198	918.30
12	50	101	405	112	2.02	0.00196	198.21	2.04	846.71	0.81	160151	0.00	0.00198	839.83

Appendix B: Example of ITS data record sheet (Mix39)

ITS Test Data Sheet

Sample	Ave diameter (mm)	Ave Length (mm)	Mass (g)	Curing days	D:L ratio	Area (m ²)	Bulk volume (cm ³)	Bulk density (t/m ³)	Tensile (kPa)
1	50	25.5	100.92	7	1.96	0.00196	50.0438	2.02	14.51
2	50	25.5	100.94	7	1.96	0.00196	50.0438	2.02	13.93
3	50	25.5	100.73	7	1.96	0.00196	50.0438	2.01	16.07
4	50	25.5	102.77	14	1.96	0.00196	50.0438	2.05	46.50
5	50	25.5	102.51	14	1.96	0.00196	50.0438	2.05	43.46
6	50	25.5	101.74	28	1.96	0.00196	50.0438	2.03	100.91
7	50	25.5	101.93	56	1.96	0.00196	50.0438	2.04	156.11
8	50	26	100.00	112	1.92	0.00196	51.0250	1.96	172.36

Appendix C: Example of slump data record sheet

Date	09-Oct-18												
Solid content	74%												
Moisture	6%												
Test	Cone		Slump	Binder		Tailing	Binder	Water	Admixture	Solid	Binder	Water	Water:Cement
#	Height (mm)	Base (mm)	(mm)	Pozzolan (%)	GPC cement (%)	(kg)	(kg)	(kg)	(%)	(% wgt)	(% wgt)	(% wgt)	W:C
1	300	200	244	0	100	9	0.28	3.26	0	74	3	35.14	11.72
2	300	200	255	0	100	9	0.28	3.26	2	74	3	35.14	11.72
3	300	200	263	0	100	9	0.28	3.26	4	74	3	35.14	11.72
4	300	200	265	0	100	9	0.28	3.26	6	74	3	35.14	11.72
5	300	200	274	0	100	9	0.28	3.26	8	74	3	35.14	11.72

Appendix D: Example of yield stress data record sheet

YIELD STRESS							
Date							
Sample description							
By							
Run #	Model	Spindle	RPM	Torque (%)	Yield stress (dyne/cm ²)	Shearing time	Comments
	Rheometer-DV3THA	V75	0.05			120 sec (2 min)	
	Rheometer-DV3THA	V75	0.1			120 sec (2 min)	
	Rheometer-DV3THA	V75	0.25			120 sec (2 min)	
	Rheometer-DV3THA	V75	0.5			120 sec (2 min)	
	Rheometer-DV3THA	V75	1			120 sec (2 min)	
Data field							
Spindle	V75						
Immersion mark	Primary						
Pre-shear speed	5	RPM					
Pre-shear time	1	Minute					
Zero speed	0.01-0.5	RPM					
Wait time	30	Seconds					
Run speed	0.01-1	RPM					
Torque reduction	100	%					

Appendix E: Example of viscosity data record sheet

VISCOSITY							
Date							
Sample description							
By							
Run#	Model	Spindle	RPM	Torque (%)	Viscosity (cP)	Shearing time	Comments
	Brookfield Rheometer-DV3THA	V75	1			120 sec (2 min)	
	Brookfield Rheometer-DV3THA	V75	2			120 sec (2 min)	
	Brookfield Rheometer-DV3THA	V75	2.5			120 sec (2 min)	
	Brookfield Rheometer-DV3THA	V75	4			120 sec (2 min)	
	Brookfield Rheometer-DV3THA	V75	5			120 sec (2 min)	
	Brookfield Rheometer-DV3THA	V75	10			120 sec (2 min)	
	Brookfield Rheometer-DV3THA	V75	20			120 sec (2 min)	
	Brookfield Rheometer-DV3THA	V75	50			120 sec (2 min)	
	Brookfield Rheometer-DV3THA	V75	100			120 sec (2 min)	
	Brookfield Rheometer-DV3THA	V75	200			120 sec (2 min)	
Data field							
Zero speed	0.01-0.5	RPM					
Wait time	30	Seconds					
Run speed	0.5-200	RPM					
Torque reduction	100	%					

Appendix F: Example of TGA data record sheet

Cure period (days)	Mass (initial) (mg)	Temp1 (°C)	Mass@temp (mg)	Temp2 (°C)	Mass@temp2 (mg)	Mass loss (mg)	CaOH ₂ (mg)	CaOH ₂ (%)
7	6.737	350	6.483	450	6.455	0.028	0.115	1.71%
7	9.272	350	8.932	450	8.89	0.042	0.173	1.86%
14	6.508	350	6.338	450	6.299	0.039	0.160	2.46%
14	9.507	350	9.275	450	9.231	0.044	0.181	1.90%
28	10.185	350	9.679	450	9.625	0.054	0.222	2.18%
56	4.438	350	4.258	450	4.236	0.022	0.090	2.04%